The role of *Tbx18* in axial mesoderm development

Thesis presented for the degree of Ph. D. by
Sarah Burbridge

MRC Centre for Developmental and Biomedical Genetics
University of Sheffield

July 2012

Figures

Chapter 1

Chapter 3

Chapter 4

Chapter 5

Chapter 6

Chapter 7

Tables

Boxes

Abstract

The axial mesoderm is a specialised population of cells lying at the midline of the embryo. It is composed of two cell populations: the anterior prechordal mesoderm (PM), bounded posteriorly by the notochord (NC). A wealth of studies have shown that both PM and NC are key organising centers that pattern and regionalise the overlying neuroectoderm into fore-, mid-, hindbrain and spinal cord. However, it is unclear how the axial mesoderm becomes regionalised into PM and NC with a sharp boundary established between the two domains. Here I use the chick embryo to address this question.

One of the reasons that studies into the development of axial mesoderm have been hampered is due to the lack of an exclusive marker of the PM. Here, I show that *Tbx18* is a novel and exclusive marker of the PM and is expressed once the axial mesoderm has fully extended.

Much emphasis has been placed in the literature upon the importance of Nodal signalling in axial mesoderm formation, however, little is known about its role in the fully extended axial mesoderm. Here, I show that Nodal initiates *Tbx18* expression in the fully extended axial mesoderm, i.e. acting to further specify PM. My studies reveal, further, that Nodal signalling is inhibited by the paraxial mesoderm and retinoic acid. Together, the antagonistic signals appear to establish the posterior limit of the PM and the anterior limit of the NC.

Finally, I find that *Tbx18* sharpens the PM-NC boundary by downregulating the NC marker 3B9 and establishing a third subpopulation of Shh- axial mesoderm that lies at the PM-NC interface. I discuss the potential significance of this third axial mesoderm population.

Chapter 1

Introduction

1.1 Introduction

The phylum Chordata includes the Cephalochordata (amphioxus), the Urochordata (tunicates such as sea squirts, salps and larvaceans) and the Vertebrata (fish, amphibians, reptiles, birds and mammals). A defining feature of this phylum is the presence of a rod-like tissue that extends in the midline. This tissue is commonly termed the notochord, and is located ventral to the neural tube. Some chordates retain the notochord throughout their lives, whereas in others it is only present during embryogenesis and larval life. Thus, the notochord is a permanent feature of amphioxus, but is lost at metamorphosis in the sea squirt *Ciona intestinalis* and is largely replaced in vertebrates by the vertebral column after embryogenesis.

Studies over many decades have detailed the importance of the axial mesodermal notochord. As detailed below, it is the source of embryonic developmental signals, co-ordinating the development of the central nervous system (CNS), non-midline mesoderm and even endodermal structures (Takya, H., 1961; Placzek et al., 1990; Yamada et al., 1993; Trousse et al., 1995; Fan and Tessier Lavigne, 1994; Brand-Saberi et al., 1993; Halpern et al., 1993; Kim et al., 1997). It also provides a mechanical supporting function in some species - giving the body some rigidity against which the axial musculature can act. Without the notochord, embryos fail to elongate leading to restricted locomotion and a malformed embryo (Talbot et al., 1995; Stemple et al., 1996).

Crucially, although the notochord does constitute the vast majority of the axial mesoderm, classic embryological studies in the early part of

the 20th century showed that the axial mesoderm is in fact composed of two major components, the anteriorly- situated prechordal mesoderm/mesendoderm, and the more posteriorly-located notochord (Spemann and Mangold, 1924 as cited in De Robertis, E. M., 2006). These can be distinguished through their different morphologies, the prechordal mesoderm's fan-like appearance contrasting with the rod-like appearance of the notochord (Adelman, H. B., 1922, 1927; Meier, 1981; Izpisúa-Belmonte et al., 1993). The anterior prechordal mesoderm (PM), bounded posteriorly by the notochord, has been shown to be present in all vertebrate species studied to date (Adelmann, H. B., 1922). As detailed below, both structures are, in fact, crucial to the establishment of the body plan, and each plays a distinct role in the organization and formation of different components of the body of the vertebrate.

1.2 Mesoderm induction and early embryonic patterning: classic phenomenological studies

Studies in Xenopus pioneered our understanding of mesoderm induction, and the phenomenological events that govern axial mesoderm induction. The Xenopus egg is polarized into a dark coloured animal and a yolky vegetal pole (Figure 1.1A). Before the zygote divides, the cortex rotates and as a result, maternal components of the Wnt signalling pathway (Box 1) are redistributed to the future dorsal side (Figure 1.1B). Cleavage occurs along the animal-vegetal axis dividing the egg into half and then again at right angles to divide it into four. As cleavage continues the egg is divided

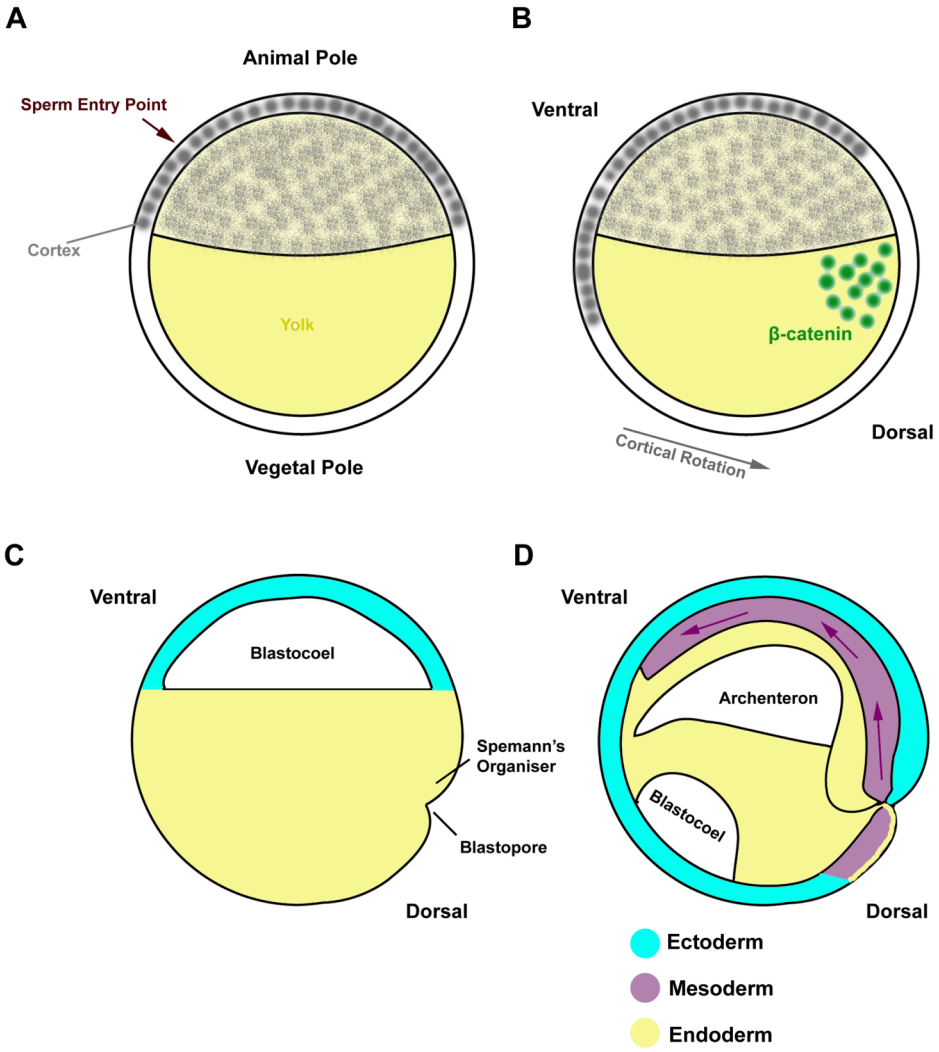

Figure 1.1 Development of the Xenopus embryo.

A Xenopus egg is divided into two halves: the dark pigmented animal pole and the yolky vegetal pole.

B Cortical rotation takes place before the zygote divides. This leads to the distribution of vesicles containing Disheveled (Dsh) protein to the dorsal side. This concentration of Dsh stabilises β catenin in this dorsal location (Tao et al., 2005).

C A slit known as the blastopore forms and the blastula is now ready to form the deeper layers of the embryo.

D Gastrulation continues as cells involute (indicated by the arrows). They move underneath the roof of the blastocoel which gets pushed to one side.

Box 1 The canonical Wnt signalling pathway

Wnts are secreted glycoproteins that bind Frizzled receptor and LRP6 co-receptor complex. Upon the binding of ligand Frizzled and LRP6 receptors are activated leading to the recruitment of a key intracellular component Dishevelled (Dsh), which interacts with a protein complex including Axin, GSK, APC and CK1 inhibiting degradation of β-catenin. Stabilised β-catenin enters the nucleus and complexes with TCF to activate Wnt target genes. In the absence of Wnt ligands, GSK-3 and CK1 phosphorylate β-catenin marking it for degradation post ubiquitnation in the cytosol. Thus, β-catenin cannot bind TCF and activate TCF responsive genes. As a result Groucho, a corepressor binds TCF in the nucleus inhibiting Wnt target gene activation. The figure below shows the simplified core pathway and does not include the antagonists of the Wnt signalling pathway. Wnt antagonists are divided into two groups: sFRP family including WIF-1 and Cerebrus which bind Wnt ligands and Dickkopf proteins which inhibit the pathway by binding to LRP coreceptors (Adapted from Wolpert, 2002).

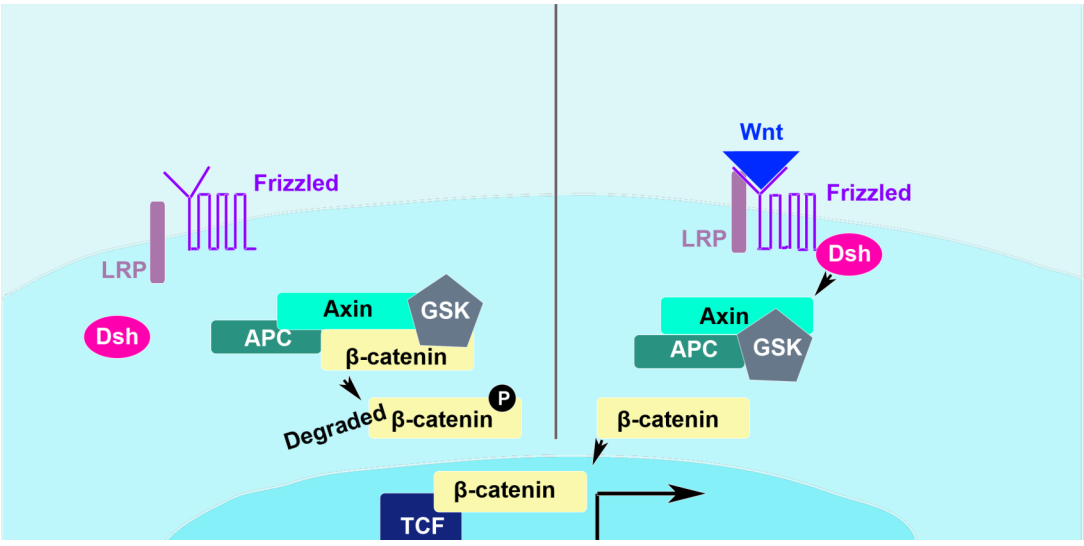

into smaller cells and then a cavity called the blastocoel develops in the animal half (Figure 1.1C). The embryo is now called the blastula, and can form its three germ layers – ectoderm, mesoderm and endoderm (Figure 1.1D).

Recombination experiments first revealed that vegetal endoderm induces the mesoderm in the animal cap cells (Nieuwkoop P, 1969; Sudarwati and Nieuwkoop, 1971). Animal cap explants cultured in isolation do not produce mesoderm *in vivo* or *in vitro*, but do so when cultured or combined with vegetal cells (Nieuwkoop P., 1969a; Nieuwkoop P., 1969b; Nieuwkoop and Ubbels, 1972). This led to the hypothesis that animal cap cells receive signals from vegetal cells instructing them towards mesodermal fate, and the repression of ectodermal fate (Sargent et al., 1986). Refined subdissections of the vegetal hemisphere, in fact, revealed that different portions of the vegetal territory have different mesodermal inducing abilities (Boterenbrood & Nieuwkoop, 1973; Dale et al., 1985; Dale and Slack, 1987 a and b). Thus, only a discrete group of cells – opposite the site of sperm entry – will induce a specialized region of mesodermal cells, termed the organiser. This specialized region of vegetal cells is termed the Nieuwkoop Centre (Gerhart et al., 1989). Lineage tracing experiments confirm that the Nieuwkoop centre does not contribute itself to the organiser or the mesoderm but has an inductive role (Gimlich, R. L., 1986).

The organiser performs three major functions: it recruits adjacent mesodermal cells to become ‘dorsal’, it induces neural tissue in the neighbouring ectoderm and it self-differentiates into the axial mesoderm (Lemaire and Kodjabachian, 1996). The instructive

properties of the organiser were shown powerfully by a classic experiment where the organiser region was isolated and grafted into the ventral side of the newt embryo. This gave rise to a fully developed secondary axis including neural tissue underlain by axial mesoderm and somites (Spemann H., 1938; Bouwmeester, T., 2001). Subsequent to these early experiments, many studies in a wide range of vertebrates have shown that structures analogous to the organiser (for instance the mouse node, the zebrafish shield and Hensen's node) have analogous properties. If transplanted ectopically into the host of a similar stage embryo, they induce and 'dorsalise' the host tissue to form neural tissue and paraxial mesoderm (Beddington, R., 1994; Shih and Fraser, 1995; Shih and Fraser, 1996, Dias and Schoenwolf, 1990). At early gastrulation the organiser begins to pattern the established mesoderm into specific fates. This results in the ventral mesoderm being patterned into kidney and blood, the intermediate lateral mesoderm into somites; the dorsal mesoderm, containing the organiser, will form the axial mesoderm composed of anterior prechordal mesoderm and posterior notochord as the dorsal lip begins to involute.

Crucial, then to the on-going development of the embryonic body plan, is the third property of the organiser – its ability to self-differentiate into axial mesoderm. Concomitant with this differentiation, the organiser- forming axial mesoderm undergoes movements that lead to a reorganisation of the blastula and the germ layers, that establish the basic body plan on which specific organs form (Harland and Gerhart, 1997). This process is known as gastrulation.

Early phenomenological studies pointed to the crucial role of the axial mesoderm as an early 'organiser' and 'patterning centre', and revealed that notochord and prechordal mesoderm have different organizing and patterning activities (Adelmann, H. B., 1930; Mangold, O., 1933; Spemann, H., 1938). If, instead of grafting early organiser tissue, different regions of the extending axial mesoderm were grafted into ectopic ventral locations, then they induced only subsets of neural tissue: the anterior extending axial mesoderm induced head-like structures, whereas posterior extending axial mesoderm induced trunk-like structures (Mangold, O., 1933 as cited in Doniach, T., 1992). This suggested for the first time that prechordal mesoderm and notochord have different inducing/patterning activities.

1.2.1 Mesoderm induction and early embryonic patterning: molecular studies

Since these early experiments, a wealth of studies have been performed, to examine the molecular events that govern these steps. Mesoderm induction occurs when a maternal T box gene, VegT, localized in the vegetal cells activates zygotic genes of the TGFβ superfamily called the Nodal-related proteins; these appear to be the main diffusible signals that act to induce mesoderm and definitive endoderm (Figure 1.2 A and B) (Box 2) (Zhang et al., 1998; Clements et al., 1999). Veg-T depleted embryos lack mesoderm and endoderm, but this phenotype can be rescued by injecting TGFβ signalling ligands, in particular the Nodal related proteins Xnr 1, -2, -4 and Derrière (Kofron et al., 1999). Conversely, inhibition of Nodal

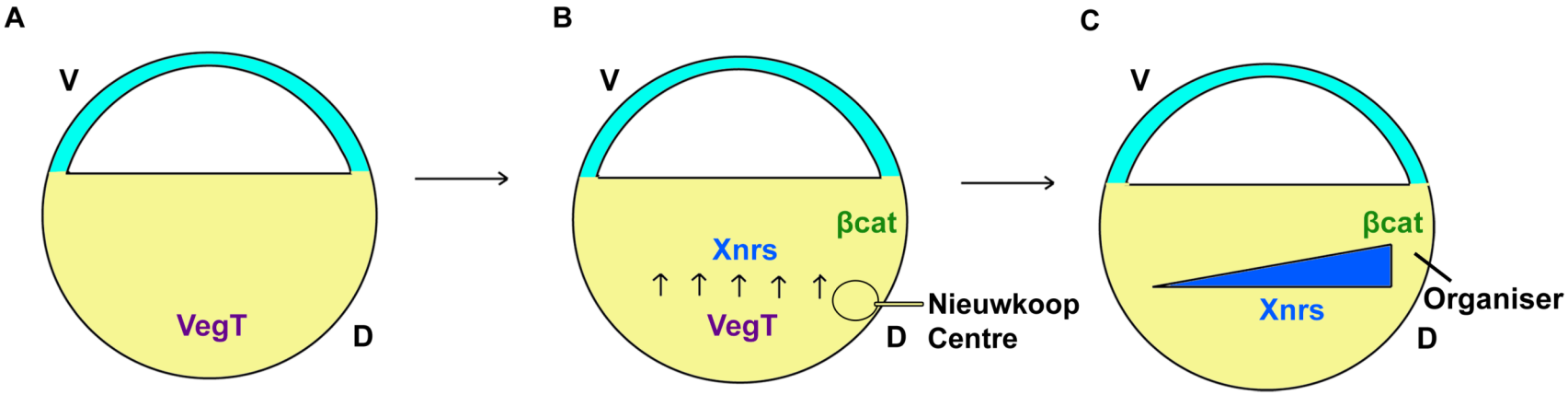

Figure 1.2 Signals required for mesoderm induction in Xenopus.

A Maternal VegT is expressed in the vegetal hemisphere of the embryo.

B VegT activates mesoderm inducers, the TGFβ signalling proteins Xnrs in the vegetal hemisphere. Xnrs along with β catenin establish the Nieuwkoop Centre on the dorsal side.

C Further βcatenin establishes a dorsoventral gradient of Xnr proteins such that there is a high concentration of Xnr proteins in the Nieuwkoop centre. This high Xnr concentration in the Nieuwkoop centre cooperates with βcatenin to establish the oragniser and transcribe organiser genes.

Box 2 TGF-β signalling pathway

The TGF-β family of signalling molecules consists of two general branches: the TGF-β/Activin/Nodal and BMP/GDF branches. Signalling is mediated by type I or type II serine/threonine receptor kinases. Ligand binding results in the association of the two types of receptor and phosphorylation of type I receptor by the type II receptor. This results in phosphorylation of Smad proteins (Smad 2/3 for TGF-β/Activin/Nodal or Smad1, 5, 8 for BMP receptor substrates). This increases their affinity for Smad4 resulting in assembly of a complex, which translocates to the nucleus and binds to transcription factors to activate target gene transcription. The figure below does not include the antagonists of the pathway that are crucial for its regulation. These antagonists include chordin, noggin, members of the DAN family including Cerberus, DAN and Gremlin, follistatin, and lefty proteins. In addition to these antagonists further negative regulation comes from Smad 6 and 7, which compete with signal transducing smads for receptor binding (Adapted from Massague and Wotton, 2000).

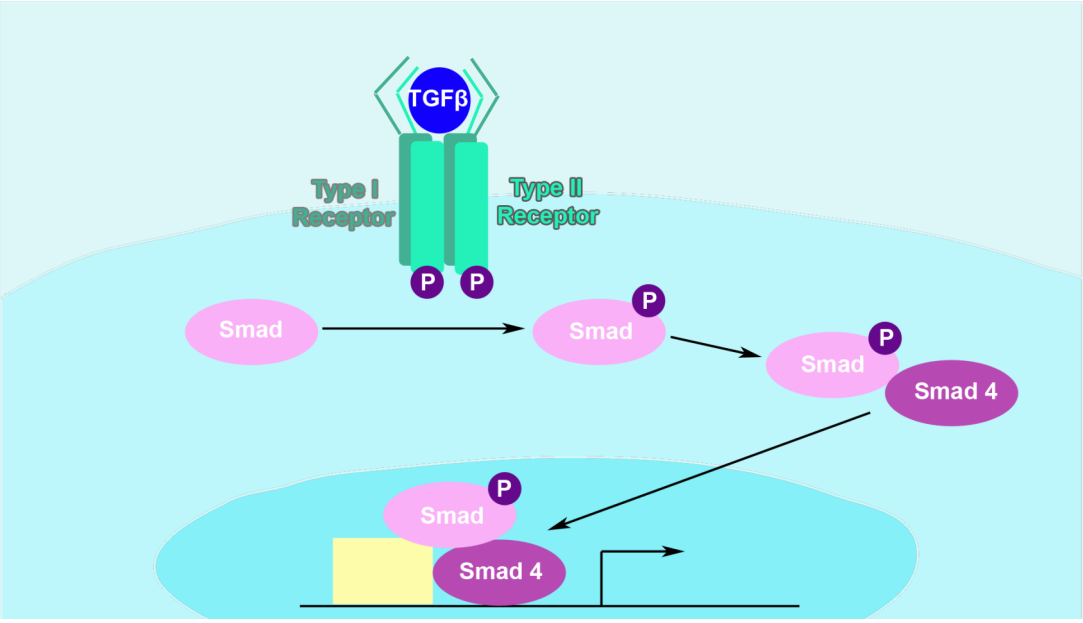

signalling in Xenopus blocks mesoderm formation (Agius et al., 2000; Osada and Wright, 1999).

Studies in Xenopus have been instrumental, not just in pointing to the role of Nodal in mesoderm induction but in establishing how Nodal signalling can lead to the establishment of different types of mesodermal cell. These studies have revealed that Nodal signalling, along with Wnt signalling pathway components that were distributed to one side of the embryo due to cortical rotation, establish the Nieuwkoop centre opposite the sperm entry point (Heasman et al., 1994; Wylie et al., 1996; Agius et al., 2000). This is now the dorsal side of the embryo and active Wnt signalling here means that its downstream factor β-catenin, stabilises and stimulates Xnr protein levels, establishing a Nodal signalling gradient along the dorso-ventral axis of the embryo (Takahashi et al., 2000) (Figure 1.2 C).

β-catenin plays a role, not only in stimulating high levels of Nodal in the Nieuwkoop Centre, but additionally co-operates with Nodal signalling components in the organiser. Here, β-catenin translocates to the nucleus and complexes with transcription factor Tcf-3, and in cooperation with high Nodal signals, activates the expression of genes such as *Siamos* and *Twin,* which then activate organiser genes such as *Gsc, Chordin, Noggin, Follistatin, Cerberus, XLim1 and Xnr3* (Brannon et al., 1997; Fan et al., 1998; Laurent et al., 1997; Fan and Sokol, 1997; Kessler, D. S., 1997; Carnac et al., 1996; Engleka and Kessler, 2001; Bae et al., 2011). *Siamos* and *Twin,* if expressed ventrally can induce the organiser and a complete secondary axis (Laurent et al., 1997; Lemaire et al., 1995).

Non-organiser mesoderm at this point has a ventral fate, promoted by high levels of BMP4 and Xwnt8 (Fainsod et al., 1994; Graff et al., 1994; Suzuki et al., 1994; Christian et al., 1991; Christian and Moon, 1993). Once the organiser is established, it begins to secrete antagonists of BMPs and Wnt, such as Chordin, Follistatin, Noggin, Cerberus and Frzb-1 (Piccolo et al., 1996; Zimmerman et al., 1996; Leyns et al., 1997; Bouwmeester et al., 1996). These appear to establish a concentration gradient, inhibiting BMP and Wnt signals, and effectively 'dorsalising' the mesoderm (Sassai et al., 1994; Piccolo et al., 1996; Sassai et al., 1995; Smith and Harland, 1992; Leyns et al., 1997; Wang et al., 1997; Bouwmeester et al., 1996).

The same BMP antagonists deriving from the early organiser appear crucial to neural induction. Prior to formation of the organiser, BMPs are uniformly expressed in the animal cap ectoderm (Hemmati-Brivanlou and Thomsen, 1995). With the onset of organiser formation, BMP antagonists that bind BMPs and prevent their binding to the receptors, are secreted (Piccolo et a., 1996; Zimmerman et al., 1996; Hsu et al., 1998; Piccolo et al, 1999; Fainsod et al., 1997; Lemura et al., 1998). Ectodermal tissue that does not receive BMP signalling acquires a 'neural fate' (Hemmati-Brivanlou and Melton, 1994; Henry et al., 1996; Lamb et al., 1993; Reversade et al., 2005). Molecular analyses reveal that, neural tissue that is induced in this early phase of development has 'anterior-like identity' (Nieuwkoop, P., 1954; Doniach, T., 1995).

As discussed above formation of the organiser leads to the establishment of the axial mesoderm and hence further dorsoventral and anteroposterior development of the embryo. The Wnt/β-catenin

pathway is not only essential for establishing the organiser by activating the transcription factors *Siamois* and *Twin,* but is also important for convergent extension movements (Kuhl et al., 2001).
The first axial mesoderm cells to extend are the prechordal mesoderm cells (Keller, R. E., 1976). For a short while, these retain the ability to induce/maintain anterior neural identity, through their continued expression of BMP and Wnt antagonists (Schneider and Mercola, 1999). By contrast, these factors are not maintained in developing notochord cells. Thus, anterior neural properties are maintained only in the prospective forebrain, while 'posteriorising' factors, including Wnts, FGFs and retinoic acid, transform other neural cells into hindbrain and spinal cord fates, through activation of genes such as the Hox genes (Games and Sive, 2000; Wilson and Edlund, 2001). This is known as 'activation-transformation' (Figure 1.3).

1.3 Patterning activities of the prechordal mesoderm and notochord

Since the initial classic experiments described above, a number of experimental studies have pointed to the different character of PM and NC, and their different abilities to induce different cell types, characteristic of particular regions in the overlying neural tissue along the rostro-caudal axis. Grafting and tissue recombination experiments show that the PM is able to induce neural tissue, which is anterior in character (Pera and Kessel, 1997; Saúde et al., 2000) and can pattern neural tissue so that it differentiates into hypothalamic and other diencephalic identities (Dale et al., 1997, 1999; Ohyama et al., 2005; Ohyama et al., 2008). The patterning

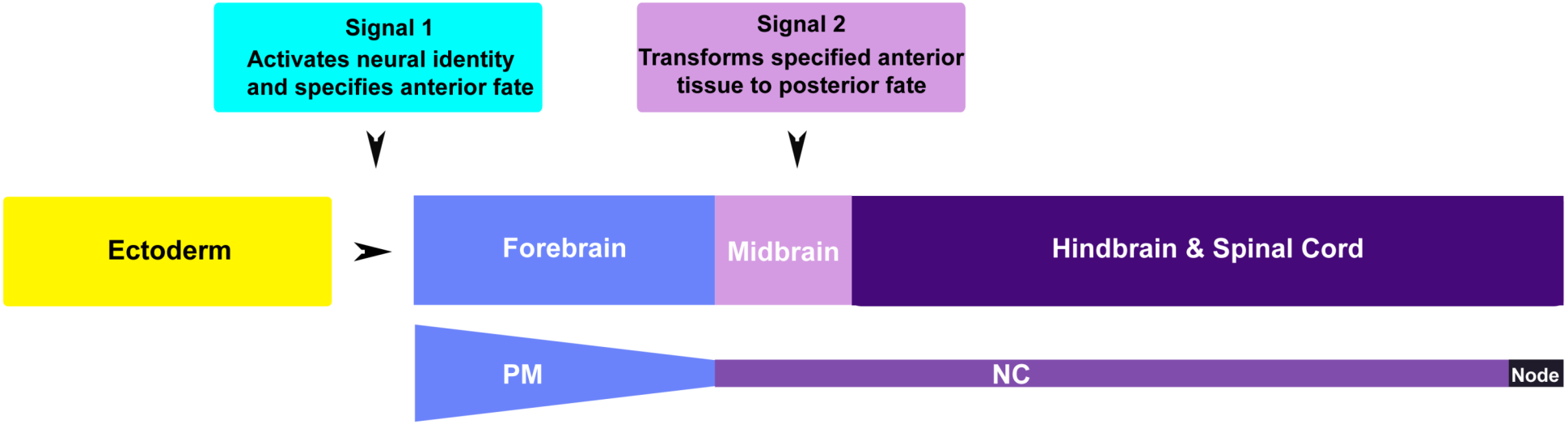

Figure 1.3 Activation- transformation model

Different regions of the central nervous system are induced according to this model first proposed by Peter Nieuwkoop (1954). Initially forebrain is induced by the first signal and BMP/Wnt antagnoists expressed by the prechordal mesoderm maintain forebrain fate. However, notochord does not express these antagnoists allowing the neural tissue to be posteriorised by Wnts, FGFs and retinoic acid and thus allowing midbrain, hindbrain and spinal cord formation. (Adapted from Stern, C. D., 2001).

activities of the prechordal mesoderm are quite distinct from those of the more posterior notochord: grafting and tissue recombination experiments show that the NC ectopically induces cell types that are characteristic of the hindbrain and spinal cord, including floor plate, motor neurons and seroternergic neurons (Placzek et al., 1993; Hynes et al., 1995; Yamada et al., 1991; 1993; Tanabe and Jessell, 1996). Conversely, removal of NC results in the absence of these cell types (Placzek et al., 1990; van Straaten and Hekking, 1991).

In fact, notochord-derived signals govern, not just the patterning of the overlying neural tube, but are instrumental in patterning other adjacent tissue. The varied roles of notochord-derived signals include patterning the somites, specifying the slow twitch muscle fibres and patterning of the early endoderm and pancreas (Barresi et al., 2000; Munsterberg and Lassar, 1995; Cleaver and Krieg, 2001; Kim et al, 1997).

Finally, notochord-derived signals appear to play various roles in early specification of the heart, and its related structures (Danos and Yost, 1995). Defects in notochord development can lead to the loss of left–right patterning of pre-cardiac mesoderm. The presumptive cardiac field, marked by the expression of the transcription factor Nkx2.5, expands if the anterior notochord is ablated, proving that signals from this region are important to limit the heart field (Goldstein and Fishman, 1998). *ntl* and *flh* zebrafish mutants fail to form the notochord, but also fail to form the dorsal aorta, implicating a role for NC in dorsal aorta formation (Fouquet et al., 1997; Sumoy et al., 1997).

Molecular studies have pointed to a number of genes that are expressed in the PM and NC and appear to mediate their properties. For example, expression of the transcription factors Goosecoid (*Gsc*) and Foxa2 in the PM appears to be important for correct anterior specification. Double mutant embryos for both transcription factors show perturbed anterior neural patterning (Filosa et al., 1997). In *Gsc* mutant mice, relatively normal patterning of the nervous system is seen although the nodes of these embryos have a weaker ability to induce neural cells (Zhu et al., 1999). Anterior endoderm and the PM share expression of the transcription factor Lim1, which has also been shown to play a role in anterior neural patterning (Shawlot et al., 1999). Lim1 knockout mice fail to develop the anterior head region (Shawlot and Behringer, 1995). In the early PM, Wnt and BMP antagonists such as Dkk-1 and Noggin are expressed, and appear to antagonize Wnt and BMP signals, preventing the posteriorisation of anterior structures. (Glinka et al., 1998; Hashimoto et al., 2000; Bachiller et al., 2000).

Intriguingly, expression of the Wnt and BMP antagonists in PM is transient, and soon after gastrulation, PM begins to express the BMP family members, BMP2 and BMP7 (Dale et al., 1997, Halilagic et al., 2003). BMPs now co-operate with Shh to pattern the prospective hypothalamus (Dale et al., 1999; Ohyama et al., 2005, 2008). The secreted signal, Shh is, in fact, expressed throughout the axial mesoderm (Echelard et al., 1993; Krauss et al., 1993; Marti et al., 1995; Roelink et al., 1995). However, in posterior regions, the NC expresses Shh but not BMP7 (Roelink et al., 1994; Rowitch et al., 1999). The exclusive expression of Shh in the notochord appears to govern many of its patterning roles, including ventralisation of the

neural tube and patterning of the somites (Yamada et al., 1991, 1993; Johnson et al., 1994; Munsterberg et al., 1995; Borycki et al., 1998)

Together, these studies show that PM and NC derive from the same general region in the embryo – the organiser – but rapidly assume quite different molecular identities. These molecular studies support the classic idea that PM and NC represent two cell types that together make up the axial mesoderm and begin to reveal how the PM and NC play significant roles in patterning the embryo. However, a major outstanding question is that of how PM and NC develop and acquire their different fates.

1.4 Role of Nodal in mesoderm induction

As briefly outlined above, the TGFβ family member, Nodal appears to play an evolutionarily conserved role in mesoderm induction (Table 1.1). The importance of the Nodal signal was first demonstrated in mouse, when a naturally occurring retroviral insertion mutation with severe gastrulation defects was shown to encode the Nodal gene (Conlon et al., 1991; Conlon et al., 1994; Zhou et al., 1993). The mice lacked mesoderm due to loss of primitive streak, essential for mesoderm induction (Zhou et al., 1993; Conlon et al., 1994). Similarly, in zebrafish, mutations in the Nodal-related genes *cyclops* and *squint* led to lack of mesoderm (Feldman et al., 1998; Rebagliati et al., 1998). Nodal was again shown to be crucial for mesoderm formation in chick, where, similar to the situation in mouse, it is required for the formation of the primitive streak (Bertocchini and Stern, 2002).

Since these observations, many studies have focused on the Nodal signalling pathway (Figure 1.4). Briefly, Nodal is thought to be secreted as a prodomain protein, which is cleaved into a mature form by the SPC convertases – Furin and Pace4 (Beck et al., 2002). Mature Nodal is thought to bind to ActRII/ALK4/5/7 receptors, and the co-receptor Cripto, to trigger signalling via phospholrylation of Smad2/3. Upon phosphorylation Smad 2/3 bind Smad4 leading to the Smad 2/3/4 complex to be translocated to the nucleus where it binds FoxH1 transcription factor to activate target genes (Schier, A., 2003).

Loss of function studies show that ActRII A and B have redundant functions but loss of both leads to severe defects in gastrulation and mesoderm formation (Matzuk et al., 1995; Song et al., 1999). Phosphorylation of Smad4 leads to activation of transcription factors including FoxH1 (Whitman, M., 2001). Mutation of these signalling components, in a range of species, supports the role of Nodal signalling in mesoderm induction (Table 1.1). Likewise, ectopic expression of Nodal signal inhibitors leads to loss of mesoderm, again supporting the key role of Nodal in mesoderm induction (Table 1.1).

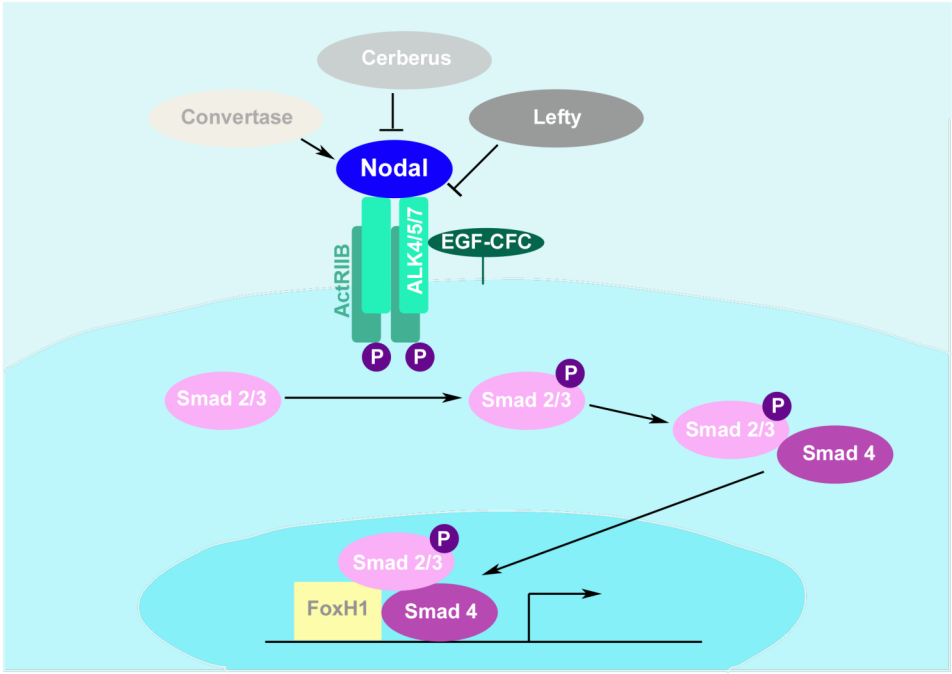

Figure 1.4 Canonical Nodal signalling pathway

Nodal ligand binds activin receptors (ActRIIB, ALK4/5/7) and the EGF-CFC coreceptor. Upon binding the receptors phosphorylate Smad 2/3 transcription factors, which bind Smad4 upon phosphorylation allowing the complex to enter the nucleus and bind FoxH1 transcription factors to stimulate target gene transcription. Nodal proproteins can be processed extracellularly by SPC1 and 4 convertases. Cerberus and Lefty proteins inhibit Nodal extracellularly. (Adapted from Schier, A. 2003)

Table 1.1 Role of Nodal and Nodal pathway components in mesoderm induction

Gene	Component	Organism	Role/Phenotype
Nodal	Ligand	Mouse	Loss of function mutation lack mesoderm (Zhou et al., 1993; Conlon et al., 1994)
Xnrs	Ligands	Xenopus	Gain and loss of functions experiments suggest that they are crucial for mesoderm induction (Osada and Wright, 1999, Kofron et al., 1999; Takahashi et al., 2000)
Cyclops; Squint	Ligands	Zebrafish	Lack of almost all mesodermal derivatives (Feldman et al., 1998)
Nodal	Ligand	Chick	Misexpression results in ectopic primitive streak formation if hypoblast is displaced (Bertocchini and Stern, 2002)
SPC1;SPC4	Convertase	Mouse	Disorganised primitive streak formation and lack of most mesoderm and endoderm (Beck et al., 2002)
Cripto	Co-Factor	Mouse	Lack of primitive streak and mesoderm (Ding et al., 1998)
One-eyed pinhead (oep)	Co-Factor	Zebrafish	Mutants lacking maternal and zygotic *oep* fail to induce mesoderm (Gritsman et al, 1999)
Lefty 1&2	Inhibitors	Zebrafish	Morpholino injections show an enlarged mesodermal domain (Agathon et al., 2001; Chen and Schier, 2002; Feldman et al., 2002)
Lefty 2	Inhibitor	Mouse	Excess mesoderm formation (Meno et al., 1999)
Cerberus-like;Lefty1	Inhibitors	Mouse	Expanded mesodermal domains due to primitive streak and multiple primtive streak formation observed in double mutant embryos (Pera-Gomez et al., 2002)
Cerberus	Inhibitors	Chick	Expressed in the hypoblast and inhibits primitive streak formation in the overlying epiblast (Bertocchini and Stern, 2002)
ActRIIA	Receptor	Mouse	No phenotype (Matzuk et al., 1995)
Act RIIB	Receptor	Mouse	No phenotype (Oh and Li, 1997)
ActRIIA&B	Receptors	Mouse	IIA-/-IIB-/- : gastrulation does not occur IIA-/-IIB+/- : primitive streak

			elongation impaired (Song et al., 1999)
ALK4	Receptor	Xenopus	Lack of mesoderm in mutants carrying a truncated mutation (Chang et al., 1997)
ALK4	Receptor	Mouse	Null mutant embryos fail to form the primitive streak and hence the mesoderm (Gu et al., 1998)
ALK4	Receptor	Zebrafish	Mesoderm induction and patterning impaired in studies using inhibitors (Sun et al., 2006)
ALK7	Receptor	Xenopus and Mouse	Constitutively active form induces mesendoderm and dominant negative form blocks Xnr1 function (Reissmann et al., 2001)
Smad2	Transcription factor	Mouse	Lack of mesoderm in homozygous mutants (Nomura and Li, 1998)
Smad2	Transcription factor	Xenopus	Required for translocation of Smad4 to the nucleus and complex with Fast-1. Dominant negative mutant activity results in partial mesoderm loss (Hoodless et al., 1999)
Smad2/3	Transcription factors	Zebrafish	Overexpression of Smad 2, Smad 3a and 3b mutants blocked mesoderm induction (Jia et al., 2008)
Smad 2/3	Transcription factor	Mouse	Embryos with loss of Smad3 and reduced Smad 2 function do not gastrulate and lack the mesoderm (Vincent et al., 2003; Dunn et al., 2004).
Smad4	Transcription factor	Mouse	Mutants fail to gastrulate and form mesoderm (Sirard et al., 1998).
FoxH1	Transcription factor	Mouse	Failure to form the node and defects in mesoderm formation (Hoodless et al., 2001; Yamamoto et al., 2001)
Schmalspur (FoxH1)	Transcription factor	Zebrafish	Lack of maternal and zygotic transcripts of FoxH1 leads to loss of the organiser and defects in mesoderm formation (Pogoda et al., 2000; Sirotkin et al., 2000)
FoxH1 (Fast1)	Transcription factor	Xenopus	Blocking antibodies reveal defects in mesoderm formation (Watanabe and Whitman, 1999)

1.4.1 Role of Nodal in axial mesoderm specification

Early experiments in Xenopus, working on the Nodal-related molecule, activin, first suggested that, not only can these induce mesoderm, but that it works in a dose-dependent manner to specify prechordal mesoderm cells versus notochord cells (Green et al., 1992, 1997; Gurdon et al., 1996). These studies showed that Activin acts dose-dependently to induce the prechordal mesodermal marker *Gsc* at high levels and the notochord marker Xbra at low levels in Xenopus animal cap cells (Jones et al., 1995; Lustig et al., 1996; Erter et al., 1998). Since these experiments, a wealth of genetic evidence has acculumated to support the idea that Nodal/Nodal-related proteins, act in a dose-dependent way to induce notochord and prechordal mesoderm (Table 1.2).

In zebrafish, loss of function mutants of *squint* and *cyclops* show defects in both PM and NC but PM appears to be particularly reduced (Hatta et al., 1991; Heisenberg and Nüsslein-Volhard, 1997, Dougan et al., 2003). This is further supported by a complete lack of PM in *one-eyed pinhead* mutants, which lack the co-factor for Nodal receptors (Schier et al., 1997). Similarly in mouse, Nodal hypomorphic mutants lack PM but not the NC, indicating that high Nodal signalling is essential for PM development (Lowe et al., 2001). Additionally, lack of PM, but not NC, is also observed in Smad 2 conditional knock-out mutants (Vincent et al., 2003). Conversely, double mutants of the Nodal inhibitors Cerberus and Lefty1 have an expanded PM (Pera-Gomez et al., 2002). In chick embryos it has been shown that an ectopic source of Cripto can alter the fate of NC to PM adding to the evidence that high Nodal signalling is required

for PM fate (Chu et al., 2005). However in mutants with a complete loss of Nodal signalling, a lack of axial mesoderm is observed. So, loss of the convertases Furin and Pace4, the co-factor Cripto and the transcription factors Smad 2, 3 and Smad 4 leads to lack of both PM and NC (Beck et al., 2002; Ding et al., 1998; Waldrip et al., 1998; Weinstein et al., 1998, Vincent et al., 2003; Dunn et al., 2004; Chu et al., 2004). Similarly, in Xenopus blocking antibodies against transcription factor FoxH1 also abolish axial mesoderm (Watanabe and Whitman, 1999).

Table 1.2 Role of Nodal and Nodal pathway components in axial mesoderm formation

Gene	Component	Organism	Role/Phenotype
Nodal	Ligand	Mouse	Hypomorphic mutants lack PM but not the NC (Lowe et al., 2001)
Cyclops	Ligand	Zebrafish	Loss of function mutation shows defects in PM and NC but particularly reduced PM (Hatta et al., 1991; Thisse et al., 1994; Dougan et al., 2003)
Squint	Ligand	Zebrafish	Same phenotypes as Cyclops (Heisenberg and Nüsslein-Volhard, 1997; Chen and Schier, 2001; Dougan et al., 2003)
SPC1;SPC4	Convertase	Mouse	Double mutant resembles Nodal mutants lacking axial mesoderm (Beck et al., 2002)
Cripto	Co-Factor	Mouse	Mutant embryos lack axial mesoderm and A-P axis is mis-oriented (Ding et al., 1998)
Cripto	Co-Factor	Chick	Ectopic expression downregulated NC markers and upregulated PM markers in the notochord (Chu et al., 2005)
One-eyed pinhead (oep)	Co-Factor	Zebrafish	Complete loss of PM in mutants (Schier et al., 1997)
Lefty 1&2	Inhibitors	Zebrafish	Ectopic expression of Lefty abolished axial mesoderm (Bisgrove et al., 1999)
Cerberus	Inhibitor	Xenopus	Injected Cer-S mRNA led to a lack of axial mesoderm in embryos (Piccolo et al., 1999)
Cerberus-	Inhibitors	Mouse	Double mutants show an expanded

like;Lefty1			prechordal mesoderm, multiple axis formation (Pera-Gomez et al., 2002)
ALK4	Receptor	Xenopus	Truncated receptor injected into embryos gave reduction in notochord specific marker (Chang et al., 1997). Secondary axis induction was observed after injecting ALK4 RNA in embryos (Armes and Smith, 1997) Also high levels induced Gsc and low levels induced Xbra in animal cap explants (Armes and Smith 1997)
Smad 2	Transcription factor	Mouse	Conditional knockout embryos lack prechordal mesoderm (Vincent et al., 2003).
Smad4	Transcription factor	Mouse	Conditional knockdown mutants gastrulate but fail to form the axial mesoderm (Chu et al., 2004)
FoxH1	Transcription factor	Xenopus	Disruption in axial mesoderm formation based on loss of function experiments using blocking antibodies (Watanabe and Whitman, 1999)

In summary, Nodal signalling is essential for the formation of both notochord and prechordal mesoderm but graded Nodal signals control cell fate decisions such that a high level of Nodal specifies prechordal mesoderm, whereas lower levels specify the notochord.

How might this gradient of Nodal signalling be set up? Firstly, Nodal signals are generated locally and are thought to diffuse short distances, so the cells closer to the source experience a higher level of Nodal signalling than those further away. It has been shown in zebrafish that *squint*-producing cells induced Gsc locally and *ntl/T* (a homologue of Brachyury) at long range (Chen and Schier, 2001). Secondly, Nodal signalling could be modulated by temporal activation of Nodal signals, so in Xenopus they are activated dorsally first and ventrally later (Lee et al., 2001). The exact mechanism involves Nodal signalling to be activated by the cooperative action of VegT and β-catenin dorsally and is attenuated later by the action of Nodal antagonists Cerberus and antivin (Lee et al., 2001). VegT

alone is responsible by the activation of Nodal signalling ventrally and commences only once its dorsal expression has been attenuated (Lee et al., 2001). But in zebrafish the time at which the Nodal signals are received does not seem to be important. Cells still respond and induce the appropriate targets genes even when they receive a delayed Nodal signal (Dougan et al., 2003). Thus, at present, the mechanisms leading to formation of the proposed Nodal gradient are not entirely clear.

Likewise unclear are the mechanisms that lead to the formation of two very discrete cell groups from a continuous concentration gradient. How does the proposed Nodal gradient ultimately results in the formation of two discrete cell types, namely the PM and the NC? A number of mechanisms could account for this. Firstly, feedback loops could operate to establish a step-gradient from a continuous gradient (Figure 1.5). In zebrafish it is postulated that the Nodal ligand *squint* autoregulates itself via a positive feedback mechanism. Both *squint* and *cyclops* can also induce the expression of Lefty inhibitors that can act at long range (Schier, A., 2003). The interactions between the ligand and the inhibitor establish a step-wise gradient, leading to the formation of PM close to the source of Nodal, and notochord at a distance (Chen and Schier, 2001; Schier, A., 2003). Alternatively, cells may operate post-signalling to sharpen the boundary between different cell types. Such a mechanism is known to operate in the spinal cord, where the Gli proteins initially translate the Shh gradient. Activator Gli1 is expressed in a ventral to dorsal gradient whereas repressor Gli proteins 2 and 3 are expressed dorsally. Shh converts Gli 2 and 3 to their activator forms thereby establishing a ventral to dorsal gradient (Box 3) (Jacob and Briscoe,

2003). Ultimately the Shh and Gli gradients lead to overlapping transcription factor expression domains along the dorsoventral axis. (Figure 1.6). These domains are sharpened through the cross-repressive interactions, leading to discrete boundaries (Briscoe and Ericson, 2001). Cells then establish different progenitor domains according to their transcriptional code (Dessaud and Briscoe, 2008).

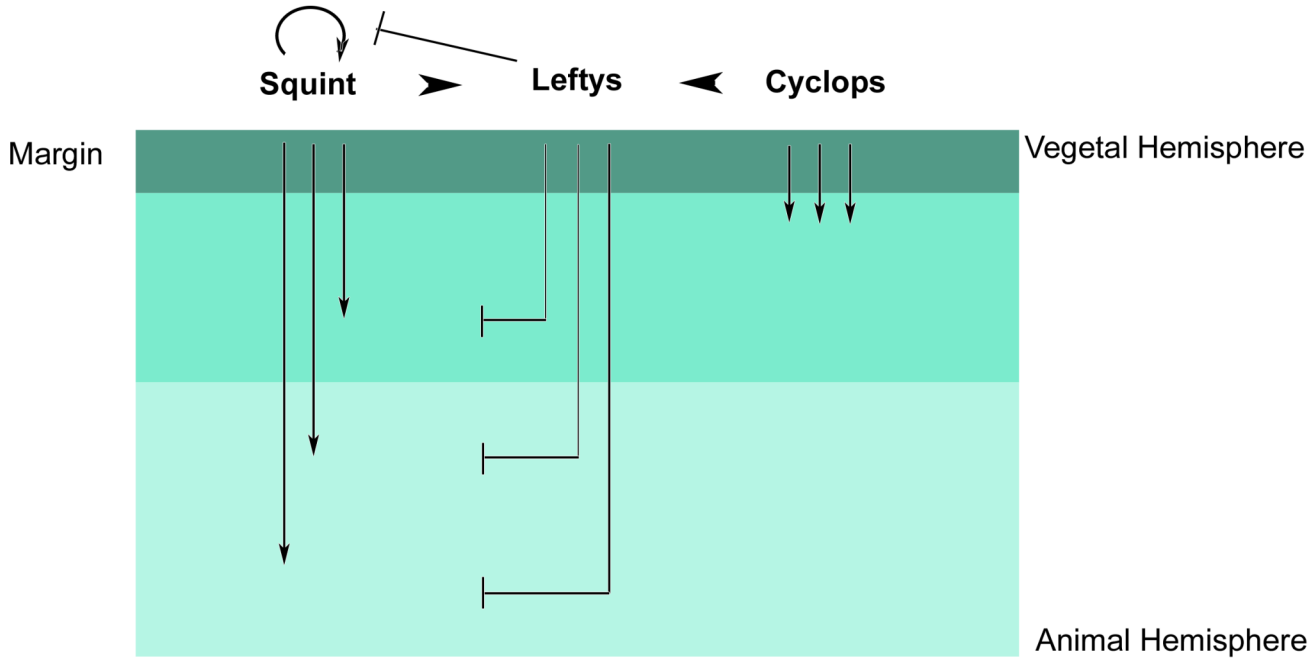

Figure 1.5 Model of induction of distinct mesodermal cell types by Nodal ligands.

Cross and autoregulatory interactions between Nodal ligands *squint* and *cyclops* with their inhibitors lefty 1&2 determine the type and extent of mesodermal cell induction. Both *squint* and *cyclops* induce the expression of leftys. *Squint* induces its own expression via a positive feedback loop and acts at long range. Leftys act at long range and inhibit *squint* creating a step gradient. *Cyclops* can only act at a short range. Collectively, the interplay between the ligands and inhibitors establishes a high Nodal concentration closer to the margin inducing PM and a lower Nodal concentration away from the margin inducing NC cells. (Adapted from Schier, A., 2003)

Box 3 Sonic Hedgehog signalling pathway in vertebrates

It is thought that in vertebrates primary cilia are crucial for the transduction of Shh signalling. (A) In the absence of Shh, the activity of Smoothened (Smo), a seven-pass transmembrane receptor is repressed by Patched1 (Ptch1) a twelve-pass transmembrane receptor, which leads to the inhibition of pathway transduction. PKA targets the zinc-finger transcription factors activator Gli (GliA) proteins to the proteasome where they are either completely degraded or truncated to their repressor form. This repressor form (GliR) translocates to the nucleus and represses the activation of Shh target genes. Any full length GliA proteins that remain are maintained in an inactive state by suppressor of fused (Sufu) (B) When Shh binds Ptch1, Smo is no longer repressed and is translocated to the primary cilium. PKA is inhibited by Smo and as a result GliA is not processed and translocate to the nucleus to activate target genes. There are three Gli transcription factors, Gli1 acts as a transcriptional activator whereas Gli2 and Gli3 can act as both activator and repressor. However, Gli2 mainly acts as an activator and Gli3 as a repressor. In the absence of Shh signal, Gli3 is truncated to its repressor form by proteolytic cleavage, whereas Gli2 is mostly degraded (Adapted from Dessaud et al., 2008).

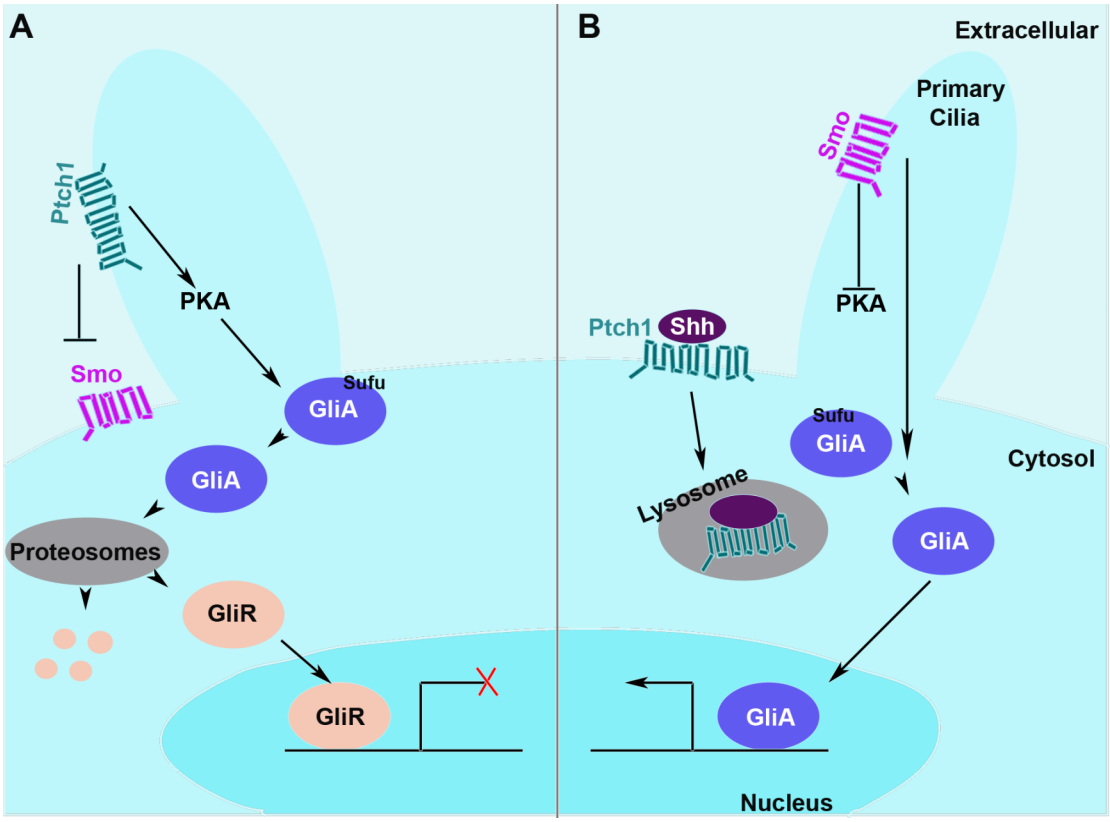

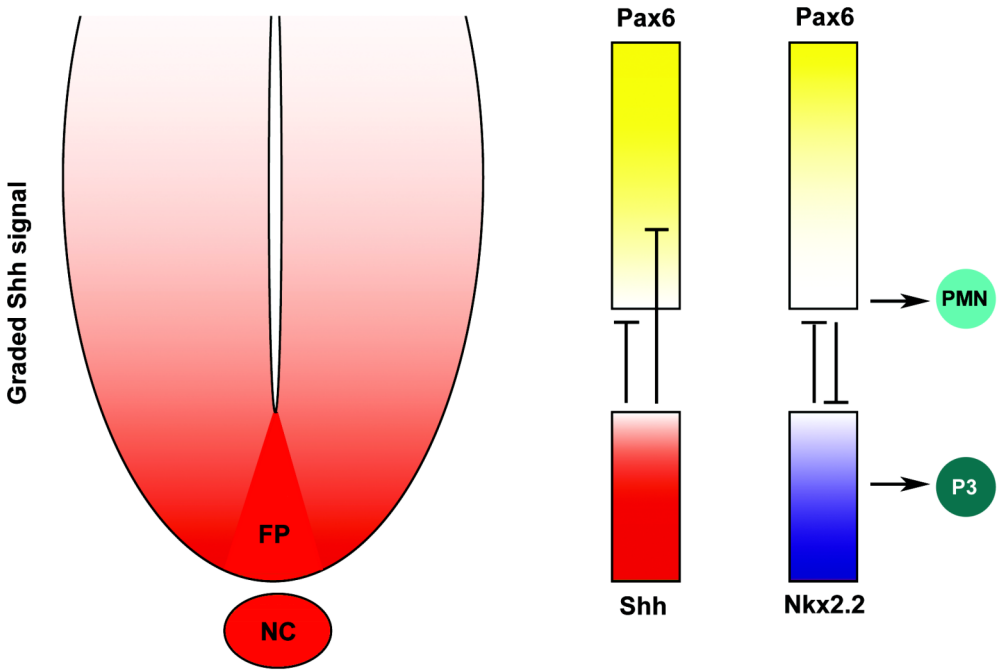

Figure 1.6 Gradient of Shh induces distinct cell types along the dorsoventral axis of the spinal cord.

Shh from the notochord (NC) and the floor plate (FP) acts in a concentration gradient to repress a number of genes including Pax6 to begin specification of progenitor domains. Post Pax6 repression, the region adjacent to the FP starts expressing Nkx2.2. Pax6 and Nkx2.2 then repress eachother to further refine the boundary between P3 and PMN progenitor domains. (Adapted from Patten and Placzek, 2000)

1.5 Mesoderm formation in the chick embryo

Studies on mesoderm induction and patterning in the chick embryo have lagged behind those in other species, but in general, it is clear that the basic mechanisms are conserved. The gastrula chick embryo is a flat bilayered blastoderm sitting on top of the yolk (Figure 1.7A). The hypoblast layer – the functional equivalent of the Xenopus vegetal pole - forms between the blastoderm and the underlying yolk and it will form extra embryonic structures. The embryo proper will form from the overlying epiblast - the equivalent of the animal pole.

As the egg travels down the oviduct, gravity determines the antero-posterior axis of the blastoderm and cells form a crescent shape next to the posterior marginal zone (PMZ), termed Koller's Sickle, at the future posterior end of the blastoderm (Figure 1.7 B and C) (Khaner and Eyal-Giladi, 1989). Cells begin to concentrate at this end to form a thickening known as the primitive streak (Figure 1.7 D and E) (Bellairs, R., 1986; Khaner and Eyal-Giladi, 1989). The PMZ cells express the TGFβ signalling molecule Vg-1 in the hours preceding streak formation and induce its formation (Seleiro et al., 1996; Shah et al., 1997). cWnt8C expressed in the marginal zone also plays a role in streak formation proved by its ability to duplicate axis if injected into Xenopus embryos (Hume and Dodd, 1993). Vg-1 and cWnt8C induce the expression of Nodal in the PMZ (Lawson et al., 2001; Skromne and Stern, 2002). Nodal together with Fgf signalling in Koller's sickle is responsible for inducing the primitive streak (Bertocchini et al., 2004). For this to occur successfully, Nodal signalling must be inhibited from the surrounding epiblast to prevent

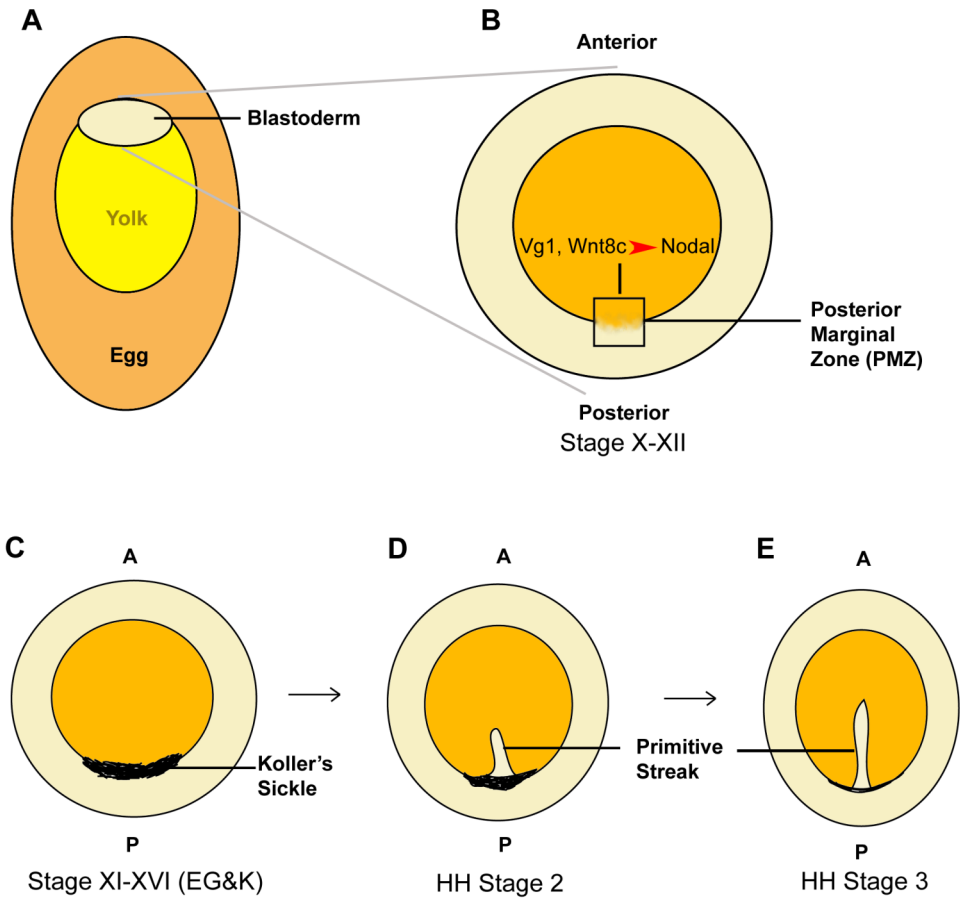

Figure 1.7 Development of the primitive streak in the chick embryo.

A The blastoderm sits on top of the yolk and the embryo will develop on its flat surface.

B The anterior and posterior axis of the embryo are defined as the posterior marginal zone forms at the future posterior end. Wnt8c is expressed throughout the marginal zone but Vg1 is expressed only in the posterior marginal zone (PMZ). Both act in cooperation to induce Nodal in the PMZ (Bertochinni etal., 2004).

C Posterior marginal zone induces a thickening of cells at the posterior margin called Koller's sickle.

D-E Further signals from the posterior marginal zone induce the primtive streak.

streak formation there, and BMP signalling must be inhibited in Koller's Sickle.

Inhibition of Nodal signalling occurs in two ways. Firstly, the hypoblast secretes the Nodal antagonist, Cerberus that prevents Nodal from inducing a premature streak (Bertocchini et al., 2002). At the time of streak formation, the hypoblast is displaced to an anterior position removing the source of Nodal antagonists posteriorly to allow Nodal to act (Bertocchini et al., 2002; Chapman et al., 2002). Secondly, the streak itself also secretes a Nodal inhibitor, which inhibits streak formation in the surrounding epiblast (Bertocchini et al., 2004).

The primitive streak further defines the antero-posterior axis of the embryo; anterior being the direction towards which it elongates and posterior marked by the beginning of the cell condensation. At the anterior tip of the primitive streak lies the homologue of the amphibian Spemann's organiser, termed the node in higher vertebrates, Hensen's node in the chick (Figure 1.8). During gastrulation cells from the epiblast migrate into the primitive streak and pass either through Hensen's node or around it to give rise to the deeper layers of the embryo (Figure 1.8). Pioneering experiments in vitro and later fate mapping studies have revealed that the position of the cells within the primitive streak dictates their migratory route and final destination (Waddington C, 1932; Schoenwolf et al., 1992; Psychoyos and Stern, 1996).

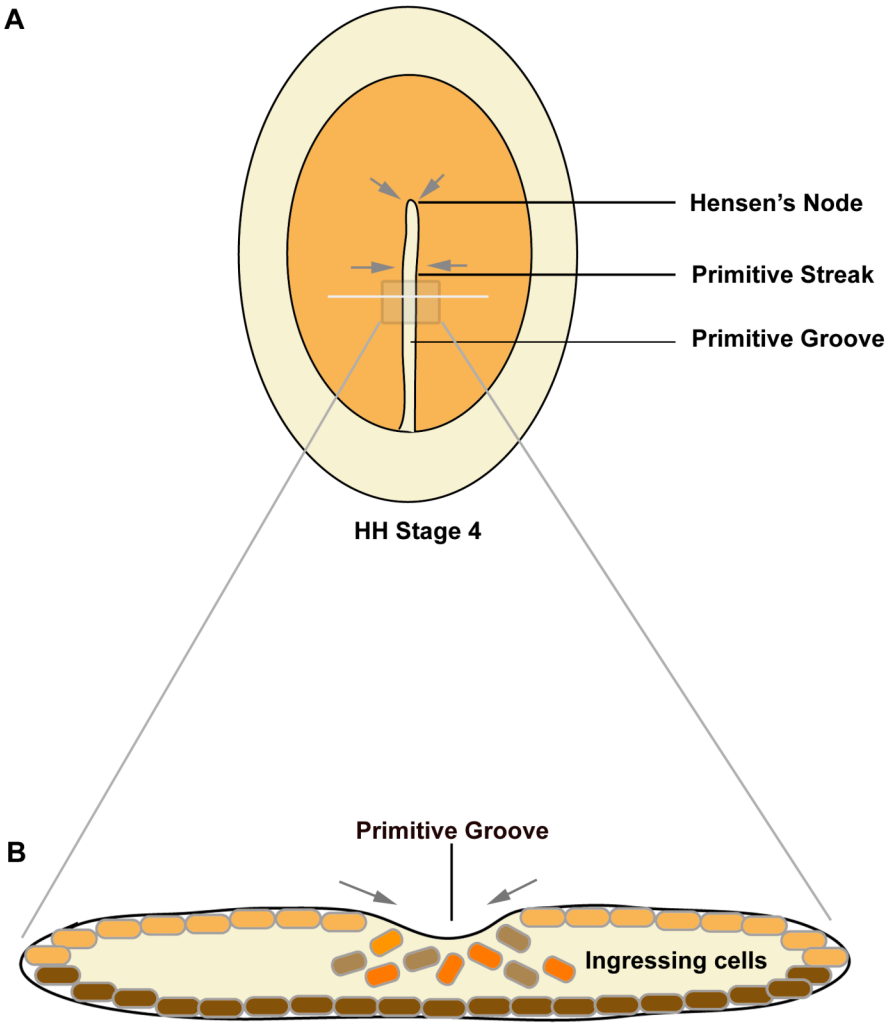

Figure 1.8 Gastrulation in the chick embryo.

A Schematic shows a fully extended primitive streak with Hensen's node at its anterior tip. At gastrulation cells move into Hensen's node and the primitive groove (indicated by arrows).

B A cross section through the primitive streak shows the ingressing mesodermal and endodermal cells. The cells will then follow various migratory routes to organise different fates within the new germ layers. Cells from Hensen's node contribute to the prechordal mesoderm and the notochord. Anterior primitive streak cells also contribute to the notochord as well as the somites (Psychoyos and Stern, 1996).

1.5.1 Development of chick axial mesoderm

The relatively large size of the chick axial mesoderm means that, in contrast to the difficulties in analyzing mesoderm induction, the chick is ideally suited to studies on the specification of distinct types of axial mesoderm cells, including notochord and prechordal mesoderm (Jurand, 1962; Psychoyos and Stern, 1996; Foley et al., 1997; Vesque et al., 2000). The cells that will give rise to axial mesoderm structures lie within Hensen's node and anterior primitive streak and their emergence requires precise spatial and temporal control (Grabowski, C. T., 1956; Schoenwolf et al., 1992; Psychoyos and Stern, 1996; Zamir et al., 2006). A head process composed of axial mesoderm precursors extends anteriorly as Hensen's node and primitive streak move posteriorly (Figure 1.9). Post- extension of the axial mesoderm at HH stage 6, the rod-like structure of axial mesoderm composed of the anterior prechordal mesoderm (PM) and the posterior notochord (NC) can be seen underlying the neuroectoderm (Figure 1.10) (Psychoyos and Stern, 1996; Foley et al., 1997; Joubin and Stern, 1999). I will refer to the migrating axial mesoderm cells as 'head process mesoderm' and once the cell populations have fully extended and resolved they will be referred to as PM and NC.

Early studies showed that the Nodal-like signal, activin, has the ability to induce chick axial mesoderm (Mitrani et al., 1990; Ziv et al., 1992). Activin is transcribed in the chick embryo prior to and post primitive streak formation and induces axial structures in isolated epiblasts cultured in vitro (Mitrani et al., 1990; Mitrani and Shimoni, 1990). Activin induces the axial mesoderm markers, *Gsc* and *Not-1*

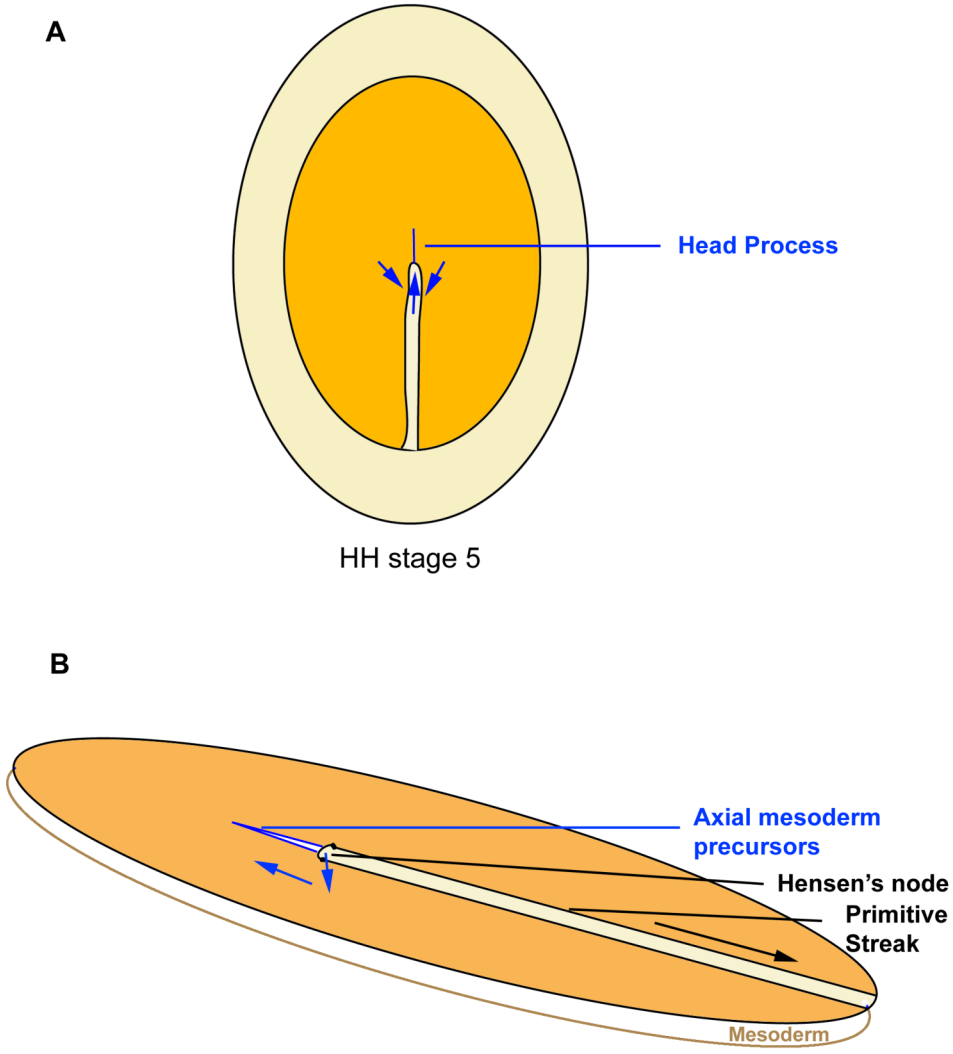

Figure 1.9 Formation of the axial mesoderm.

A Axial mesoderm precursors move into Hensen's node and migrate anteriorly (indicated by blue arrows) (Psychoyos and Stern, 1996). Head process consisting of axial mesoderm precursors emerges and extends away from the primitive streak.

B As the axial mesoderm cells migrate anteriorly away from the primitive streak and Hensen's node, primitive streak and Hensen's Node begin to regress posteriorly (indicated by black arrow).

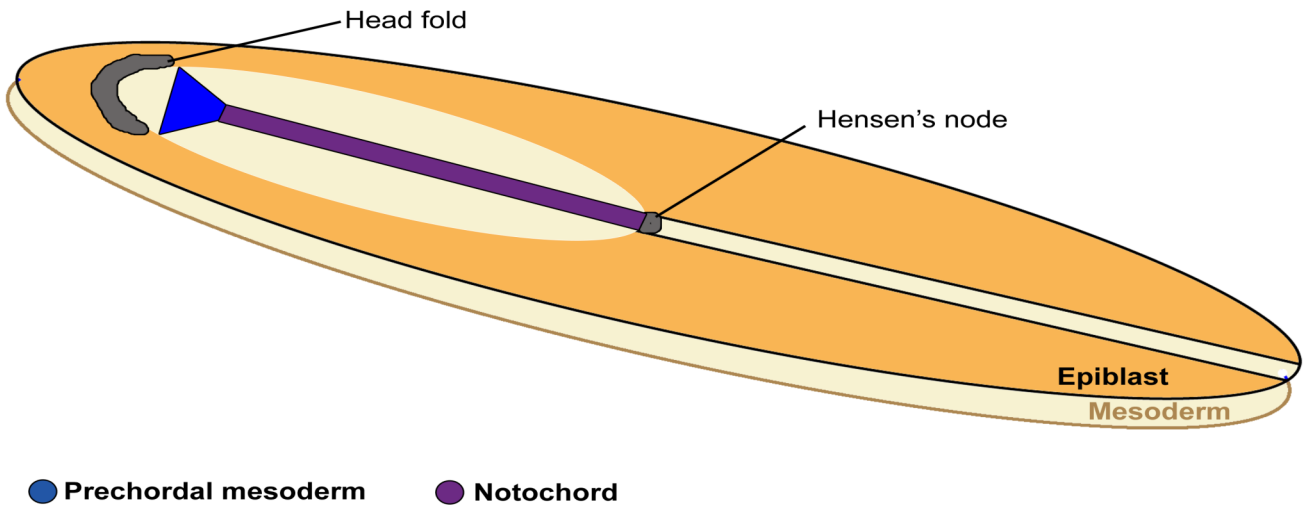

Figure 1.10 Prechordal mesoderm and notochord at HH stage 6.

Schematic shows that at HH stage 6 axial mesoderm can be seen composed of the anterioir prechordal mesoderm and the posterior notochord. The axis will continue to extend posteriorly beyond HH stage 6 but the components of the axial mesoderm have been laid down.

(a NC marker) at higher concentrations than are required to induce other types of mesoderm (Stern et al., 1995). The activin receptors ActR II-A and B are also expressed in the chick primitive streak and are capable of inducing axial structures if injected into Xenopus embryos, further supporting a role for Nodal-like signals in axial mesoderm development in the chick (Stern et al, 1995). Also, as mentioned earlier, an ectopic source of Cripto, which is a co-receptor in Nodal signalling pathway is able to alter the fate of notochord to prechordal mesoderm (Chu et al., 2005). Thus, Activin and Nodal signalling is required for prechordal mesoderm and notochord specification.

1.5.2 Prechordal mesoderm and notochord commitment

An unknown question, however, in any species, remains that of when prechordal mesoderm and notochord actually commit to each fate. Such studies have been addressed primarily in chick, where they suggest a late-specification. Fate mapping studies reveal that labeled cells move into the node from HH stage 3 and transiently acquire PM/NC properties whilst in the node but then lose those properties as they migrate out, suggesting that the cells in the head process are not committed and can change their character (Joubin and Stern, 1999). This idea that these cells are not fully committed in Hensen's node is supported by experiments carried out by Foley et al., 1997; Vesque et al., 2000. DiI labelling experiments revealed that head process that initially migrates out of Hensen's node at HH stage4+ consist of intermingled cells that at a later stage will contribute to both PM and NC (Foley et al., 1997). Additionally, early head process at HH stage

4+ has a different neural inducing potential to late head process at stage 5. Early head process at HH stage 4+ upon grafting into the extraembryonic region of another embryo, confers neural fate onto the host cells (Foley et al., 1997). However, anterior head process isolated at HH stage 5 is specific in its neural inducing properties (Foley et al., 1997). Transplantation experiments show that explants of anterior head process only confer forebrain character to prospective neural tissue alone and not other kinds of tissues such as the extraembryonic tissue (Foley et al., 1997). This shows that head process mesoderm extending out of Hensen's node at stage 4+ does not have set properties and must be specified.

Additionally, at HH stages 4+ and 5 head process mesoderm shares characteristics of both PM and NC, including expression of *Gsc* and Chordin but again their full character is yet to be determined (Vesque et al., 2000). These studies suggested that, in chick as head process cells migrate away from the node they are exposed to TGFβ signals from the anterior endoderm, as a result of which PM character is promoted and NC character is suppressed. These studies suggest that sustained TGFβ signalling is essential to maintain PM and suppress NC identity. However, the factors that may mediate this, and set PM fate, are unclear.

1.6 T-box genes

T-box genes are a family of transcription factors characterised by a conserved DNA binding domain called the T-box (Figure 1.11). The first T-box gene to be identified is called Brachyury or *T*. Mice which

Figure 1.11 Conserved T domain of the T-box gene family.

Members of the T-box gene family are characterised by the presence of the T domain, which is conserved across all species. T domain binds DNA and is additionally involved in protein dimerisation. A domain at the N terminus is thought to bind cofactors and residues at the C terminus control transcriptional activation or repression. (Adapted from Minguillon and Logan, 2003)

have a naturally occurring mutation in Brachyury have a short tail phenotype (Dobrovolskaia-Zavadskaia, N., 1927 as cited in Schulte-Merker et al., 1994). Brachyury binds the T domain as a dimer, each monomer occupies a T-half site (Papapetrou et al., 1997). T-box genes are expressed widely during early embryonic development and have been linked to many developmental disorders. Amongst many roles of T-box genes, a growing body of work suggests a vital role of T-box genes in mesoderm function. The role of a few key T-box genes is discussed below.

1.6.1 Role of T-box genes in mesoderm development

As mentioned earlier, Brachyury plays a crucial role in mesoderm development. Mutation in Brachyury leads to a defective primitive streak and an absence of the posterior notochord (Gluecksohn-Schoenheimer, 1938). Notochord precursors fail to migrate away due to defects in cell adhesion (Yanagisawa et al., 1981).

As mentioned earlier, a similar phenotype has been reported when the brachyury homologue Xbra mRNA is blocked in Xenopus (Smith et al., 1991). Further it was found by Xbra overexpression experiments that Xbra is required for the differentiation and maintenance of the differentiated state of notochord cells (Cunliffe and Smith, 1992). The role of Brachyury is also conserved in zebrafish (Halpern et al., 1993). This shows that T-box genes are evolutionarily conserved and are important for mesoderm formation and subsequent morphogenesis.

Brachyury acts cell autonomously as a transcriptional activator and several studies have been conducted to find its downstream targets (Kispert et al., 1995). Embryonic fibroblast growth factor eFGF has been identified as one target (Casey et al., 1998). A study by Tada et al. (1998) identified, a second target, showing that, homeobox gene Bix 1 was induced by Xbra in the mesoderm and specifies ventral mesoderm. Thus Brachyury is capable of specifying mesodermal character.

Since the characterisation of Xbra, it has become clear that a cascade of T-box genes operates subsequently and temporally. The T-box gene Eomesodermin, is expressed one to two hours before Xbra. It is capable of initiating mesoderm induction and is one of the first mesoderm inducing genes to be expressed in the early gastrula. Ectopic expression of Eomesodermin leads to activation of other mesodermal genes such as Gsc, Xwnt8 and Xbra (Ryan et al., 1996). Culture studies suggest that it may act in a dose-dependant way to promote notochord and muscle fate. Impaired function of the gene leads to gastrulation arrest and a loss of mesoderm gene activation.

Prior to this, T-box transcription factor Veg T, is expressed in the vegetal pole of the Xenopus embryo. It acts on the neighbouring cells influencing their fate and establishing three primary germ layers (Stennard et al., 1996, Zhang et al., 1998). It can induce Eomesodermin and vice versa, as well as other mesodermal genes including Xbra and Xwnt8 (Stennard et al., 1996). Depletion of VegT leads to loss of key signalling molecules required for mesoderm induction and thus the loss of mesoderm itself (Kofron et al., 1999).

In addition to playing crucial roles in mesoderm induction and axial mesoderm development, T-box genes have been shown to play an important role in paraxial mesoderm development. Paraxial mesoderm gives rise to the vertebral column and the muscles of the body. At HH stage 6 it can be seen unsegmented either side of the neural tube but by H stage 7 it has begun segmentation into somites by the process of epithelialisation. Tbx6 is downstream of Eomesodermin and Brachyury and is expressed in the primitive streak, paraxial mesoderm, presomitic mesoderm and the tail bud in the mouse (Chapman et al., 1996). Its expression pattern has also been studied in Xenopus and zebrafish and is broadly similar to that in mouse (Uchiyama et al., 2001; Hug et al., 1997).

Tbx6 expression in the presomitic mesoderm highlights its role as a key gene involved in the correct specification and segmentation of somites. Studies of mutant Tbx6 mouse embryos have revealed that some somites form in an irregular fashion indicating that Tbx6 is required for correct somitic segmentation (Chapman and Papaioannou, 1998). Tbx6 activates the transcription factor *Mesp2,* which is responsible for determining the segment boundary of somites (Yasuhiko et al., 2006). Its crucial role in somite patterning is further demonstrated by its naturally occurring mutation, called Rib-vertebrae, presenting a severe phenotype of vertebral malformations. The cause has been described as defective anterior-posterior (AP) patterning, size and morphology of somites (Watabe-Rudolph et al., 2002).

Similarly, Tbx18 is also involved in somite development. It is expressed in the paraxial mesoderm and specifically in the anterior

half of the developing and the newly formed somites (Kraus et al., 2001; Haenig and Kispert, 2004). In the mutant Tbx18 mouse embryo, somites develop but the posterior half of the somite expands and invades the anterior territory (Bussen et al., 2004). Overexpression of Tbx18 leads to thinning of the posterior portion of the somites. This raises the possibility that Tbx18 is required for the anterior-posterior somite boundary, rather than somite specification (Takahashi et al., 2000). Subsequent studies support this idea showing that Tbx18 may control the integrity of the somite compartments by regulating the adhesion properties of the cells, such that loss or misexpression of Tbx18 leads to loss or gain of new adhesion properties, disrupting the sharp boundary set up between the distinct compartments (Bussen et al., 2004; Farin et al., 2007).

During inner ear development Tbx18 is again crucial for boundary formation between otic fibrocytes and otic capsule (Trowe et al., 2008). Otic fibrocytes fail to undergo a mesenchymal to epithelial transition to form basal cells that form an epithelium separating the different compartments of the cochlea, specifically the stria vascularis in Tbx18 deficient mice (Trowe et al., 2008). Again the authors propose that the role of Tbx18 is either to govern a repulsive signal or to govern the adhesion properties of the cells.

Tbx18 is also required to specify ureteral mesenchyme whose proliferation and differentiation in smooth muscle cells is essential for the development of a functional ureter (Airik et al., 2006). In the absence of Tbx18, prospective ureteral mesenchymal cells lose their ability to aggregate around the ureter stalk but disperse to mix with other kidney tissues. Tbx18+ cells are thought to promote preferential

adhesion between themselves and the ureteric epithelium and are specified to remain ureteric and not differentiate into other tissues (Airik et al., 2006).

Finally, Tbx18 along with other T-box genes, including Tbx 1, 2, 3, 5 and 20 plays a role in the cardiac specification as well (Greulich et al., 2011). They are expressed in different progenitor pools and act in complex regulatory networks to pattern the developing heart, although the mechanisms are not clear. Together, however, these studies indicate that a common role for Tbx18 might be in regulation of adhesive properties and boundary formation.

Due to their wide variety of roles in mesoderm development, T-box genes are good candidates for playing a role in axial mesoderm development. In this study, I particularly wished to explore the possibility that a T-box gene may play a role in PM development, since this developmental domain of the axial mesoderm is currently poorly understood.

1.7 Thesis aims

One of the main reasons that studies into prechordal mesoderm development have been hampered is due to a lack of an exclusive marker for the prechordal mesoderm. Thus, my first objective was to identify a marker expressed only in the prechordal mesoderm. Gain and loss of function studies of such a factor would allow me to study the development of prechordal mesoderm specifically. As discussed above, I particularly focused on the T-box gene family, as they are

strong candidates, playing a variety of roles within the developing mesoderm.

Secondly, I aimed to study the role of Nodal signalling in prechordal mesoderm development. As described above, Nodal signalling has already been shown to play a crucial role in axial mesoderm development. However, most of these studies focus on its early role in axial mesoderm development i.e. its role in their establishment over the period HH stage 3-5 in the chick. It is unknown if prechordal mesoderm specification and/or maintenance is dependant on Nodal signalling post extension i.e. over the period HH stage 6-13. I hypothesised that Nodal signalling is required for prechordal mesoderm specification over this time period.

Thirdly, I aimed to understand how Nodal signalling is regulated in the axial mesoderm of the chick embryo so that prechordal mesoderm forms anteriorly and notochord posteriorly. I wished to examine how the extent of the prechordal mesoderm is determined and the boundary between prechordal mesoderm and notochord defined.

CHAPTER 2

Materials and Methods

2.1 Molecular Biology methods for DNA preparation

2.1.1 Bacterial cell culture and DNA extraction

DHα5 competent bacteria (Invitrogen) were transformed with plasmid and then grown on static Luria Bertani (LB)-Agar plates containing the appropriate antibiotic at 37 ^{o}C. A single colony of cells was grown first in LB broth and antibiotic (ampicillin, 50μg/ml) on a shaker at 225rpm for 8 hours at 37^{o}C and then 2ml of the culture was transferred to 200ml LB broth containing antibiotic and cultured overnight on the shaker at 225rpm at 37^{o}C. The next day the culture was spun at 6000g for 15 minutes at 4^{o}C using Beckman centrifuge (Avanti centrifuge J-25). DNA was extracted from the pellet and purified using HiSpeed Plasmid Maxi kit (QIAGEN) according to manufacturers instructions.

2.1.2 siRNA vector synthesis

The siRNA vectors were made as decribed by Das et al, 2006. Tbx18 siRNA vectors were targeted to the following sequences:
A; AAGCTTGACACTCTCATCTTCT,
B; AAGGAGTGCACTTACTTAGCAG,
C; AAGCTTTGGTGGAGTCTTACGC and chosen using the design tool at https://www.genscript.com/ssl-bin/app/rnai. The vectors used a chicken specific U6 promoter, which drove the expression of a modified chicken microRNA operon (Figure 4.10). The three vectors were transfected together or co-electroporated to increase knockdown efficiency as described in 2.4.2 and 2.4.3.

2.2 Analytical molecular biology techniques

2.2.1 RNA extraction and cDNA synthesis

Total RNA was extracted from whole chick embryos or heads of chick embryos using the RNAeasy kit (Stratagene). The concentration of purified RNA was measured on NanoDrop ND100 (Labtech). cDNA was synthesized by reverse transcribing 2µg of purified RNA using SuperScript III Reverse Transcriptase (Invitrogen) and random primers (Promega).

2.2.2 Reverse transcription polymerase chain reaction (RT-PCR)

A typical RT-PCR reaction was set up consisting of H_2O (Sigma), 1x PCR Buffer (Promega), 1mM $MgCl_2$ (Sigma Aldrich), 200µM dNTPs (Invitrogen), 0.5µl cDNA template, 200nmol of forward primer, 200nmol of reverse primer and 7.5units of Taq polymerase per 25µl (Sigma Aldrich). The PCR reaction was started with an initial denaturation step at 95^{o}C for 3 minutes, 30 cycles for each gene consisting of denaturation step at 95^{o}C for 1 minute, primer annealing at individual temperature for one minute and product extension at 72^{o}C for 1 minute. A final elongation step at 72^{o}C for 8 minutes ended the reaction. Table 2.1 gives a summary of primers used at individual annealing temperature. Nucleic acids were detected by mixing with a loading buffer and running on 1%agarose gel

Table 2.1 Summary of RT-PCR primers

Gene	primer-FWD	primer-Rev	Annealing temperature
cβActin	GATGGTCAGGTCATCACCATTG	CATCGTACTCCTGCTTGCTGATC	56
cTbx2	GGGAAGGCCGACCCGGAGAT	CGGGTTTGCAGGGCTCCTCG	59.3
cTbx3	CTTCGCGCAGTCCTCCTGCC	TCGGTCTGGACCGTGAGGGG	59.3
cTbx18	CTGACTCCCCGGTACCGCCT	GCATCCCCGTCATTGCCGCT	57.8
cEomesodermin	CACTGGCGCTTCCAAGGGGG	GCACGCTGTATCGGGCACCA	57.8
cTbx6	GTGGCTCTCTCGGCTGTGCG	CTGCCAGGAGCGGGGGAATC	61

containing ethidium bromide in 1xTAE buffer. 1kb (Promega) or 500bp (New England Biolabs) DNA ladders were used to confirm bands were of the expected size.

2.2.3 Protein analysis

Sample preparation

Nodal proteins were obtained either from cell supernatants (see 2.3.2) or as commercial recombinant proteins (R&D systems). Proteins were denatured and reduced in LDS sample buffer (NuPAGE – Invitrogen) containing 1x reducing agent at 70 ^{o}C for 10 minutes.

SDS PAGE

Samples were immediately loaded on NuPAGE 4-12% Bis Tris gradient precast gels (Invitrogen) and run at 160V (constant voltage) in MOPS buffer (Invitrogen) using the X-Cell Novex MiniCell system (Invitrogen). A BenchMark Prestained Protein Ladder (Invitrogen) was run along side the samples to confirm the band sizes.

Western Blotting

Proteins were transferred onto Hybond-C Extra nitrocellulose membrane (Amersham Biosciences) according to standard techniques. Briefly transfer was conducted at 90V for 1.5 hours using Biorad wet transfer system. After blotting the membrane was blocked in PBS containing 0.1%Tween20 (Sigma Aldrich) and 5% milk powder (Marvel) for one hour at room temperature. Membrane was then probed with anti-Nodal rabbit polyclonal (1:4000, gift from M.Shen) in blocking solution overnight at 4^{o}C. Membrane was then washed in PBS containing 0.1%Tween20, anti-Rabbit HRP (1:6000,

Jackson labs) was applied in blocking solution for 45 minutes at room temperature. Finally proteins were detected using ECL Plus Western Blotting Detection System (GE Healthcare).

2.3 In vitro manipulations

2.3.1 Purification of proteins

ProNodal and Cerberus Short proteins were produced using 293T cells. Cells were grown in DMEM containing 10% of fetal calf serum and transfected with mFlagNodal-H246L for ProNodal (Constam and Robertson, 1999), pCS2-cer-S for Cerberus Short (Piccolo et al., 1999) or empty pCS2 vector (gift from Daniel Constam) for controls using lipofectamine (GIBCO) in OPTIMEM (GIBCO) without serum. Medium was replaced after 5 hours and cells were cultured for a further 72 hours. Supernatants were collected and concentrated 20 fold using 10kD cut off Centri-plus columns (Millipore) then diluted in explant culture medium to the required concentration.

2.3.2 Cell Pellets

293T cells were transfected as above with mFlagNodal-H246L for ProNodal or empty pCS2 vector. Transfected cells were cultured for 24 hours and then transferred to DMEM containing 10% fetal calf serum for a further 24 hours. Cell pellets were then generated in overnight hanging drop cultures by trypsinising and plating 20ul drops at 100K cells per ml.

2.3.3 Chick embryo dissection

All embryos were accessed *in ovo* by making a small window in the eggshell and removing the overlying membranes. Embryos were then harvested from the yolk, staged and dissected in cold Leibowitz's L15-Air medium (GIBCO).

2.3.4 Explant culture

Explants of the PM and NC were prepared by dissecting the head and trunk region anterior to Hensen's node and primitive streak of stage 6 embryos using sharp tungsten needles. Mesoderm was isolated from the neurectoderm using Dispase (1mg/ml) and the axial mesoderm, identifiable by its morphology was dissected. It was then further sub dissected into the prechordal mesoderm and the notochord. Explants were cultured in collagen beds as described by Dale et al., 1999. Proteins used are described in Table 2.2.

Table 2.2 Proteins used in explant cultures

Protein	Concentration	Source
ProNodal	0.25x, 1x and 3x	See 2.3.1
Mature Nodal	50ng/ml, 100ng/ml and 250ng/ml	R&D systems
Cerberus Short	0.25x, 0.5x and 1x	See 2.3.1
ALK inhibitor (SB431542)	25µM	Sigma Aldrich
FgfR3-fc	600ng/ml	R&D systems
All-trans retinoic acid	10^{-6}M	Sigma

2.3.5 *In vitro* lipofection

The following solutions were prepared:
Solution 1: 0.5μg of construct in 50μl of OPTIMEM medium
Solution 2: 5μl of lipofectamine (Invitrogen) in OPTIMEM medium
Solutions were combined and incubated for 30 minutes at room temperature. The DNA and lipofectamine complex medium was then added to explants for 2 hours. Explants were then mounted on collagen beds and cultured in fresh explant medium for a further 13 hours before fixation and preparation for analysis via immunohistochemistry and in situ hybridisation. These studies have not been included due to low efficiency of transfections (9% efficiency) and variable viability.

2.4 In vivo manipulations

2.4.1 Cell pellet implantation

A small window was made into the eggshell and membranes overlying the embryo were removed. To visualise the embryo blue food dye (Dr Oetker, Tesco) was mixed with L15-Air medium (1:10) and injected under the embryo. In order to access the axial mesoderm, a small incision was made next to the neural tube of a HH stage 6 or 10 chick embryo. Cell pellets were then implanted into the hole and placed next to the notochord by applying gentle pressure.

After implantation the eggs were sealed and incubated for 24 hours. They were then dissected in cold L15-Air medium, fixed and processed to be analysed by immunohistochemistry and in situ hybridisation.

2.4.2 *In ovo* lipofection

The DNA and lipofectamine complex (described in 2.3.5) was also applied directly onto stage 4 embryos prepared by first removing the vitelline membrane above Hensen's Node. The eggs were sealed and incubated for 24 hours. They were then dissected in cold L15-Air medium, fixed and processed to be analysed by immunohistochemistry and in situ hybridisation. These studies have not been included due to low efficiency of transfections. Prechordal mesoderm and notochord were targeted using *in ovo* electroporation instead (see 2.4.3), which was more efficient.

2.4.3 *In ovo* electroporation

HH stage 3-10 embryos were accessed by making a small window into the eggshell. Membranes overlying the embryo were removed and the embryo was visualised by injecting blue food dye L15-Air medium mixture under the embryo. DNA was injected in Hensen's node, prechordal mesoderm or notochord as described in Table 2.3. pCAGGS-cTbx18 (gift from Cheryl Tickle) was co electroporated with pCAGGS-RFP (50ng/µl and 30ng/µl respectively). pCAGGS vector and pCAGGS-RFP used as controls at the same concentration.

Tbx18 SiRNA (see 2.1.2) and empty control vector (gift from Stuart Wilson) were used at a final concentration of 50 ng/µl. Electrodes were then placed as described in Table 2.3, 4mm apart with cathode in contact with the albumen and the anode piercing the yolk directly underneath the cathode. Current was applied as described in Table 2.3 (4 – 6 x 50ms pulses) across the electrodes using TSS20 Ovodyne electroporator (Intracel). Eggs were then sealed and incubated for 24 hours, dissected in cold L15-Air medium, fixed and processed to be analysed by immunohistochemistry and in situ hybridisation.

Table 2.3 Summary of different in ovo electroporation techniques tried to target axial mesoderm

Electrode placement	**Stage**	**DNA injected**	**Voltage**	**Number electroporated**	**Number survived**	**Successful axial mesoderm electroporation**
Parallel to the axis	4-10	Hensen's node and neural groove	30V	27	11	0
Right angles to the axis	4-6	Hensen's node	40V	200	34	4
Right angles to the axis	4-5	Hensen's node	60V	76	24	0
Right angles to the axis	8-10	PM	40V	55	31	0
Right angles to the axis	8-10	PM	60V	12	8	0
Right angles to the axis	8-10	NC	40V	73	42	1
Same plane as the axis	3-4	Hensen's node	10V	180	43	6

2.5 Immunohistochemistry

Immunohistochemistry analysis was performed according to established techniques (Placzek et al., 1993). Embryos and explants were fixed at 4°C in 4% Paraformaldehyde (0.12M Phosphate Buffer) for two hours and then transferred to 30% sucrose (0.1M Phosphate buffer). The tissue was then cryosectioned (15μm thickness) and collected onto Superfrost Plus slides (Thermo Scientific). Tissue was pre-treated in a blocking solution of phosphate buffered saline (PBS) containing 1% heat inactivated goat serum (HINGS) and 0.1% Triton X-100 for one hour. Primary antibodies were applied in blocking solution overnight at 4°C. Tissue was washed in PBS and then secondary antibody in blocking solution was applied for one hour at room temperature. Finally slides were mounted using Vectashield mounting medium containing 4',6-diamidino-2-phenylindole (DAPI) (Vector laboratories) and glass coverslips.

Table 2.4 Primary and secondary antibodies used to detect proteins

Antibody	**Concentration**	**Source**
Primary Antibodies		
68.5E1 anti-Shh	1:50	Johan Ericson
Anti-3B9	1:50	DSHB
Anti-Phosphorylated Smad 1/5/8	1:500	Cell signalling technologies
Anti-RFP	1:1000	Chemicon
Secondary conjugates		
Cy3	1:200	Jackson labs

Alexa 594	1:500	Molecular Probes
Alex 488	1:500	Molecular Probes

2.6 *In situ* hybridisation

In situ hybridisation analysis was performed according to established techniques (Vesque et al., 2000). Slides were post-fixed for ten minutes in 4%PFA and then incubated with acetylation mix of triethanolamine (Fluka) and acetic anhydride (Sigma). They were then incubated in prehybridisation solution for a minimum of two hours at 68^{o}C prior to incubation in a hybrisation solution containing RNA probe overnight. Slides were washed in SSC/formamide solutions before blocking with 10%HINGS in TBST. They were incubated in blocking solution containing alkaline phosphotase conjugated anti-DIG antibody (ROCHE) for 90 minutes. Slides were developed in NTMT containing NBT and BCIP (both from ROCHE). The following DNA templates were used to synthesise digoxygenin labeled antisense RNA probes using conventional methods.

Table 2.5 Plasmid DNA used to synthesise RNA probes

Plasmid	**Linearised with**	**Transcribed with**	**Source**
Pcvhh-1 (Shh)	Sal1 (Promega)	SP6 (NEB)	Thierry Lints
cNR1(Nodal)	Not1 (Promega)	T7 (NEB)	Clifford Tabin
pcGsc	EcoR1 (Promega)	SP6 (NEB)	Clifford Hume
pMT23-Chordin	EcoR1 (Promega)	SP6 (NEB)	Kevin Lee

pcBMP7	Xho1 (Promega)	T3 (NEB)	Brian Houston
cTbx18	BamH1 (Fermentas TS)	T7 (NEB)	Malcolm Logan

NEB = New England Biolabs, Fermentas TS = Fermentas Thermo Scientific

2.7 Microscopy and Image analysis

Brightfield and fluorescent images were taken using Olympus BX60 running Spot software (Diagnostic Instruments Inc) and Zeiss Apotome microscope with Axiovision software (Zeiss). Photoshop CS3 (Adobe) and ImageJ (NIH, http:rsb.info.nih.gov/ij) were used to process images. Schematics were drawn using Illustrator CS5 (Adobe).

2.8 Statistical analysis

Percentage marker expression was calculated by measuring the area of positive expression and comparing that to the total area of the PM explant (Figure 5.8 B). In NC explants however, NC length was measured, rather than area, as contamination can occur from the endoderm below, and the paraxial mesoderm lying parallel to, the NC, whereas it can be cleanly isolated anteriorly and posteriorly. So, the length of the NC with positive marker expression was measured and then compared to total length of the explant (Figure 5.4 B). The values shown in figures represent the mean percentage calculated by analysing the number of explants anlaysed given in brackets.

Prism 5.03 software (GraphPad Software Inc.) was used to perform all statistical analyses. P-values were determined using two-tailed students t test.

CHAPTER 3

Tbx18: a novel and specific marker of prechordal mesoderm

3.1 Introduction

Chick embryo development is studied with reference to morphology and according to the Hamburger-Hamilton (HH) stageing system (Hamburger and Halmilton, 1951). Axial mesoderm development begins around 18-24 hours of development of the chick embryo. Head process mesoderm consisting of axial mesoderm cells can be clearly observed at stage 5 migrating anteriorly away from Hensen's node (Figure 3.1 A, A* and A**) (Hamburger and Halmilton, 1951; Kochav and Eyal-Giladi, 1971). A fully extended axial mesoderm can be seen from HH stage 6 onwards (Figure 3.1 B – E).

As described in the main Introduction (Section 1.5.1) the anterior tip of the axial mesoderm, known as the prechordal mesoderm (PM) has a broader fan-shaped morphology (Figure 3.1 B-E). PM underlies neuroectoderm that will give rise to the forebrain. Transverse sections through the PM over HH stage 6-13 reveal it to be broad and flat (Figure 3.1 B*-E*).

Posterior to the PM is the long rod-like notochord (NC). The NC is positioned underneath the prospective midbrain, hindbrain and the spinal cord and is surrounded by paraxial mesoderm on either side (Figure 3.1 B-E). Compared to the PM, NC has a round morphology (Figure 3.1 B**-E**).

As outlined in the main Introduction, the events that lead to the development of PM or NC have been studied in many vertebrates. Evidence suggests that in the chick, Nodal-like morphogens operate prior to gastrulation begin to specify PM or NC (Mitrani et al., 1990;

Figure 3.1 Morphology of head process mesoderm and axial mesoderm in the chick embryo.

A-E
Schematic of whole chick embryos HH stages 5-13. By stage 5 the head process mesoderm has begun extending anteriorly away from Hensen's node (HN). At stages 6-13 fully extended PM and NC can be seen at the midline of the embryo.

A*
Transverse sections indicated by line marked A* shows anterior head process mesoderm lying underneath the neurectoderm.

A**
Transverse sections indicated by line marked A** shows posterior head process mesoderm lying underneath the neurectoderm.

B*-E*
Transverse sections as indicated by lines marked B*-E* in B-E reveal a flat PM underlying the neurectoderm (forebrain).

B-E****
Transverse sections as indicated by lines marked B**-E** in B-E show a round NC underlying the neurectoderm (spinal cord).

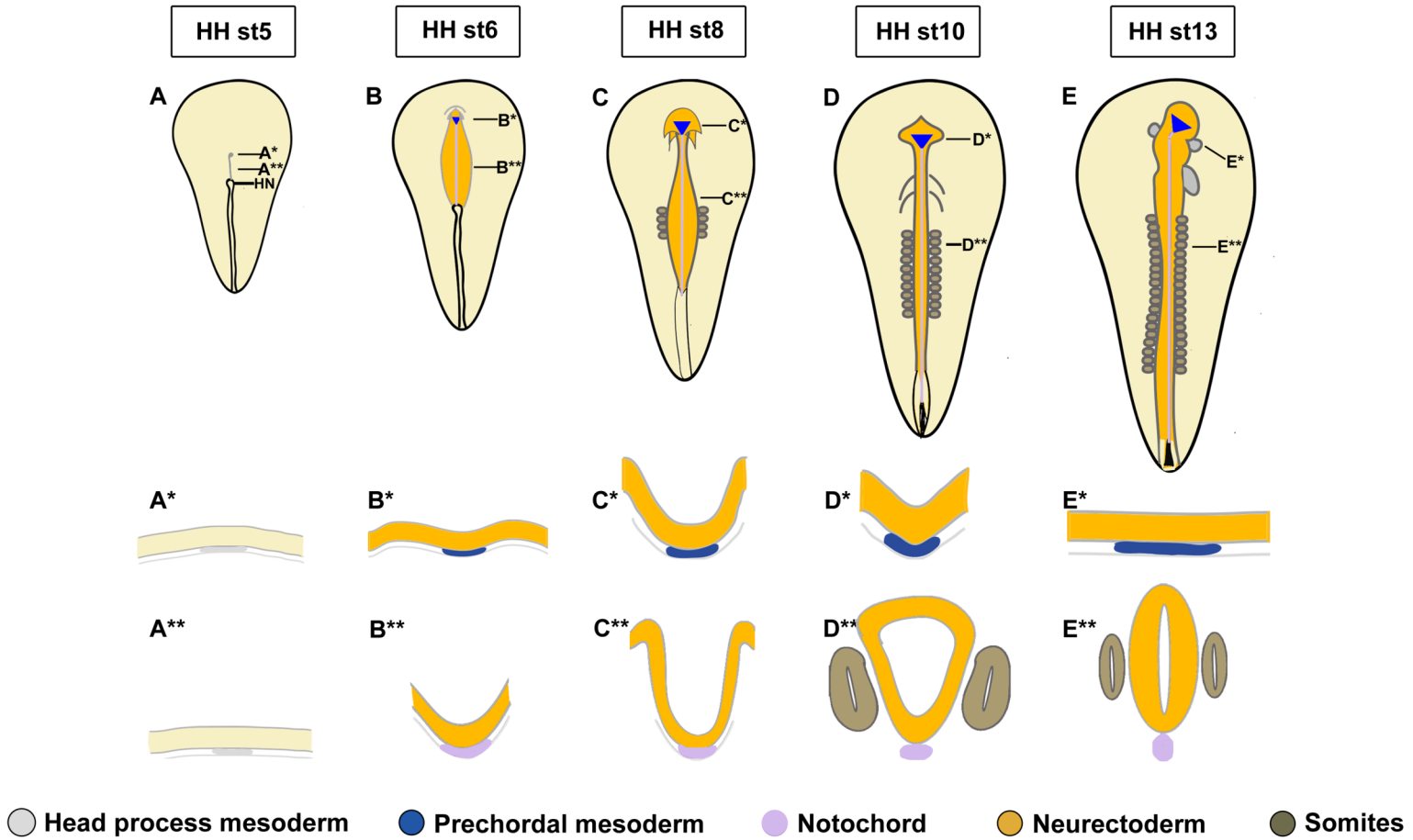
HH st5
HH st6
HH st8
HH st10
HH st13
A
B
C
D
E
A*
A**
HN
B*
B**
C*
C**
D*
D**
E*
E**
A*
B*
C*
D*
E*
A**
B**
C**
D**
E**
Head process mesoderm
Prechordal mesoderm
Notochord
Neurectoderm
Somites

Mitrani and Shimoni, 1990; Ziv et al., 1992; Stern et al, 1995). The mechanism of exact separation of PM and NC cells into their distinct identities is unclear (See section 1.5.2). However, *in vitro* observations show that head process mesoderm is composed either of a common progenitor that co-expresses notochord and prechordal mesoderm markers or cells are arranged in a mixed 'salt and pepper' arrangement (Vesque et al., 2000 and Foley et al., 1997). These studies suggest that PM and NC begin to resolve when the tip of head process encounters signals from the anterior endoderm. Thus, culture of early NC with anterior endoderm leads to the downregulation of NC markers and the upregulation of the PM marker *Gsc* (Vesque et al., 2000). Regardless of which of these mechanisms is true, it is clear that notochord and prechordal mesoderm are not fully resolved in head process mesoderm as mixed expression and/or mixed cells are readily detected (Foley et al., 1997; Vesque et al., 2000; Chapter 3).

One reason that studies into PM versus NC specification have been hampered is that few definite markers exist for either one and particularly for PM. To further understand the molecular events that govern the specification of PM and NC, I first aimed to establish a profile of markers of the differentiated PM and NC and in particular identify a PM-specific marker.

3.2 Results

To begin to characterise the axial mesoderm I analysed the expression profiles of various signalling molecules and transcription factors. I began this analysis at HH stage 5, a time when axial

mesoderm is migrating anteriorly as head process mesoderm I ended the analysis at HH st13, the time when PM begins to regress.

3.2.1 *Gsc* and *BMP7* mark the PM

I first confirmed the expression profiles of Goosecoid (*Gsc)* and BMP7, both previously described to mark the PM in the chick embryo (Izpisúa-Belmonte et al., 1993; Dale et al., 1999; Vesque et al., 2000). Consistent with previous studies, I find that the transcription factor *Gsc* and the signalling ligand *BMP7* are expressed in head process mesoderm and the PM (Figure 3.2 and 3.3).

Transverse sections through the chick PM show that *Gsc* is expressed at stage 5 in the anterior and posterior head process mesoderm (Figure 3.2 A and F). Additionally it is also detected in the PM at HH stage 6 (Figure 3.2 B) and then in both the PM and the overlying floor plate at HH stages 8 and 10 (Figure 3.2 C and D). I do not detect any *Gsc* expression in the PM at HH stage 13 (Figure 3.2 E). I did not detect *Gsc* at any of the stages analysed in the NC (Figure 3.2 G-J).

BMP7 has a similar expression as *Gsc* in the axial mesoderm. It is first detected at stage 5 in head process mesoderm and then in the PM from stage 6 (Figure 3.3 A-D). By stage 8 its expression is detected in both the PM and the overlying floor plate (Figure 3.3 C-D). Expression is stronger at earlier stages when compared with later

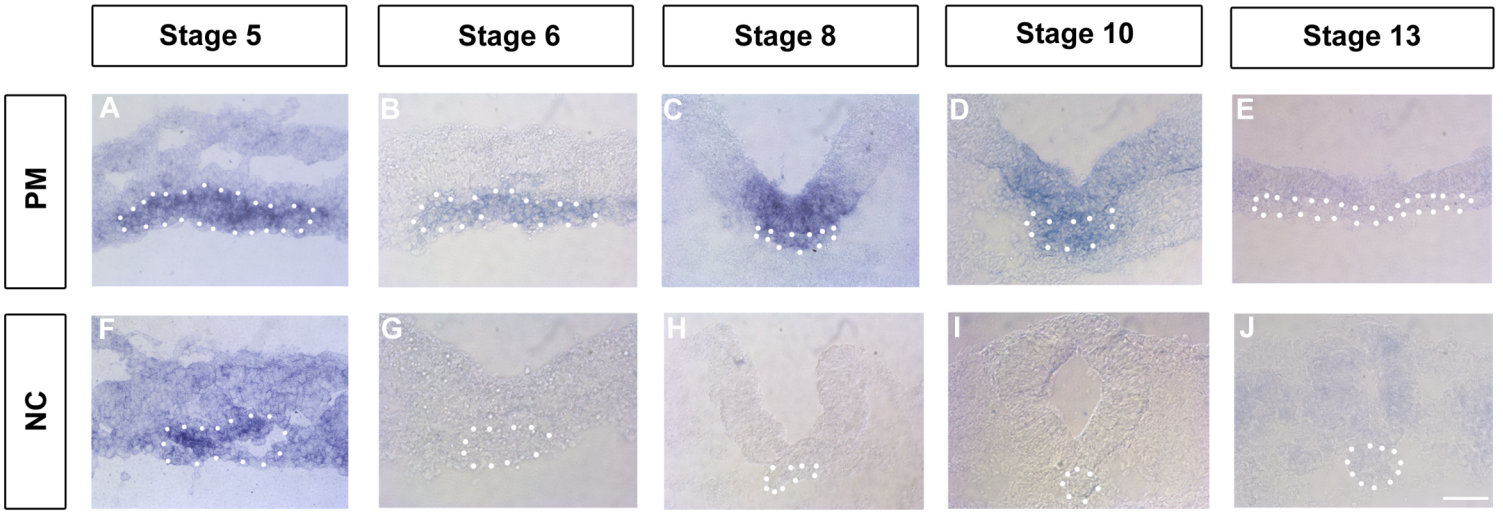

Figure 3.2 Expression of *Gsc* at HH stage 5 – 13

A-E
Transverse sections show that *Gsc* is expressed in the anterior head process mesoderm (outlined by dotted lines) at stage 5 and in the PM (outlined by dotted lines) at HH stages 6-10. At stage 8-10 its expression can also be detected in the overlying neuroectoderm. At stage 13 *Gsc* is not expressed in the PM or in the neurectoderm.

F- J
Gsc is expressed in the posterior head process mesoderm (outlined by dotted lines) at stage 5. Transverse sections through the trunk (as described in Figure 1) show that *Gsc* is absent from the NC from stage 6-13 (outlined by dotted lines). Scale bar = 50 µm

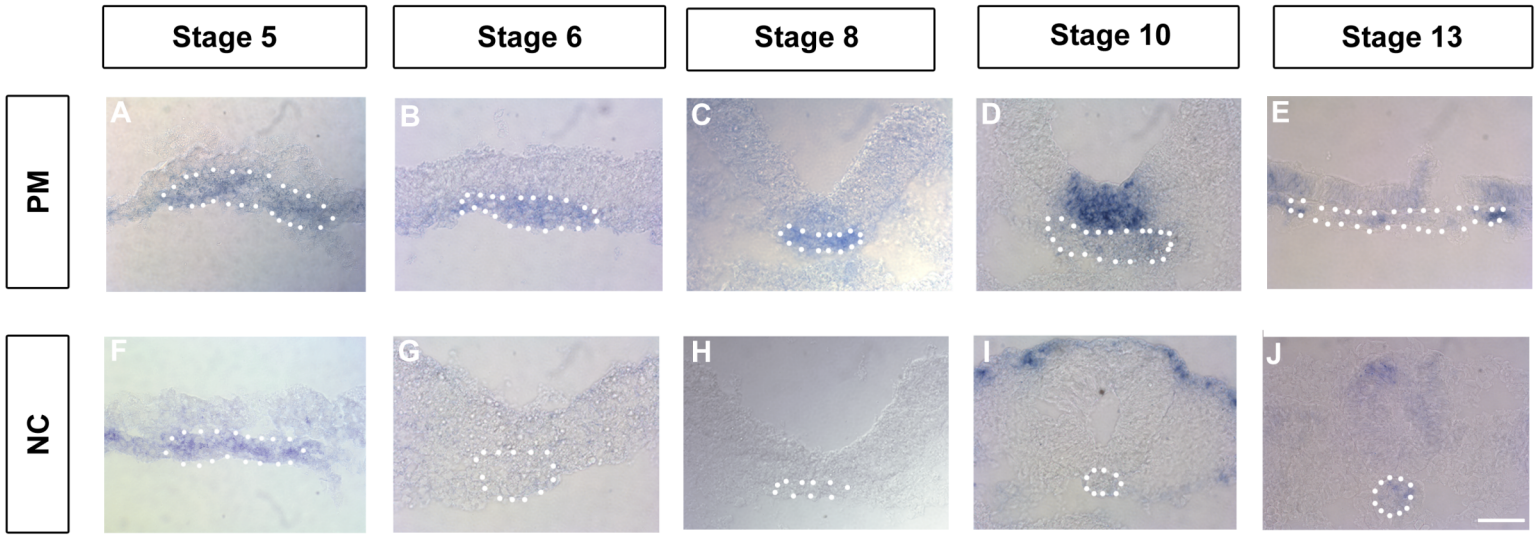

Figure 3.3 Expression of *BMP7* at HH stage 5 – 13

A-E
Transverse sections show that *BMP7* is expressed in the anterior head process mesoderm (outlined by dotted lines) at stage 5 and in the PM (outlined by dotted lines) at HH stages 6-13. At stages 8-13 its expression can also be detected in the overlying neuroectoderm.

F- J
BMP7 is detected in the posterior head process mesoderm (outlined by dotted lines) at stage 5. Transverse sections through the trunk (as described in Figure 1) show that *BMP7* is absent from the NC from stage 6-13 (outlined by dotted lines). Scale bar = 50 μm.

stages. At HH stage 13, expression does not appear uniform throughout the PM but is intermittent, restricted to only a few cells (Figure 3.3 E). *BMP7* expression can also be faintly observed in the region of NC immediately posterior to the PM from stage 8 (data not shown), however, it is absent in the majority of the notochord (Figure 3.3 G-J).

3.2.2 SHH marks both NC and PM

The signalling ligand SHH is expressed throughout the axial mesoderm from stage 6 but I do not detect it at stage 5 (Figure 3.4). Like *Gsc* and *BMP7*, SHH is expressed in the PM but not in the overlying neuroectoderm at HH stage 6, but expression extends to the overlying floor plate at HH stages 8 and 10 (Figure 3.4 B-D). At HH stage 13 SHH protein is no longer detected in the PM but persists in the overlying floor plate (Figure 3.4 E). SHH is expressed at all stages in the NC but its expression begins in the floor plate of the spinal cord after HH stage 6 (Figure 3.4 G-J).

3.2.3 *Chordin* and 3B9 mark the NC

The secreted molecule *Chordin (Chrd)* is expressed in head process mesoderm at stage 5 (Figure 3.5 A and F). It is also detected in the NC and the floor plate of the spinal cord over the period HH stage 6 to 10 (Figure 3.5 G-J). At HH stage 13 *Chrd* is only expressed in the NC and is absent from the overlying floor plate (Figure 3.5 J). *Chrd* expression is not expressed in the PM (Figure 3.5 B-E).

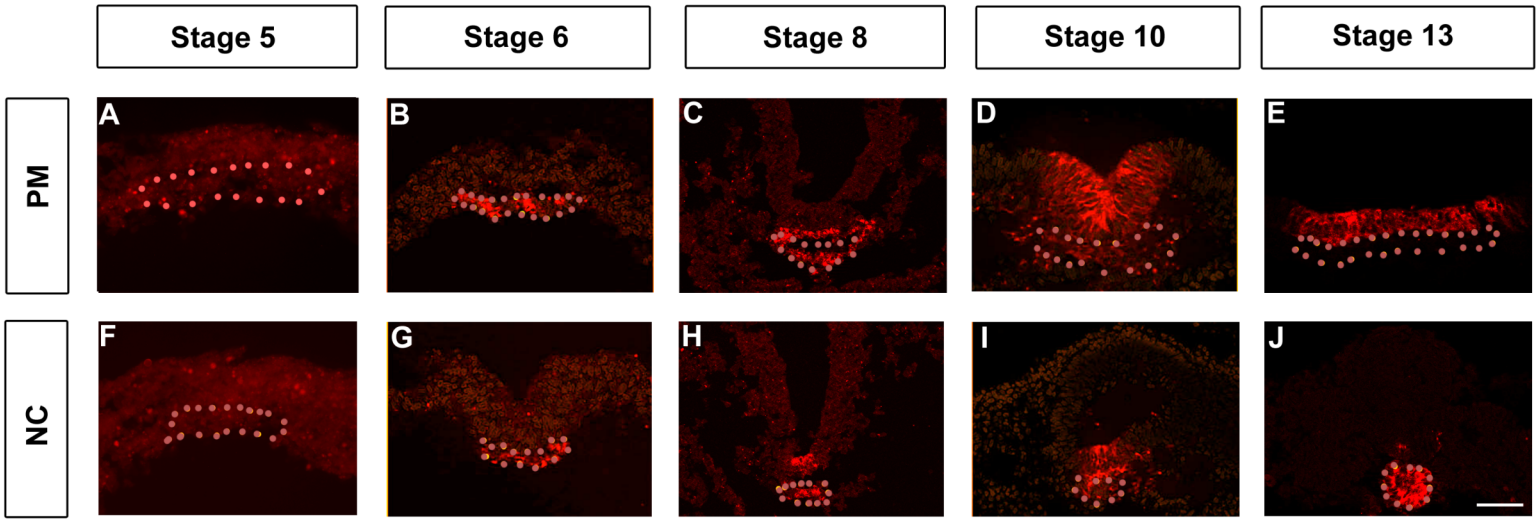

Figure 3.4 Expression of SHH at HH stage 5 – 13

A-E
Transverse sections show that SHH is not detected in the anterior head process mesoderm at stage 5 (outlined by dotted lines). Its expression begins in the PM (outlined by dotted lines) at HH stages 6, remains till stage 10 but is absent at stage 13. At stages 8-13 SHH can also be detected in the neuroectoderm.

F- J
At stage 5 SHH is not detected in posterior head process mesoderm (outlined by dotted lines), however, transverse sections through the trunk (as described in Figure 1) show that it is expressed in the NC from stages 6-13 (outlined by dotted lines) and the overlying neuroectoderm from stages 8-13. Scale bar = 50 μm

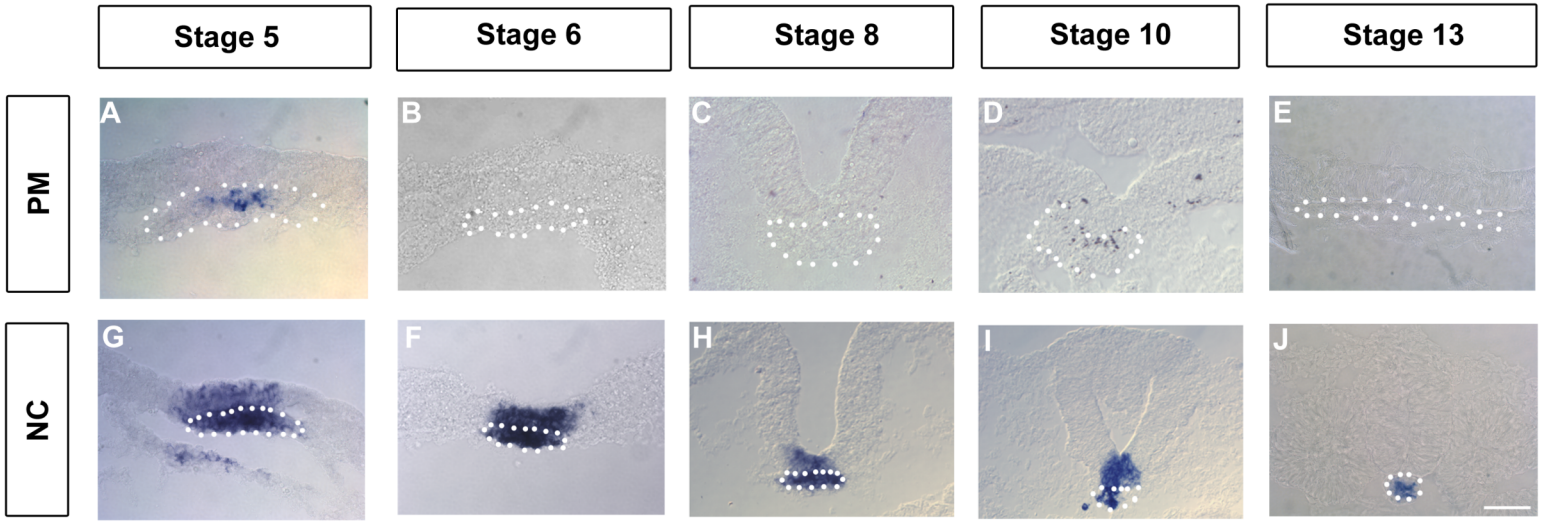

Figure 3.5 Expression of *Chordin* at HH stage 5 – 13

A-E
Transverse sections show that *Chordin* is detected in the anterior head process mesoderm (outlined by dotted lines) at stage 5. Its expression however is absent in the PM (outlined by dotted lines) at HH stages 6-13.

F- J
At stage 5 *Chordin* is expressed in posterior head process mesoderm (outlined by dotted lines), however, transverse sections through the trunk (as described in Figure 1) show that it is expressed in the NC and the overlying neuroectoderm from stages 6-13 (outlined by dotted lines).
Scale bar = 50 μm

Similarly, the surface molecule 3B9 is a marker for the NC and not the PM (Figure 3.6). However, unlike *Chrd* it is only expressed in the NC and not in the floor plate (Figure 3.6 G-J). I did not detect 3B9 in head process mesoderm at stage 5 (Figure 3.6 A and F).

3.2.4 Expression profiling in prechordal mesoderm and notochord explants

To determine whether the PM and NC maintain their marker profile in vitro, explants of PM and NC were dissected at HH stage 6 and cultured on collagen beds for 15 hours, until the equivalent of HH stage 8/9 *in vivo* (Figure 3.7). Explants were then fixed, processed by in situ hybridisation or Immunohistochemistry and scored in a semi-quantitative manner (Figure 3.8 K, for quantitation see materials and methods section 2.8). Prechordal mesoderm explants continued to express *Gsc*, *BMP7* and SHH but not *Chordin* and 3B9 (Figure 3.8 A-E). Over 60% of the area of each PM explant expresses *Gsc, BMP7* and SHH (Figure 3.8 K). NC explants also maintained their unique character in vitro and expressed SHH, *Chordin*, 3B9 and *BMP7* but not *Gsc* (Figure 3.8 F-J). *Chordin* and 3B9 were expressed in over 90% along the length of each NC explant (Figure 3.8 K). Expression of *BMP7* could be observed faintly in the NC, with 20% of the explant expressing *BMP7* (Figure 3.8 G and K).

So, *Gsc* and *BMP7* can be used *in vitro* as marker of the PM and 3B9 and *Chordin* as markers of the NC. However, my analyses reveal that *Gsc* and *BMP7,* are not exclusive to the PM and label also the neurectodermal midline. The lack of definitive markers hampers

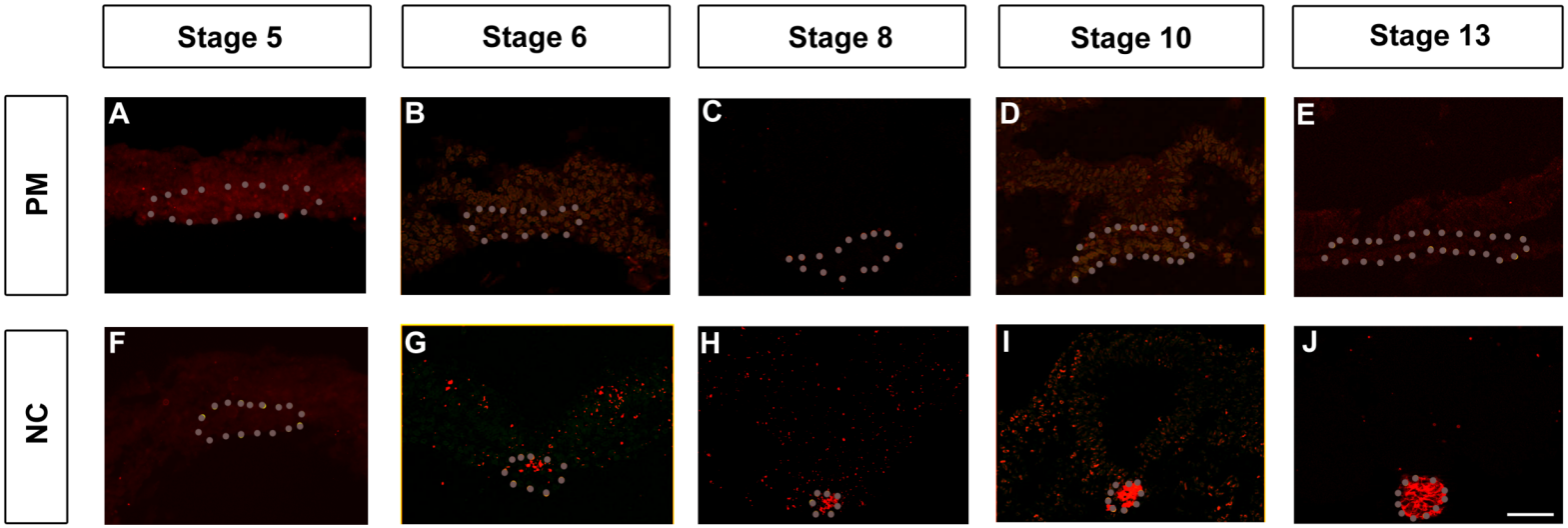

Figure 3.6 Expression of 3B9 at HH stage 5 – 13

A-E
Transverse sections show that 3B9 is absent from the anterior head process mesoderm (outlined by dotted lines) at stage 5 and the PM from HH stages 6-13 (outlined by dotted lines).

F- J
At stage 5 3B9 is absent from the posterior head process mesoderm (outlined by dotted lines), however, transverse sections through the trunk (as described in Figure 1) show that it is expressed in the NC alone from stages 6-13 (outlined by dotted lines).
Scale bar = 50 μm

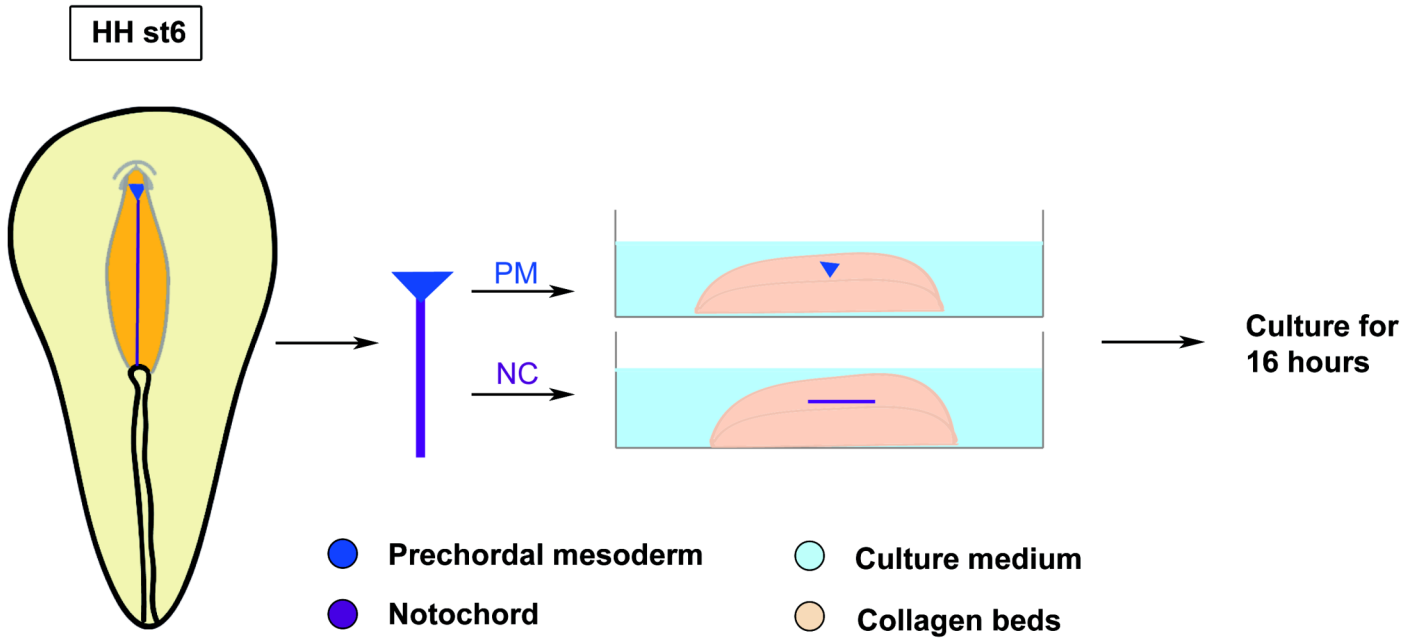

Figure 3.7 *In vitro* culture of axial mesoderm explants

Axial mesoderm dissected from HH stage 6 embryo is further subdissected into PM and NC. The PM and NC are then cultured on collagen beds for 16 hours, equivalent to HH stage 8/9 *in vivo*.

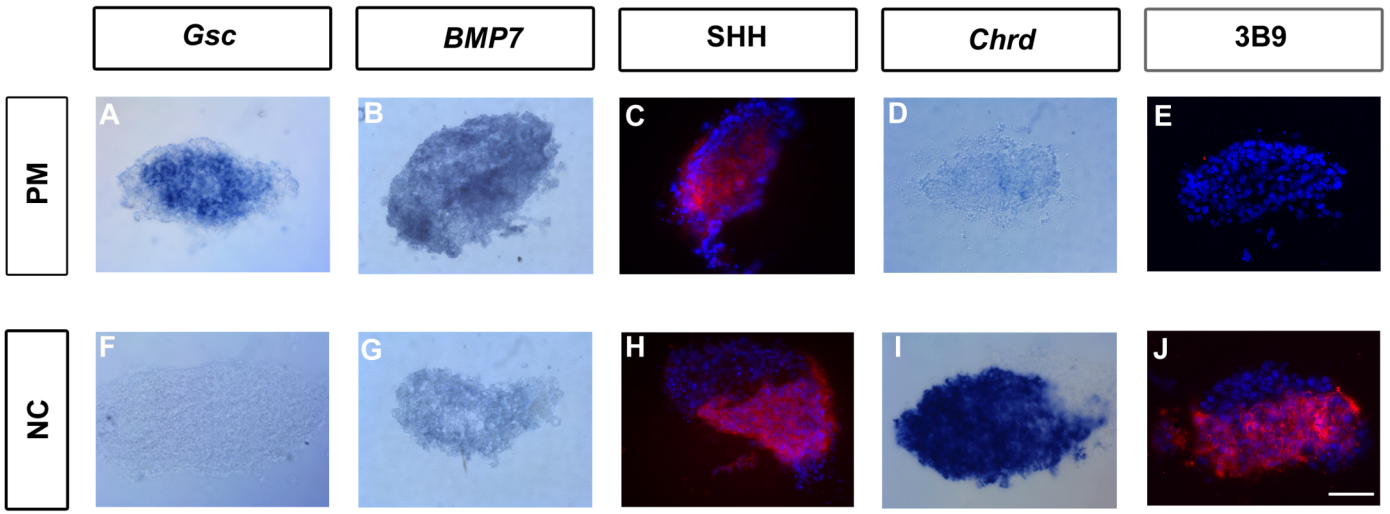

K

	PM	NC
Gsc	66% (8/8)	0% (4/4)
BMP7	70% (4/4)	20% (2/2)
SHH	70% (20/21)	69% (8/9)
Chrd	0% (5/5)	93% (23/25)
3B9	0% (5/5)	97% (25/28)

Figure 3.8 Expression of genes in PM and NC explants

A-E

Gsc, *BMP7*, SHH continue to be expressed strongly in vitro in the PM, where as *Chrd* and 3B9 are absent.

F-J

Gsc is not expressed in the NC explant, *BMP7* is weakly expressed whereas SHH, *Chrd* and 3B9 are strongly expressed in the NC. Scale bar = 50 µm

K

Explants were scored by measuring the percentage area with positive expression and comparing that to the total area of of PM explants. For NC, length of positive expression was measured and compared to the total area of the NC (see materials and methods 2.8). Numbers in brackets represent the number of explants with positive expression compared to the total number of explants analysed.

analysis of PM development (van Straaten et al., 1989; Placzek et al., 1990; Yamada et al., 1991; Placzek M., 1995; Catala et al., 1996; Teillet et al., 1998; Le Douarin et al., 1998; Placzek et al., 2000; LeDouarin and Halpern, 2000; Patten et al., 2003). I therefore sought to identify additional markers that specifically mark the PM.

3.2.5 Expression analysis of T-box genes in the axial mesoderm

As outlined in the main introduction (section 1.6.1) I decided to study the expression of T-box genes, given that previous studies have shown that they play a role in other regions of the developing mesoderm (e.g. Papaioannou and Silver, 1998; Naiche et al., 2005; Wardle and Papaioannou, 2008; see also references in section 1.6.1). I focused on those T-box genes that have been shown to either regulate or are regulated by BMPs and Nodal as previous studies support a role for these molecules in PM specification (Mitrani et al., 1990; Mitrani and Shimoni, 1990; Ziv et al., 1992; Stern et al, 1995; Vesque et al., 2000).

Tbx2 and *3* are expressed with BMPs in the cardiac mesoderm (Yamada et al., 2000). BMPs directly regulate their expression: overexpression of BMP ligands induces *Tbx2* and *Tbx3* in non-cardiogenic tissue (Yamada, 2000). *Tbx2* and *Tbx3* also act with SHH and BMP signalling to specify posterior digit identities in the chick limb (Suzuki et al., 2004).

Studies in chick, mouse, Xenopus and zebrafish have shown that *Tbx6* and *Tbx18* are critical for the correct specification of somites

(Chapman et al., 2003; Chapman and Papaioannou, 1998; Bussen et al., 2004; Begemann et al., 2002; Haenig and Kispert, 2004; Tanaka and Tickle, 2004; Uchiyama et al., 2001). The expression of *Tbx6* can be induced by BMP ligands in Xenopus and zebrafish (Uchiyama et al., 2001; Szeto and Kimelman, 2004).

Low levels of BMP signalling are also required for the correct expression of *Tbx18* expression in the proepicardium of the developing heart (Schlueter et al., 2006). Conversely, in the uretral mesenchyme the authors proposed that *Tbx18* regulates BMP and SHH signalling pathways (Airik et al., 2006).

I also wanted to study Eomesodermin, which has a pivotal role in mesoderm delamination during gastrulation as well as specification of the anterior primitive streak (Arnold et al., 2008). It interacts with Nodal signalling to promote correct anterior posterior axis formation and epithelial to mesenchymal transition of the ingressing mesoderm (Arnold et al., 2008).

To begin to analyse the expression of T-box genes in the axial mesoderm I first used RT PCR to detect RNA for these T box genes. cDNA was prepared from whole chick embryos and from the heads of the chick embryos at HH stage 6, 8, 10 and 13.

Tbx2, Tbx3, *Tbx18*, and Eomesodermin were detected in whole chick embryo and heads (Figure 3.9 B-E). Tbx6 could only be detected in whole embryos at all stages but was only detected in the head at HH stage 6 (Figure 3.9 F).

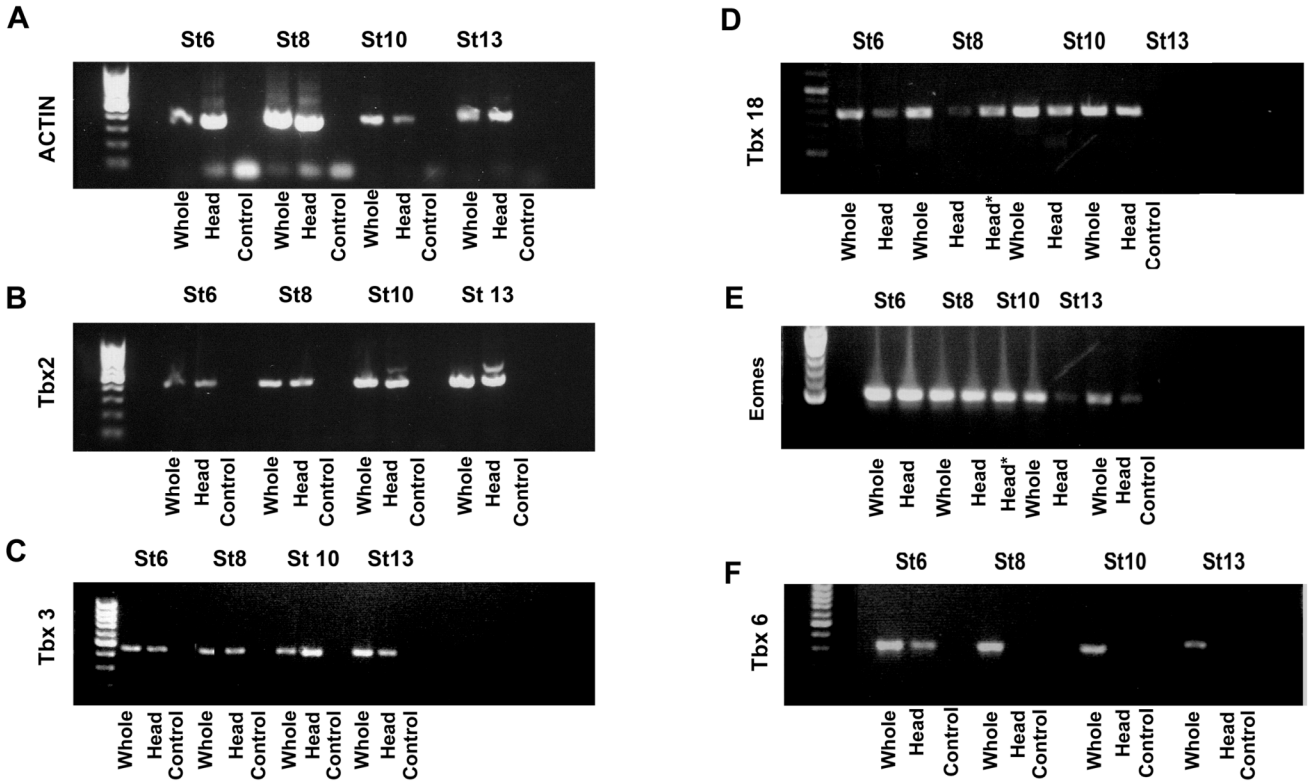

Figure 3.9 Expression of T-box genes using RT PCR in heads and whole chick embryos

cDNA used to perform was obtained from either whole chick embryos (whole), heads of chick embryos (head) or heads after dissecting out the cardiac tissue (head*). Marker gene tested is on the left and stage analysed from HH stage 6-13 is indicated on the top.

Using immunohistochemistry and in situ hybridisation I studied the expression of these genes in chick embryos (data not shown). Expression was detected in a variety of structures including the eyes and the hypothalamus. However, only *Tbx18* marked the PM. *Tbx18* was detected in the PM over HH stages 6-10 (Figure 3.10 B-D). Expression appeared relatively transient and could no longer be detected at stage 13 (Figure 3.10 E). *Tbx18* expression was not detected in the PM prior to stage 6 nor was expression detected in the NC at any stage (Figure 3.10 A, G-K). To determine whether *Tbx18* might act as a useful marker in *in* vitro experiments I examined its expression in PM explants. Tbx18 is maintained *in vitro* explants of the PM (74% of explants express *Tbx18*, n=19/20) (Figure 3.10 F). *Tbx18* expression was largely absent in NC explant (Figure 3.10 L). In some NC explants small patches of *Tbx18* expression were detected in 12% of NC explant (n=7/12) (Figure 3.10 F and L). Thus, broad and robust expression of *Tbx18* is seen in the PM explants and it is largely absent from the NC explants.

3.3 Discussion

In summary I have identified a transcription factor, *Tbx18,* that *in vivo* exclusively marks the fully extended PM in the chick embryo. Expression of *Tbx18* has been described in mouse, zebrafish and Xenopus, however, its expression in the PM has not been studied (Kraus et al., 2001; Begemann et al., 2002; Jahr et al., 2008). To see if the expression of *Tbx18* in PM is conserved across species, these studies need to be repeated with a particular focus on the PM.

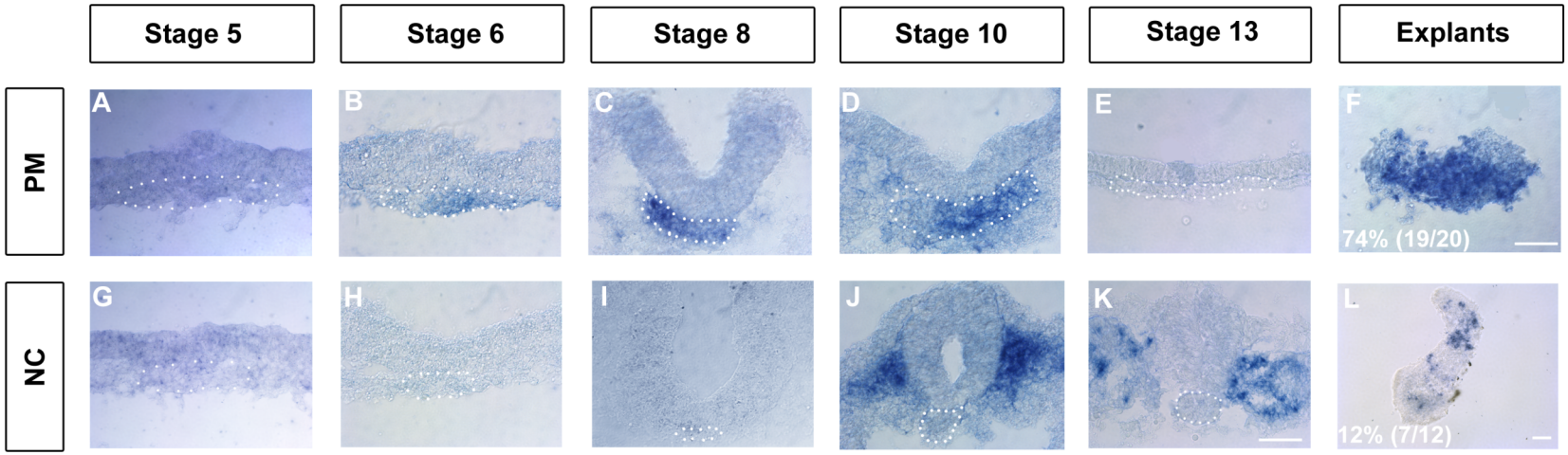

Figure 3.10 Expression of *Tbx18 in vivo* and *in vitro*

A-E
Transverse sections show that at stage 5 *Tbx18* is absent from the anterior head process mesoderm (outlined by dotted lines) but is expressed in the PM (outlined by dotted lines) at HH stages 6-10. At stage 13 *Tbx18* is not detected in the PM.

G-K
Tbx18 is absent from the posterior head process mesoderm (outlined by dotted lines) at stage 5. Transverse sections through the trunk show that *Tbx18* is not expressed in the NC (outlined by dotted lines).

F&L
Explants of PM and NC both show *Tbx18* expression, however, it is stronger in the PM with 74% of the explant expressing *Tbx18* compared with 12% in the NC explant. Scale bar = 50 μm

My studies show that, not only is *Tbx18* expressed exclusively in the PM, but also that it is a relatively late marker of the PM, being expressed only from stage 6 onwards. As such it contrasts with *Gsc* and *BMP7*, which are also expressed at stage 5. This raises the possibility that Tbx18 may have a late role in PM specification and/or maintenance. Interestingly *Tbx18* is although specific to the PM *in vivo*, I observe that it is detected in NC explants in low amounts. This suggests that the expression of *Tbx18* is tightly regulated in vivo to preserve the unique identity of PM.

Mouse and Drosophila knockout studies of Gsc do not show any obvious phenotype in gastrulation (Rivera-Perez et al., 1995; Yamada et al., 1995; Zhu et al., 1999; Goriely et al., 1996). Defects in neural patterning are however, observed in Drosophila, zebrafish and Xenopus but the expression of *Gsc* in both PM and neuroectoderm makes it difficult to distinguish between a direct role of Gsc in the neuroectoderm or the prechordal mesoderm (Seiliez et al., 2005; Steinbiesser et al., 1995; Hahn and Jaeckle, 1996). Other transcription factors of the PM including Lim1, Hesx1, Frizzled, Crescent, Dkk, HNF3ß, Otx2, blimp1 are also expressed in the neuroectoderm and/or the anterior visceral endoderm located anterior to the PM (Ang et al., 1996; Ang and Rossant et al., 1994; Brickman et al., 2000; Chapman et al., 2004; de Souza et al., 1999; Jones et al., 1999; Ladher et al., 2000; Martinez Barbera et al., 2000; Shawlot and Behringer, 1995; Sun et al., 2008). Thus up until now it has been complicated to study the specification and role of the PM due to the lack of an exclusive marker of the PM. The specific expression of *Tbx18* in the PM provides an opportunity to study whether it plays an important role in PM specification. Studies analysing how PM

specifies and the factors involved in its specification/development are currently difficult to interpret. Thus, the specific expression of *Tbx18* in the chick PM now presents an opportunity to study the factors involved in the specification/maintenance of PM and the role that *Tbx18* itself is playing in the PM.

Chapter 4

Tbx18 inhibits notochord character and induces the formation of a third type of axial mesoderm at the PM/NC boundary

4.1 Introduction

As outlined in Chapter 3 (introduction), i.e. prechordal mesoderm and notochord are not fully resolved in head process mesoderm as mixed expression and/or mixed cells are readily detected (Foley et al., 1997; Vesque et al., 2000; Chapter 3).

However, from HH stage 6-7, notochord and prechordal mesoderm resolve – in-situ hybridisation and immunohistochemical analyses show distinct expression boundaries between the two cell types. This raises the possibility that a factor may be expressed in either one or both axial mesoderm cell type, and inhibit characteristics of the second. For instance, hypothetically, prechordal mesoderm cells may begin to express a transcription factor that inhibits notochord character.

In theory, such a transcription factor could exert an effect through a number of mechanisms. Elsewhere in the embryo, for example in the neural tube (see section 1.4.1) such sharp expression boundaries arise through the mutual repression of cells in adjacent domains, maintained by particular transcription factors (Briscoe and Ericsson, 2001). The best characterised of these are the homeodomain transcription factors Nkx2.2 and Pax6, that mutually repress each other (Briscoe et al., 2000). Thus, a transcription factor expressed in the PM could repress NC fate directly, downregulating notochord character. Such cells might then

1. die as a consequence of downregulating NC characteristics (Figure 4.1 A),

2. change fate and form PM, upregulating PM markers (Figure 4.1 B),
3. become a third type of axial mesoderm cell that expresses the transcription factor but not NC or other PM characteristics (Figure 4.1 C), or,
4. express particular adhesive properties, or chemorepulsive signals, so that they act as a barrier or push away any cells that do not express the same properties (Figure 4.1 D),
5. behave due to a combination of such properties (e.g. 2 and 4 or 3 and 4).

As described in Chapter 3, *Tbx18* has the correct profile to act as such a factor. It is not expressed in the head process mesoderm formation when NC and PM are mixed/intermingled. However, it is expressed from HH stage 6 i.e. the time at which NC and PM appear to resolve *in vivo*. Moreover, in other regions of the embryo, T box genes can repress cell identities (Bussen et al., 2004; Farin et al., 2007; Kapoor et al., 2011). As described in the main Introduction (section 1.6.1), *Tbx18* in particular has been associated with boundary formation in three distinct territories in the developing embryo – the somites, the inner ear and the ureter (Bussen et al., 2004; Farin et al., 2007; Trowe et al., 2008; Airik et al., 2006). The mechanism through which *Tbx18* acts to form boundaries in all these structures is unclear, but it is widely speculated that *Tbx18* may either confer distinct adhesive properties to cells which then adhere to cells with the same properties or it may promote the expression of a chemorepellent. So, there might be a common molecular program through which *Tbx18* operates to form sharp boundaries in these tissues.

Figure 4.1 Possible mechanisms of boundary formation between PM and NC

FactorX expressed by PM cells inhibits NC fate and those cells may take the following possible routes to create the boundary between PM and NC:

A
Cell positive for FactorX undergo apoptosis.

B
Cells may downregulate NC characteristics and upregulate PM characteristics for instance, Tbx18 and Gsc.

C
Cells positive for FactorX downregulate NC characteristics but do not upregulate PM characteristics, thereby creating a third type of axial mesoderm.

D
Cells positive for FactorX aggregate together by expressing the same adhesion properties and repel cells that do not posses the same adhesion properties as themselves.

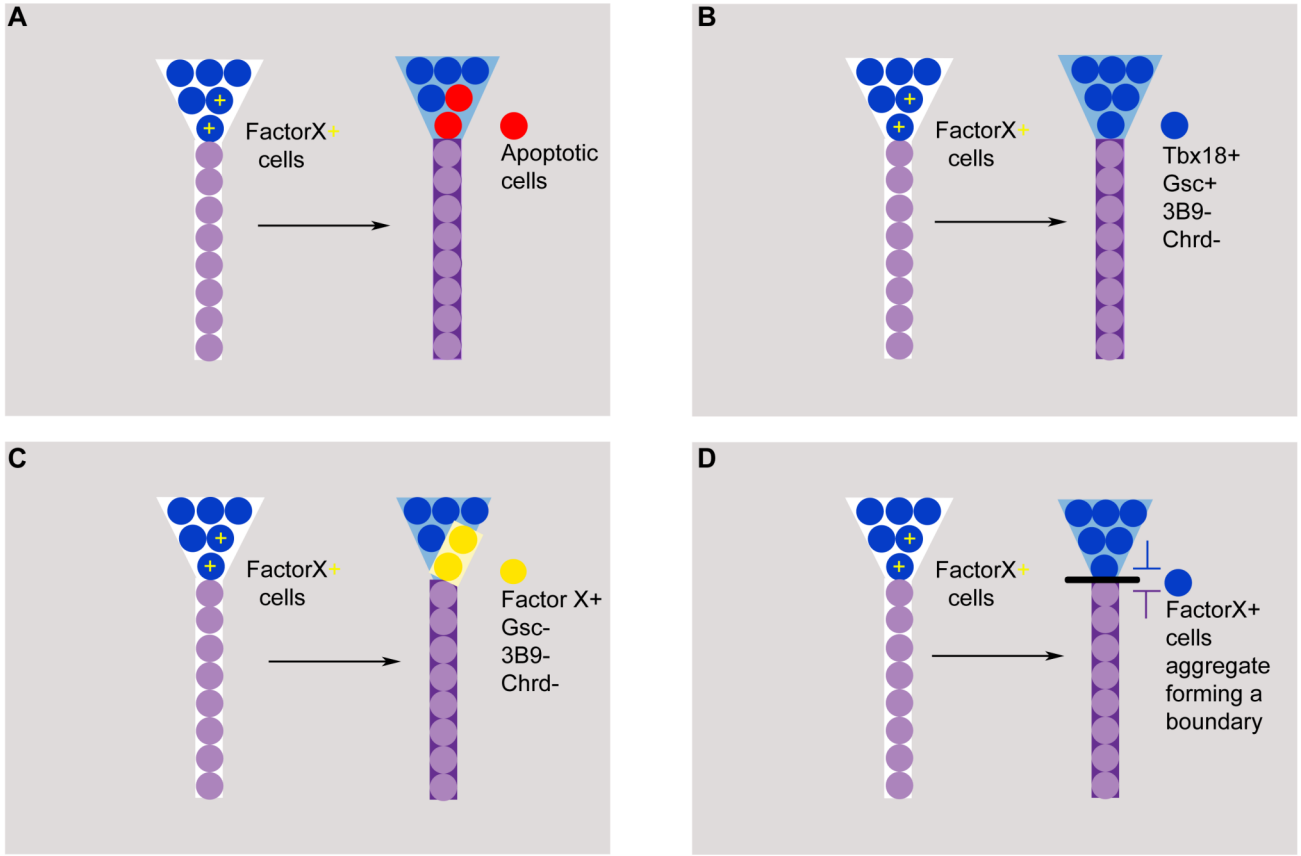
A
FactorX+
cells
Apoptotic
cells
B
FactorX+
cells
Tbx18+
Gsc+
3B9-
Chrd-
C
FactorX+
cells
Factor X+
Gsc-
3B9-
Chrd-
D
FactorX+
cells
FactorX+
cells
aggregate
forming a
boundary

In this chapter I set out to address whether *Tbx18* is likely to play a role in the establishment of a sharp boundary between notochord and prechordal mesoderm. To be able to do this, I performed *in ovo* gain and loss-of-function electroporation experiments. Thus, I aimed to misexpress *Tbx18* in the notochord and additionally aimed to electroporate small interefering RNAs targeted to *Tbx18* into the prechordal mesoderm.

4.2 Results

4.2.1 Electroporation of the axial mesoderm

Whereas analysis of gene function by misexpression in the neural tube of the chick embryo has become a routine method in recent years, electroporation of the axial mesoderm remains challenging (Yasugi and Nakamura, 2000; Swartz et al., 2001; Nakamura et al., 2004; Das et al., 2006; Croteau and Kania, 2011). The neural tube can be accessed easily and the lumen of the neural tube serves as a vehicle to hold DNA before transfection. The axial mesoderm in comparison underlies the neural tube making access difficult and the lack of lumen adds to the challenge of precise transfection. The prechordal mesoderm is a particularly difficult cell to target as it is a transient structure, allowing limited time for an efficient gene misexpression or knockdown.

To attempt to robustly target axial mesoderm cells I experimented with a variety of methods (see materials and methods). Most success

resulted when cells were targeted pre-gastrulation, i.e. before axial mesoderm cells extend out of Hensen's node and thus at a time point when they are easily accessible. Vectors were introduced into Hensen's node using standard *in ovo* electroporation techniques (Gray and Dale, 2010, Figure 4.2). Initially a pCAGGS empty vector and a pCAGGS-RFP vector were co-electroporated into HH stage 4 and embryos developed to HH stage 10. Whole mount analyses revealed that RFP expression could be observed in the midline of the embryo (Figure 4.3 A). Sections through the trunk of such embryos showed RFP expressed in a mosaic manner with an average of 20% NC cells electroporated (no. of cells =36/180) (Figure 4.3 B).

4.2.2 Misexpression of *Tbx18* in the notochord

To begin to investigate the role of *Tbx18,* I misexpressed *Tbx18* and ascertained its effect on notochord. A DNA expression construct (cTbx18), containing cDNA for *Tbx18* cloned into the pCAGGS vector (Tanaka and Tickle, 2004) and was co-electroporated with pCAGGS – RFP to allow detection of electroporated cells (in the vector to reporter ratio of 1.7:1) (Table 4.1). Empty pCAGGS vector and pCAGGS – RFP were co-electroporated as control (Table 4.1). Analysis was restricted to those embryos that showed robust expression of RFP in the midline (Figure 4.4 A and C). Embryos with such clear RFP in the notochord intriguingly, (n=2/3) also showed increased expression of RFP in the prospective heart region of embryos misexpressing *Tbx18* in the notochord compared to the controls (n=0/2) (Figure 4.4 marked by arrowheads). The limitation of co-electroporation were considered in these analysis i.e. it cannot

be ruled out that there is a possibility that not all RFP cells are expressing cTbx18 gene. Therefore it was important to compare the embryos misexpressing cTbx18 in the notochord to be compared to the controls carefully to conclude that there is a possibility that embryos misexpressing cTbx18 had an enlarged heart domain but the control embryos did not. To confirm this observation it is important to repeat this experiment and analyse a bigger sample.

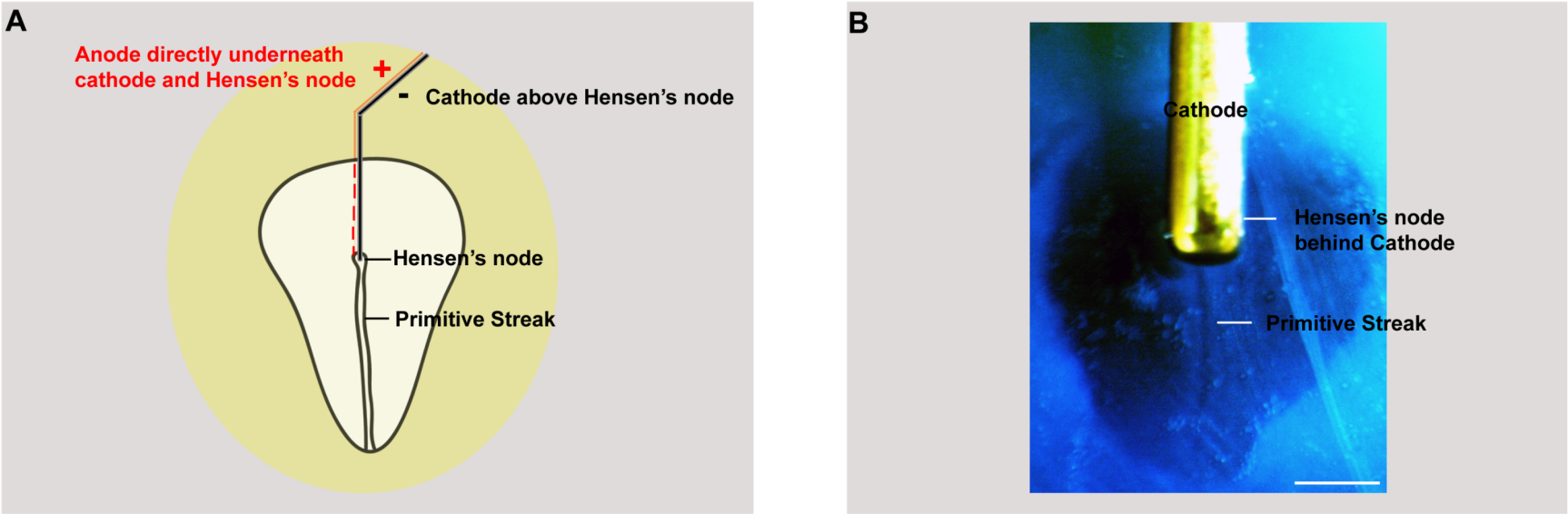

Figure 4.2 Electoporation set-up for misexpressing genes in axial mesodermal cells

Schematic (A) of the example set-up for in ovo electroporation into axial mesoderm progenitors at HH stage 4 in B. The embryo is accessed by windowing the egg shell and is visualised by injecting blue food dye underneath it. DNA is injected above and into Hensen's node. The electrodes are placed such that the anode is underneath the node (not visible in B as masked by cathode) and the cathode touches Hensen's node as shown in panel B. The current allows the DNA to enter the cells by creating pores in their plasma membrane. Scale bar = 5μm

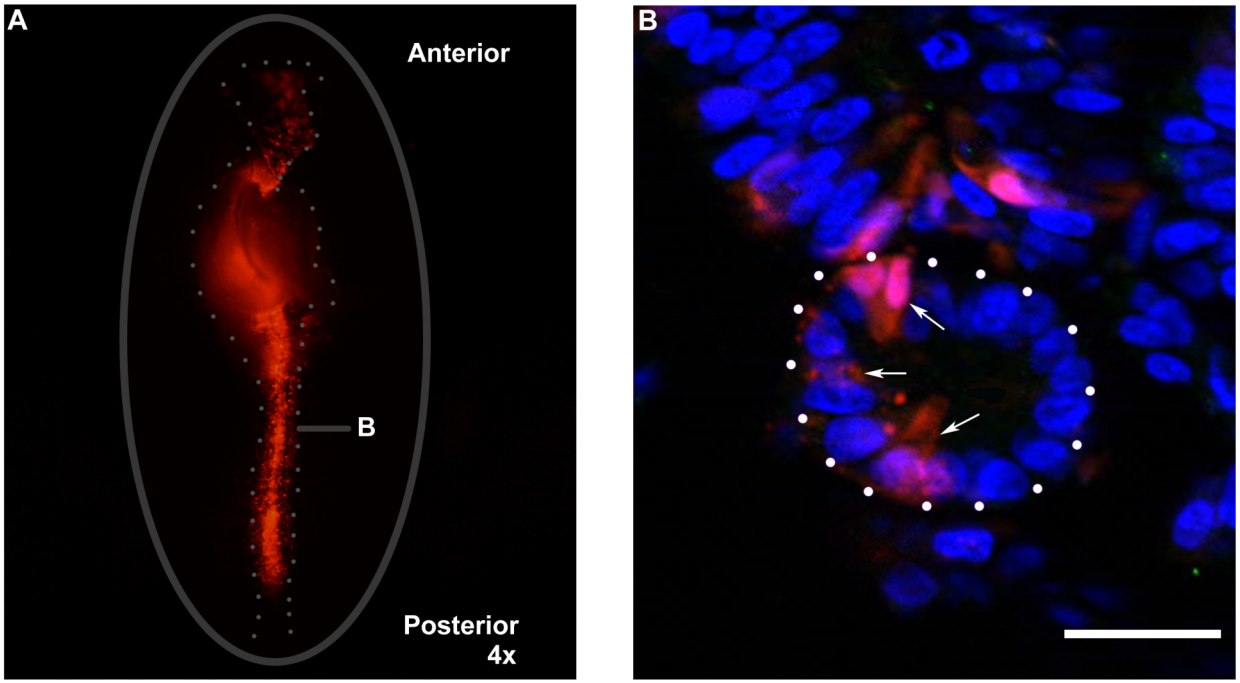

Figure 4.3 RFP is expressed in embryo co-electroporated with pCAGGS empty vector and pCAGGS-RFP.

A Wholemount embryo co-electroporated with pCAGGS empty vector and pCAGGS-RFP at stage 4 and developed to stage 9 post electroporation. RFP expression is detected in the midline of the embryo.

B Transverse section through the embryo shows RFP expression (marked by arrows) in the notochord (outlined by dotted lines) and cells of the overlying floor plate. Scale bar = 25μm.

Table 4.1 Summary of in ovo electroporations

Vector	Electrode placement	Stage	DNA injected	Voltage	Number electroporated	Number survived	Number expressing RFP in the midline	Number expressing RFP in the NC or PM
pCAGGS-Tbx18 and pCAGGS-RFP	Same plane as the axis	3-4	Hensen's node	10V	60	28	16	2 (NC)
pCAGGS-Tbx18 and pCAGGS-RFP	Right angles to the axis	4-6	Hensen's node	40V	42	26	8	1 (NC)
pCAGGS and pCAGGS-RFP	Same plane as the axis	3-4	Hensen's node	10V	36	12	6	2 (NC)
Tbx18 SiRNA	Same plane as the axis	3-4	Hensen's node	10V	48	18	11	2 (PM)
Luciferase control	Same plane as the axis	3-4	Hensen's node	10V	36	14	10	1 (PM)

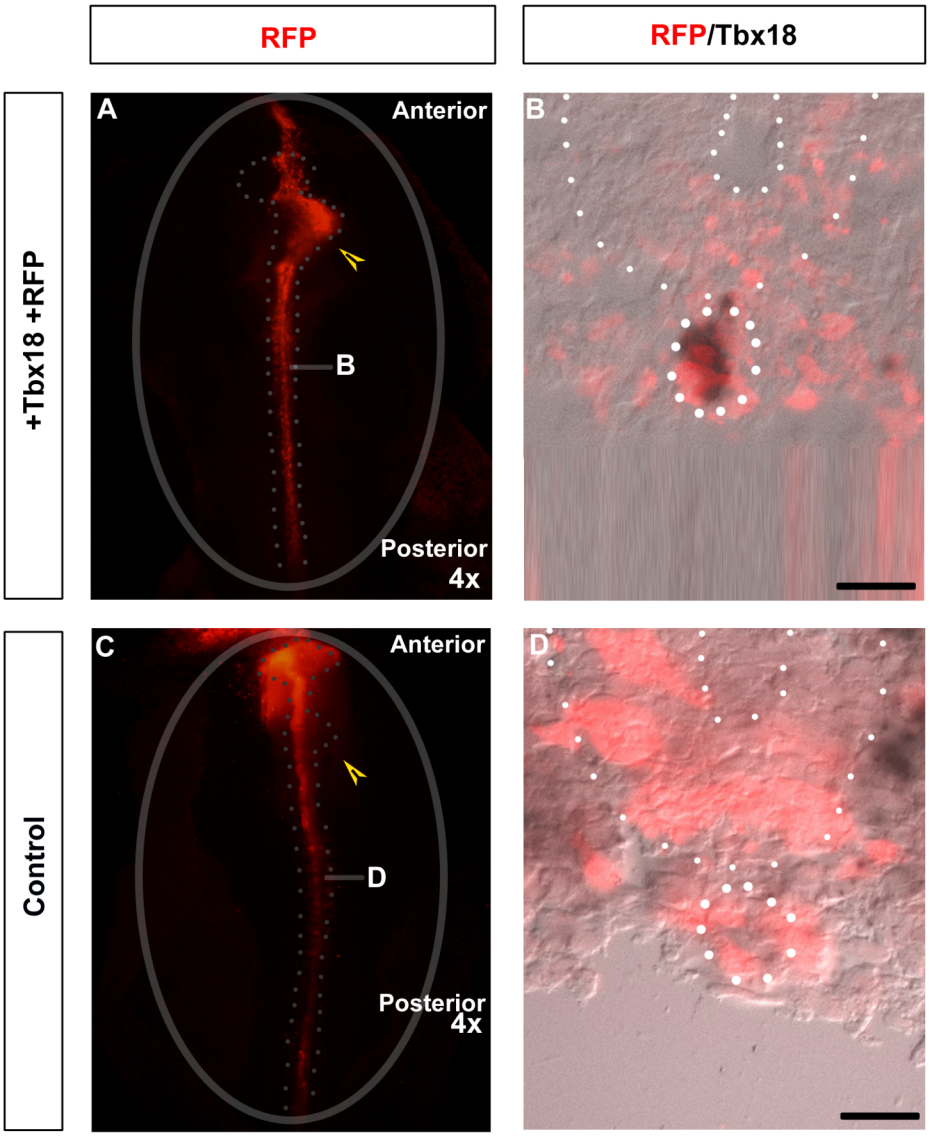

Figure 4.4 *Tbx18* is expressed in the NC of pCAGGS-cTbx18 and pCAGGS-RFP (+Tbx18 +RFP) but not in pCAGGS and pCAGGS-RFP (control) co-electroporated embryos.

A Expression of RFP is detected throughout the midline as well as the heart (marked by arrowhead) of pCAGGS-cTbx18 and pCAGGS-RFP (+Tbx18 +RFP) co-electroporated embryo.
B Transverse section through the embryo (marked by line in A) shows robust expression of *Tbx18* in the NC (marked by dotted line).
C Expression of RFP is detected throughout the midline but not in the heart of the pCAGGS and pCAGGS-RFP (control) co-electroporated embryo.
D Trasverse section through the embryo (marked by line in C) shows that *Tbx18* is not expressed in the NC (marked by dotted line).
Scale bar = 25 μm.

Misexpression of *Tbx18* in the NC was first confirmed by in situ hybridisation. Expression of *Tbx18* was detected in the NC of pCAGGS – cTbx18 electroporated embryos (no. of embryos = 3/3) whereas the NC of control embryo did not express *Tbx18* (no. of embryos =2/2) (Figure 4.4 B and D). Notably, *Tbx18*+ cells were almost always aggregated together in pCAGGS-cTbx18; single Tbx18+ cells were rarely observed (Figure 4.4 B).

To ask whether *Tbx18* can downregulate NC characteristics, I analysed expression of the NC markers 3B9 and *Chrd*. 3B9 was not detected in pCAGGS-cTbx18 electroporated notochord cells (no. of embryos = 3/3, no. of cells =5/54), whereas control electroporated cells robustly expressed 3B9 (no. of embryos = 2/2, no. of cells =20/28) (Figure 4.5 A and B). As Tbx18 is a transcription factor it is expected to act in a cell autonomous manner however, electroporated and non-electroporated cells alike lose the expression of 3B9 (marked by arrows in Figure 4.5). This suggests that there might be a secondary non-cell autonomous effect. This further implies that *Tbx18* might play a role in suppressing the notochord marker 3B9 in prechordal mesodermal cells but requires further investigation to successfully conclude this by analyzing a larger sample of embryos. Due to repeated technical difficulties, expression of *Chrd* could not be studied.

To further test the properties of *Tbx18*- cells (as set out in Figure 4.1), I first asked whether *Tbx18*+ 3B9- cells are undergoing apoptosis, by observing DAPI, which labels the nuclei. Chromatin condensation was not observed in the nuclei in pCAGGS-cTbx18 (no of embryos = 3/3, no of cells =55/60) or control electroporated cells (no of embryos

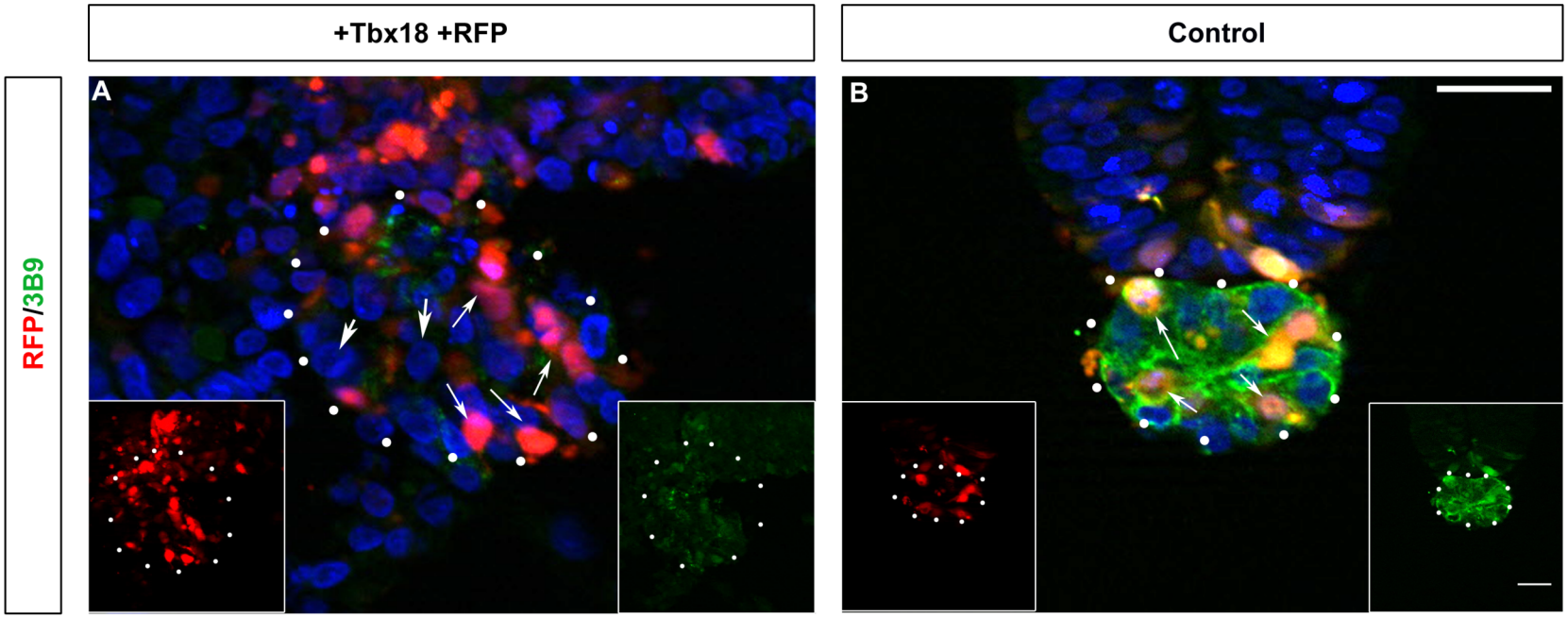

Figure 4.5 3B9 is downregulated in the notochord of pCAGGS-cTbx18 and pCAGGS-RFP (+Tbx18 +RFP) but not in pCAGGS and pCAGGS-RFP (control) co-electroporated embryos.

A Expression of 3B9 is absent from the pCAGGS- cTbx18 and pCAGGS-RFP (+Tbx18 +RFP) co-electroporated cells and non-electroporated cells in the notochord (marked by arrows).

B 3B9 is expressed in the cells of the notochord (marked by arrows) in pCAGGS and pCAGGS-RFP (control) co-electroporated embryo. Scale bar = 25 μm

= 2/2, no of cells =60/61) (Figure 4.6). This suggests that 3B9- cells are healthy and do not undergo apoptosis post-Tbx18 misexpression.

Next I tested the hypothesis that cells alter their fate to prechordal mesoderm and begin to express *Gsc*. Expression of *Gsc* was not detected in pCAGGS-cTbx18 electroporated NC cells or in control vector electroporated cells (Figure 4.7). This suggests that *Tbx18*+ cells downregulate 3B9 but do not upregulate the prechordal mesoderm marker *Gsc,* i.e. are not altering their fate to prechordal mesoderm. This suggests that they instead exist as a third type of axial mesodermal cell, which is *Tbx18*+, *Gsc*- and 3B9-.

Previous studies in the lab have, in fact, suggested the presence of a third population of axial mesoderm cell types *in vivo,* that exists at the boundary of PM and NC and unlike the PM and NC, does not express SHH (Figure 4.8, M.P. unpublished observations). Thus, I tested if misexpression of *Tbx18* in the NC results in the downregulation of SHH, potentially indicating the creation of this third type of axial mesoderm. Expression of SHH in pCAGGS-cTbx18 electroporated as well as non electroporated NC cells was weaker (no of embryos 3/3, no of cells = 14/67) than those in control suggesting that SHH is downregulated in NC cells misexpressing *Tbx18* (no of embryos 2/2, no of cells = 30/42) (Figure 4.9). This suggests that there is a possibility that *Tbx18* misexpressing cells alter their fate from NC to a third type of axial mesoderm sitting at the boundary between PM and NC.

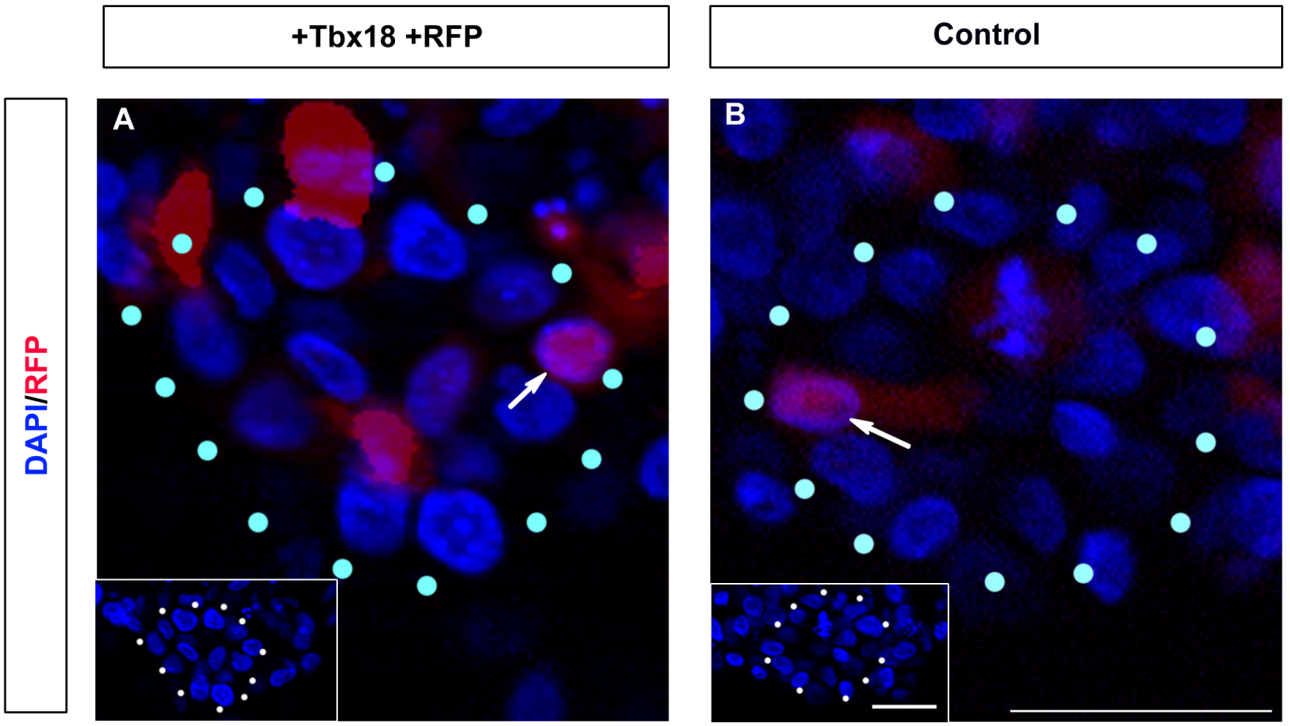

Figure 4.6 Absence of apoptotic cells in pCAGGS-cTbx18 and pCAGGS RFP (+Tbx18 +RFP) and pCAGGS and pCAGGS RFP (control) co-electroporated NC.

A DAPI labelling does not show nuclear fragmentation in pCAGGS-cTbx18 and pCAGGS RFP (+Tbx18 +RFP) electroporated RFP+ cell (marked by arrow)
B pCAGGS and pCAGGS RFP (control) co-electroporated cell (marked by arrow) also does not show nuclear fragmentation suggesting that cells are not apoptotic. Scale bar = 25 μm

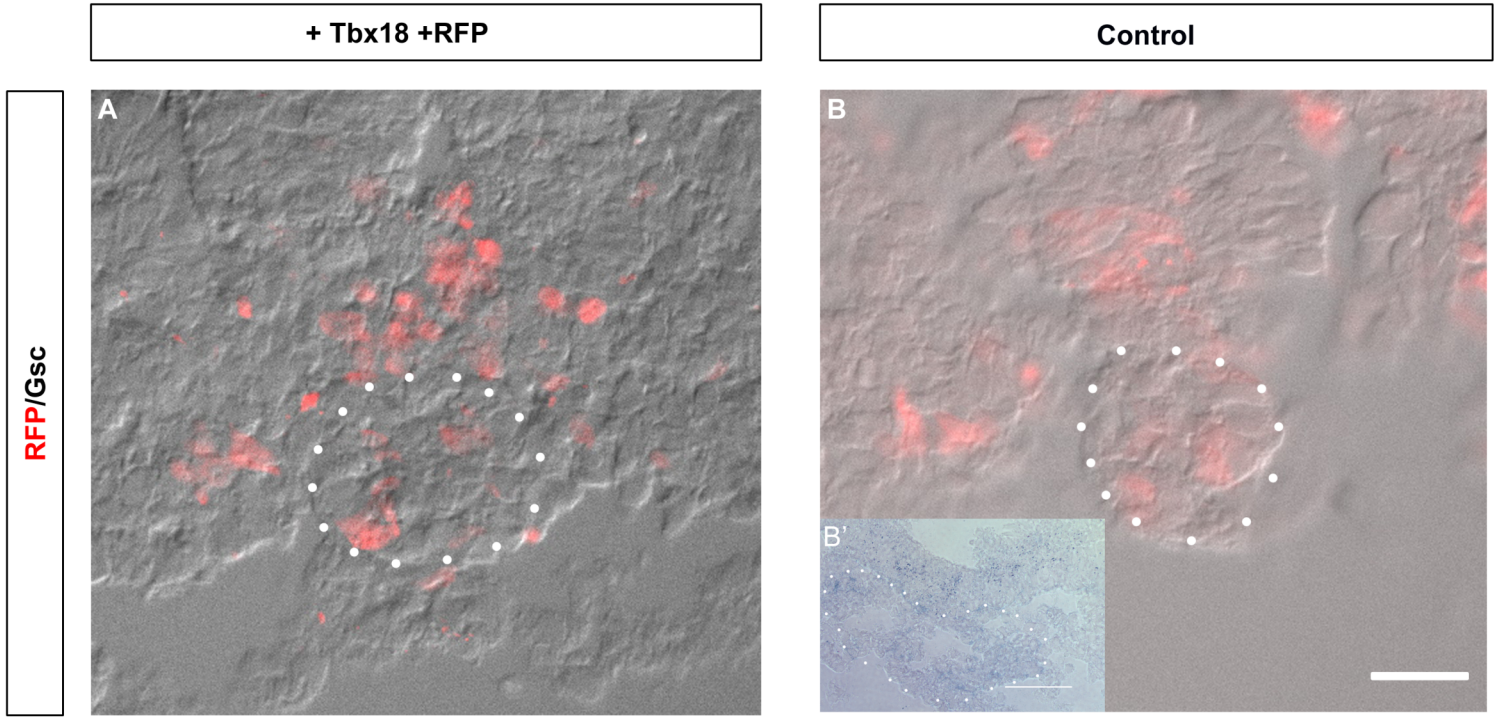

Figure 4.7 *Gsc* is not expressed in notochord cells of pCAGGS-cTbx18 and pCAGGS-RFP (+Tbx18+RFP) and pCAGGS and pCAGGS-RFP (control) co-electroporated embryos.

A Expression of *Gsc* is not detected in NC cells of the embryo co-electroporated with pCAGGS-cTbx18 and pCAGGS-RFP (+Tbx18+RFP) vector.

B *Gsc* is also not expressed in pCAGGS and pCAGGS-RFP (Control) co-electroporated NC cells.

B' *Gsc*+ prechordal mesoderm section is shown as positive control. Scale bar = 25 μm

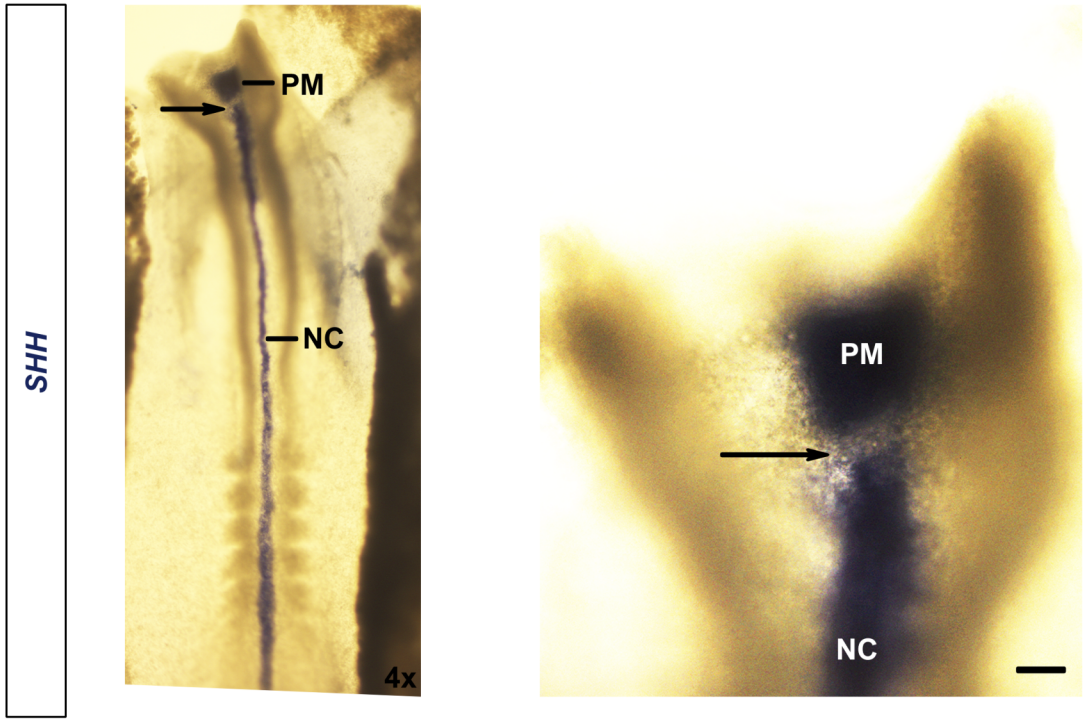

Figure 4.8 Expression of *Shh* at HH stage 8.

Shh is expressed in the PM and the NC at HH stage 8, however, it is absent from a small region posterior to the PM and anterior to the NC (marked by arrow). Scale bar = 50 μm .

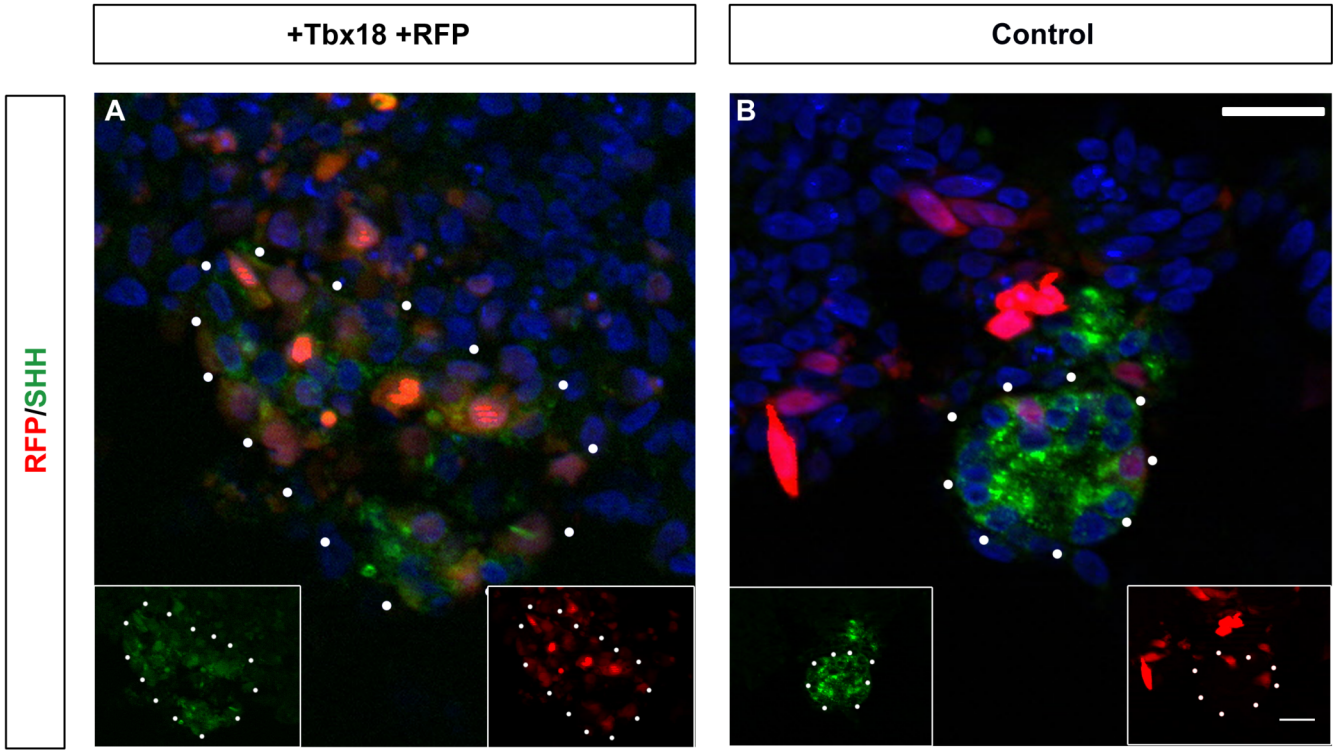

Figure 4.9 SHH is downregulated in pCAGGS-cTbx18 and pCAGGS-RFP (+Tbx18 +RFP) co-electroporated notochord cells but not in pCAGGS and pCAGGS-RFP (control) co-electroporated notochord cells.

A Weak expression of SHH is detected in NC cells co-electroporated with pCAGGS-cTbx18 and pCAAGS-RFP as well as non electroporated cells.
B SHH is robustly expressed in pCAGGS and pCAGGS-RFP (control) co-electroporated NC cells. Scale bar = 25 μm

4.2.3 *Tbx18* loss-of function in the prechordal mesoderm

To directly establish the role of *Tbx18* in the prechordal mesoderm siRNA vectors targeted to *Tbx18* were also designed as described earlier (Shiau et al., 2008; see materials and methods). Target sequences were amplified by PCR and cloned into pRFPRNAiC backbone (Figure 4.10). Their transcription is driven by a chicken specific promoter, Chick U6 promoter. The plasmid also contains a RFP cassestte driven by ß-actin promoter to allow visualization of the electroporated cells. Work is currently ongoing to successfully electroporate the vectors into the prechordal mesoderm.

4.3 Discussion

Studies described here show that *Tbx18* might play a role in suppressing notochord identity although further testing is required by analysing a larger sample of embryos. Misexpression of *Tbx18* in the notochord suppressed the expression of the notochord marker 3B9 in a cell non-autonomous way, with transfected and non-transfected cells downregulating 3B9 (Figure 4.5).

The mechanism through which *Tbx18* exerts this effect is not mediated by apoptosis of NC cells (Figure 4.6). Neither does it govern the expression of the prechordal mesoderm marker, *Gsc*, suggesting that it does not induce or maintain prechordal mesoderm identity (Figure 4.7). Instead the analysis of SHH in serial adjacent

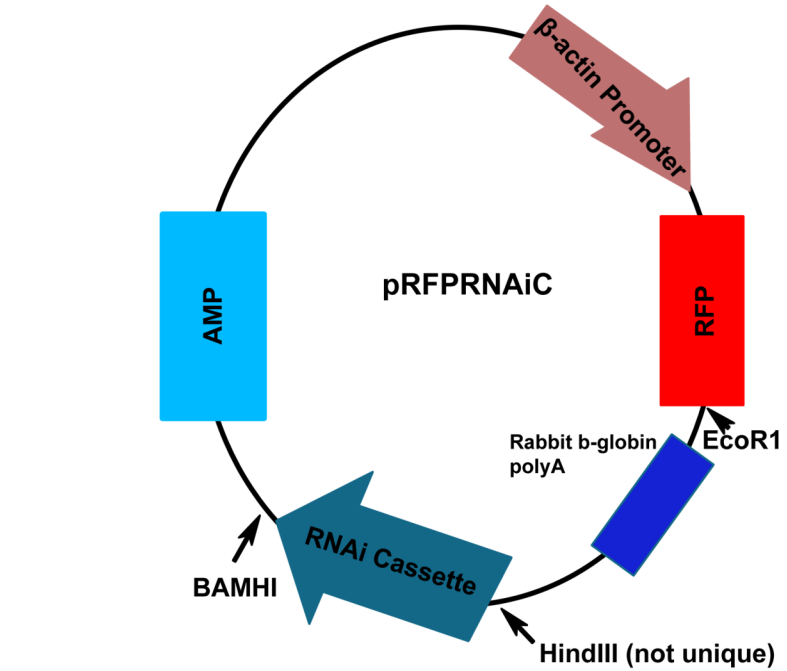

Figure 4.10 SiRNA synthesis

Schematic shows the pCAGGS backbone of the SiRNA vectors. RFP is cloned into the EcoR1 site of the BamH1-HindIII fragment. SiRNA hairpin is cloned into the RNAi cassette driven by chick U6 promoter. (Adapted from Shiau et al., 2008).

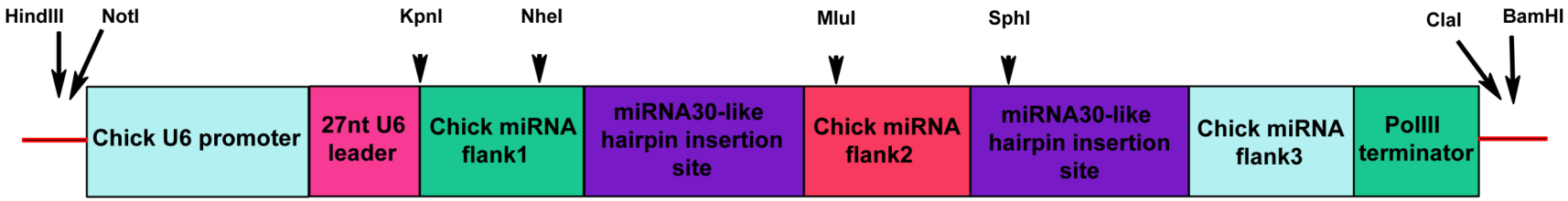

sections suggests that these cells might have a profile of a third type of axial mesoderm cell (Figure 4.9).

This third type of axial mesoderm cell may sit at the boundary of PM and NC (Figure 4.9). In future it will be critical to characterise this region *in vivo* to see if it is *Tbx18*+, *Gsc*- and 3B9-, supporting the hypothesis that *Tbx18* creates a boundary between PM and NC by creating a cell population with a distinct marker profile. This will suggest a novel way of restricting cell mixing in the axial mesoderm and protecting distinct prechordal mesoderm and notochord cell populations. Further future studies are required to address the mechanism through which Tbx18 operates to confer these distinct cell properties.

One possibility suggested by studies of *Tbx18* in other regions (Bussen et al., 2004; Airik et al., 2006; Trowe et al., 2008) is that *Tbx18* regulated adhesive properties of PM cells. An intriguing observation from these studies is that, post-electroporation, cells misexpressing *Tbx18* cells were almost always found in a cluster. This suggests that *Tbx18* may confer an adhesive property to these cells such that they adhere to one another thus creating a boundary between themselves and their neighbours. Alternatively cells may gain chemo-attractant or repulsive characteristics allowing them to aggregate together and repel cells that do not possess the same properties as themselves. Interestingly, the receptors EphA4 and EphA3 (involved in chemotaxis) are expressed in the notochord of the chick embryo, expression of Eph/Ephrin family members has yet to be reported in the prechordal mesoderm; however, wholemount in-situ hybridisation suggests EphrinB2 as a particular candidate (Baker

and Antin, 2003). In zebrafish Eph/Ephrin signalling has been shown to be involved in cell movements of prechordal mesoderm and notochord cells during gastrulation such that disruption of the pathway led to prechordal mesoderm cells lying outside of their domain (Chan et al., 2001). Future work is required to establish the mechanism of boundary formation by *Tbx18,* involving analysis of the expression of chemo-repellant and cell adhesion molecules in the axial mesoderm and the manner in which their expression pattern may be governed by *Tbx18.*

My studies suggest that *Tbx18* may lead to the establishment of a third type of axial mesoderm that sits at the NC-PM interface. No study thus far has described this cell population; given the central role that axial mesoderm plays in patterning the overlying neural tube, one can speculate that the loss of SHH from this small region may have profound effects on the patterning of the overlying mid-forebrain. Future experiments are required to examine this in detail. A critical question is that of the future fate of this third population of axial mesoderm. Studies in the lab show that it appears to be a transient structure, thus, later in development no gap in *Shh* expression is detected (Dale et al., 1999; Manning et al., 2006). Intriguingly, as Figure 4.4 shows, embryos misexpressing *Tbx18* in the notochord appear to have an enlarged heart domain. Previous studies have pointed to a link between anterior notochord and the heart field (Goldstein and Fishman, 1998), so, perhaps cells from this region contribute to the heart (I will return to this idea in Chapter 7).

In conclusion, studies described here suggest that the hypothesis that *Tbx18* might play a role in PM/NC boundary formation by

1. inducing the formation of a third type of axial mesoderm that sits at the boundary between PM and NC,
2. conferring an adhesive property to the cells so that they cluster together and
3. by inhibiting notochord characteristics in particular NC marker 3B9

Further studies are required to address the mechanism through which *Tbx18* acts to form the boundary between PM and NC. However, a second unanswered question is that of how *Tbx18* expression is governed in the prechordal mesoderm. In the next chapter, I set out to address how the expression of *Tbx18* is controlled in the PM.

CHAPTER 5

Tbx18 is governed by both canonical and non-canonical Nodal signalling pathways

5.1 Introduction

Nodal signalling plays a conserved role in the formation of the prechordal mesoderm as described in the main Introduction (see Chapter 1 Table 1.1). For example, mouse embryos that are mutant for FoxH1, one of the target genes of Nodal, lack anterior and midline structures (Hoodless et al., 2001; Yamamoto et al., 2001. The zebrafish mutant *schmalspur*, that lacks FoxH1 function, also shows broad anterior and midline defects including defects in the PM (Pogoda et al., 2000; Sirotkin et al., 2000). Xenopus studies using blocking antibody for FoxH1 and injection of dominant negative FoxH1 also eliminate PM (Watanabe and Whitman, 1999). These studies demonstrate that Nodal plays an early and conserved role in the formation of prechordal mesoderm.

The loss of PM in these studies is unsurprisingly accompanied by a loss of PM expressed genes including *Gsc*. The loss of tissues precludes any understanding of whether Nodal signalling directly governs *Gsc* expression. However, other experiments suggest that it does play a direct role in *Gsc* expression. For example, *Gsc* domain is expanded when Xenopus Nodal gene *Xnr1* mRNA is injected into Xenopus embryos and conversely its expression is blocked when mRNA for a specific Nodal inhibitor Cerberus Short was injected into the embryos (Agius et al., 2000). Similarly in zebrafish, mRNA for Nodal ligands *squint* and *cyclops* can induce *Gsc* in wildtype embryos (Feldman et al., 1998; Sampath et al., 1998; Gritsman et al., 2000). Also mouse *Nodal* mRNA is capable of inducing *gsc* in zebrafish embryos (Toyama et a., 1995). Additionally, it has been shown that Nodal-related molecules control *Gsc* transcription through

a distal responsive element within the Xenopus *Gsc* promoter region (Watabe et al., 1995). Transduction of Nodal-related signal results in a complex of transcription factors Smad2/4 and mixer on distal promoter element activating *Gsc* transcription (Germain et al., 2000). The motif identified as crucial in transcription factor mixer for mediating Smad2 interaction is also present on FoxH1, so a common mechanism exists for Smad recruitment to the distal element (Germain et al., 2000). Further, a specific FoxH1 binding site has also been identified in the mouse *Gsc* promoter, which is required for *Gsc* transcription by Nodal signalling (Labee et al., 1998). Thus, Nodal signalling is able to directly activate *Gsc* transcription.

Most of the studies describing the role of Nodal in prechordal mesoderm development, focus on an early role for Nodal signalling, examining its ability to govern the early induction of *Gsc* in PM precursors (Varlet et al., 1997; Feldman et al., 1998). So, these studies focus on the role of Nodal signalling as the PM is migrating out of the organiser and has not fully extended.

Recent evidence in the Placzek lab suggests that Nodal signalling has an additional role, governing the PM post-extension. These studies show that Nodal maintains the expression of SHH in the PM over the period HH stage 6-12 (Ellis et al., in revision). However, interestingly, it is the unprocessed Pro form (ProNodal) that is essential for SHH maintenance. Moreover, ProNodal appears to operate in this case by binding and activating Fgf receptor 3 (FgfR3) rather than the canonical ALK receptors, through which proteolytically cleaved Mature Nodal acts.

As yet, no study has yet investigated whether Nodal signalling governs other later characteristics of the PM when it has fully extended in part because no marker has been shown to be expressed post-extension. My analyses show that *Tbx18* can be detected only from HH stage 6 chick embryo, which allows me to ask whether *Tbx18* is governed by Nodal signalling? Here I set out to address this question and ask additionally whether Nodal acts in its pro-form via the novel FgfR3 pathway and/or its mature form, via the canonical ALK receptor pathway, to regulate *Tbx18* in the PM.

5.2 Results

5.2.1 Expression of *Nodal* in the PM

If Nodal signalling functions in the PM then its expression may well persist post gastrulation from stage 6 in the chick embryo. Figure 5.1 shows that indeed *Nodal* is expressed in the PM and is absent from the NC at HH stage 8 (Ellis et al., *in revision*). I did not analyse the expression of *Nodal* at any other stages, because it has such weak expression in the PM, requiring long development.

5.2.2 Expression of FgfR3 in the PM

As mentioned in the Introduction (Table 1.1 and 1.2) a wealth of evidence shows that Mature Nodal acts through the canonical ALK receptor pathway. By contrast ProNodal acts via the novel FgfR3 pathway (Ellis et al., in revision). If either Mature Nodal or ProNodal

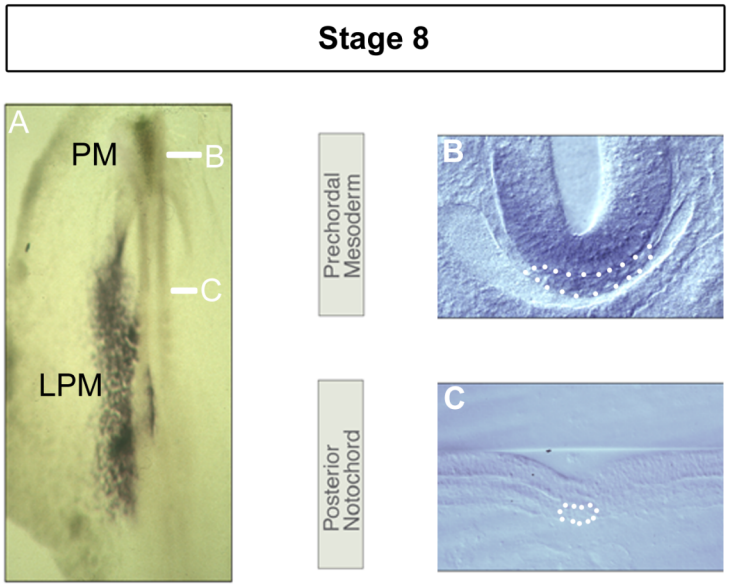

Figure 5.1 Expression of *Nodal* at HH Stage 8.

A
Nodal is expressed in the PM and the lateral plate mesoderm (LPM) of a stage 8 chick embryo.

B-C
Transverse sections show that Nodal is expressed in the PM (outlined by dotted line) and the overlying neurectoderm but it is absent from the posterior NC (outlined by dotted line).

With permission from Professor Marysia Placzek (University of Sheffield).

operate in the fully extended PM, expression of ALK receptors and FgfR3 should be detected in the PM post-gastrulation.

Unfortunately due to a lack of functional antibodies and RNA probes targeted to ALK receptors, I was unable to confirm its expression pattern in the PM. However, it has been shown in Xenopus that ALK4 is expressed in the PM and notochord (Chen et al., 2005). Also ALK co-receptor, Cripto is expressed and has a function in the chick PM (Colas and Schoenwolf, 2000; Chu et al., 2005).

I was, however, able to confirm that *FgfR3* is expressed in the PM and the overlying neuroectoderm at HH stages 6-10 (Figure 5.2 B-D). I did not detect any expression earlier (at stage 5) and only weak expression was seen at stage 13 (Figure 5.2 A and E). In the posterior head process mesoderm, *FgfR3* is similarly absent at HH stage 5, but it is broadly detected in the NC and overlying neuroectoderm at HH stages 6-10 (Figure 5.2 F-I). *FgfR3* expression becomes more complicated in the NC at stage 13, when weak expression persists in the anterior NC (data not shown) but not in the posterior NC (Figure 5.2 J).

5.2.3 ProNodal and Mature Nodal can upregulate *Tbx18* in the NC

I next set out to establish the role of Nodal signalling in the specification of chick assaying both ProNodal and Mature Nodal for their ability to induce PM markers.

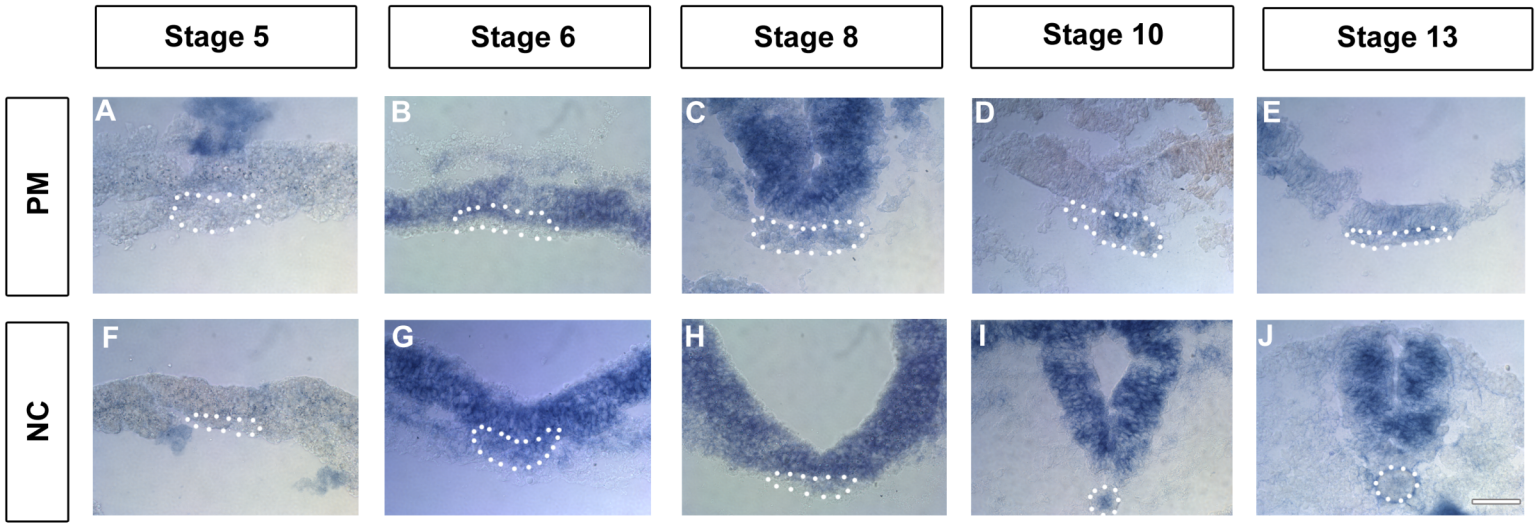

Figure 5.2 Expression of *FgfR3* at HH stage 5 – 13.

A-E
Transverse sections show that *FgfR3* is not expressed in the anterior head process mesoderm (outlined by dotted lines) at HH stage 5 but it is expressed in the PM and the overlying neurectoderm (outlined by dotted lines) at HH stages 6-10. Its expression is weak in the PM stages 6 and stage 13.

F- J
It is absent at HH stage 5 from the posterior head process mesoderm. Transverse sections through the trunk show that *FgfR3* is expressed in the NC and the neurectoderm from stage 6-10 (outlined by dotted lines). At stage 13 its expression cannot be detected in the NC but it persists in the neurectoderm. Scale bar = 50 μm

ProNodal was obtained from 293T cells transiently transfected with plasmid encoding a cleavage mutant form of Nodal, which secretes only the ProNodal form into the supernatant. Western blot analysis of conditioned medium showed a protein band of the correct molecular mass (Figure 5.3 A, Ellis et al., *in revision*). In addition a recombinant mature Nodal (R&D systems) was assayed, having first performed western blot analysis to confirm a protein with the correct molecular mass (Figure 5.3 B).

HH stage 6 NC explants were used as a test bed, to determine if ProNodal and/or Mature Nodal are sufficient to induce expression of *Gsc* and *Tbx18* in extended axial mesoderm (Figure 5.4 A). Before asking whether ProNodal/Mature Nodal can upregulte PM markers I asked if NC is able to respond to ProNodal/Mature Nodal by downregulating standard NC markers. To determine the extent of downregulation, the length of the entire NC, and the length of expression pattern of the protein/gene tested, were measured and percentage expression was then calculated and compared to controls (Figure 5.4 B, see materials and methods section 2.8).

This experiment was performed at three concentrations for both proteins, to determine an optimal concentration. The concentration range was based on an independent assay in which a similar concentration range of Nodal antagonises BMP7 (Ellis et al., in revision). Although the precise concentration of ProNodal obtained from cell supernatant is unknown, by running it alongside the known concentration of Mature Nodal we were able to estimate a comparable concentration range for use in these assays. This was

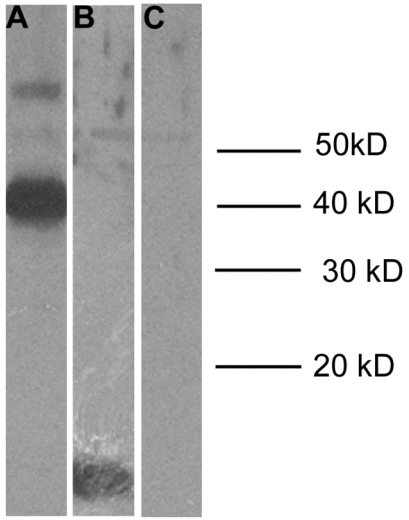

Figure 5.3

Western Blot analysis of ProNodal (from transfected 293T cell supernatant) and Mature Nodal (R&D systems).

A ProNodal: 45kD
B Mature Nodal: 15kD
C Mock Transfected control

Proteins were detected with anti-Nodal Rabbit polyclonal at 1:4000.

With permission from Pam Ellis (Placzek lab, University of Sheffield).

done by comparing the strength of the ProNodal protein band to the Mature Nodal protein band.

NC cultured with ProNodal downregulates 3B9 at 1x and 3x but not at 0.25x compared to controls (Figure 5.4 C-F). At 1x 53% of the NC continued to express 3B9 compared to 80% at 3x. *Chrd* was downregulated at 0.25x (60%) and 1x (63%) but not at 3x (78%) (Figure 5.4 G-J). It is surprising to see that 0.25x and 1x downregulated NC markers more than 3x. This might be due to the high concentration of protein activating a negative feedback mechanism preventing downregulation of NC markers.

In response to Mature Nodal, 3B9 was downregulated at 250 ng/ml and 100 ng/ml but not at 50 ng/ml compared with controls (Figure 5.5 A-D). *Chrd* was downregulated at all three concentrations (Figure 5.5 E-H). However, at 250 ng/ml, downregulation was most robust, with, only 36% of the NC continuing to express 3B9 and 40% expressing *Chrd* compared, to 76% 3B9 and 60% *Chrd* at 100 ng/ml (the second highest).

Thus, NC markers were maximally suppressed using 1x ProNodal and 250 ng/ml Mature Nodal. These protein concentrations are within a similar range to each other, based on band intensities revealed by Western blot (Figure 5.3). Thus, ProNodal at 1x and Mature Nodal at 250 ng/ml were chosen for analysis of higher number of explants in which, (a) serial adjacent sections were analysed for downregulation of NC markers and concomitant upregulation of PM markers and (b) statistical analyses were performed to point the significance of my results.

Figure 5.4 Downregulation of NC markers in NC explants at different concentrations of ProNodal.

A
Schematic showing NC explants dissected from HH stage 6 embryo cultured on collagen beds for 16 hours.

B
Schematic demonstrates the method of scoring used to indicate the change in expression markers in the NC post culture. % of positive expression calculates in indicated in brackets in C-J.

C-F
NC explants cultured with medium containing ProNodal at 0.25x, 1x and 3x (B-D) or under control conditions (E) for 16 hours. NC marker 3B9 is downregulated the most post culture with medium containing ProNodal at 1x.

G- J
NC explants cultured with medium containing ProNodal at 0.25x, 1x and 3x (G-I) or under control conditions (J) for 16 hours. NC marker *Chrd* is downregulated the most post culture with medium containing ProNodal at 1x.

Scale bar = 50 μm

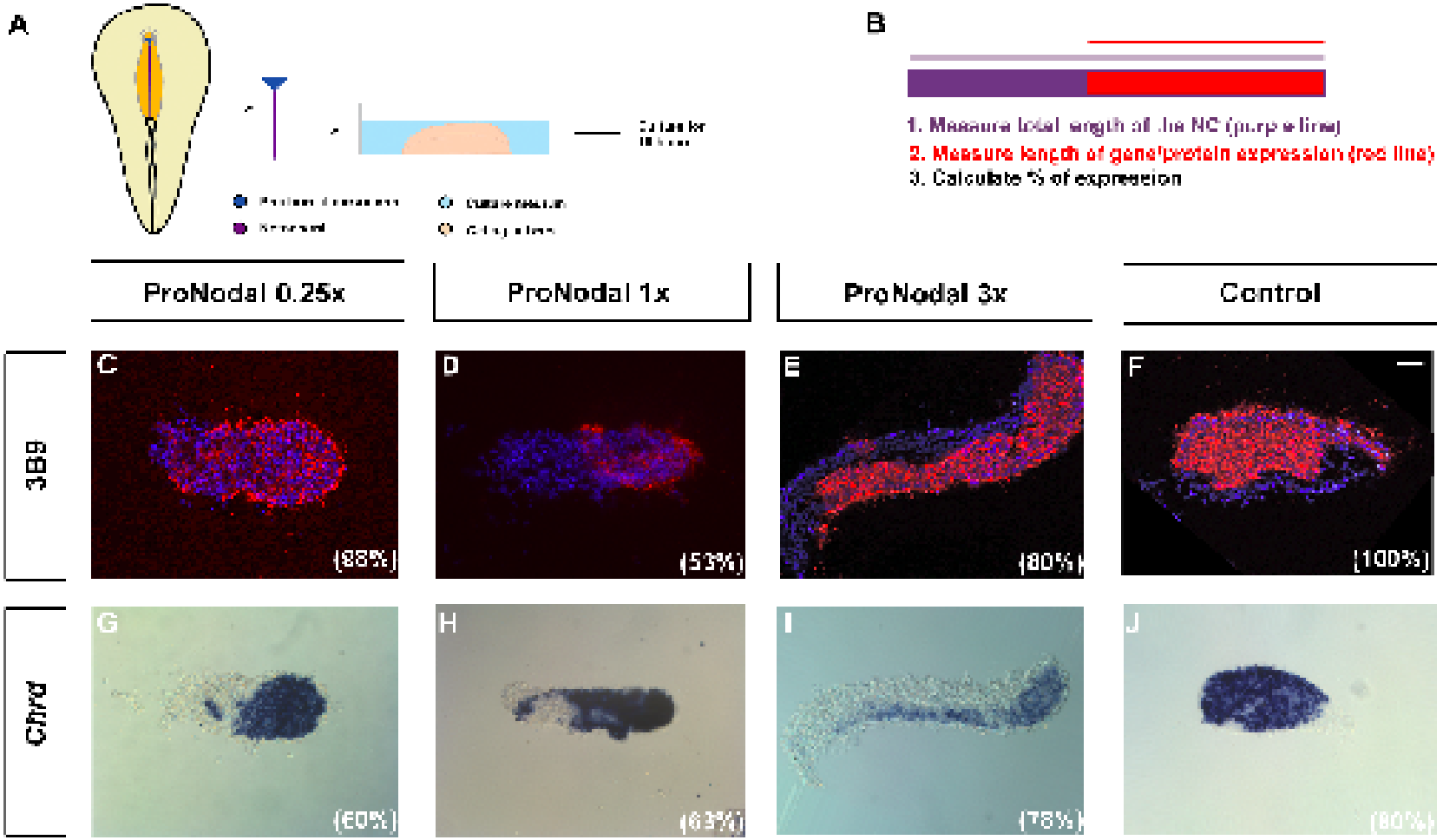
A
B
1. Measure total length of the NC (purple line)
2. Measure length of gene/protein expression (red line)
3. Calculate % of expression
ProNodal 0.25x
ProNodal 1x
ProNodal 3x
Control
3B9
Chrd
C
D
E
F
G
H
I
J
(88%)
(53%)
(80%)
(100%)
(60%)
(63%)
(75%)
(80%)

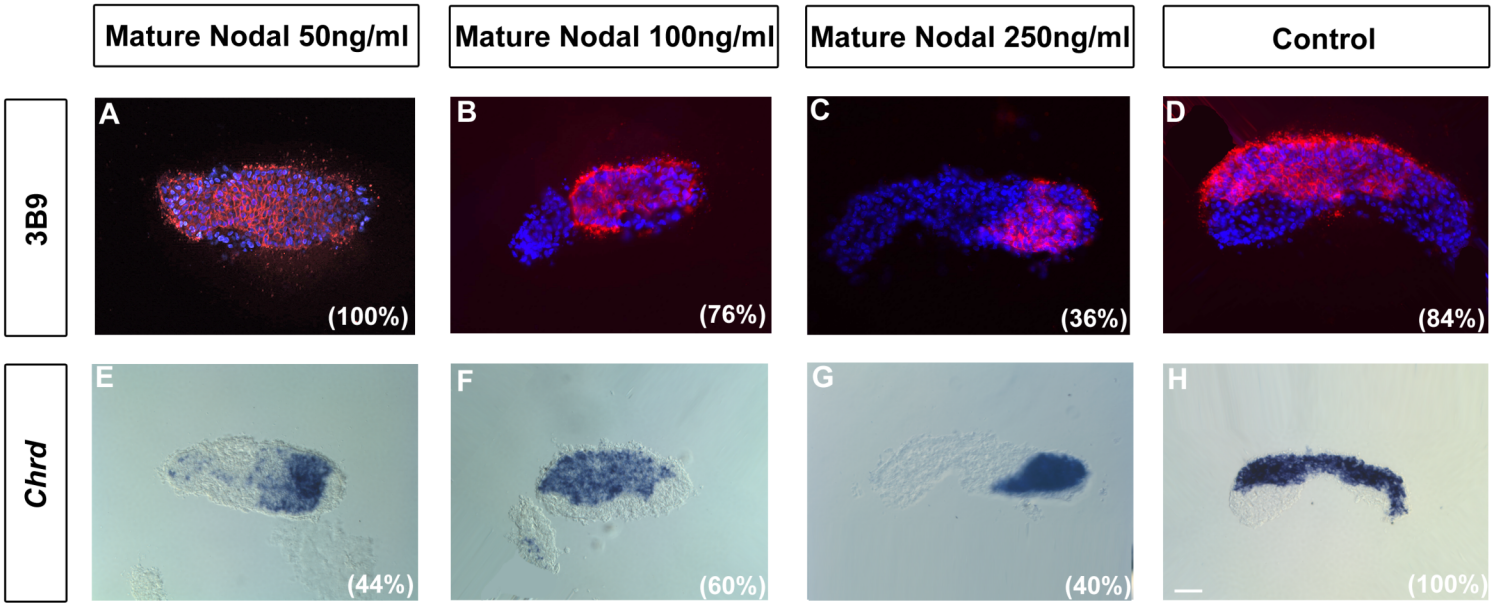

Figure 5.5 Downregulation of NC markers in NC explants cultured with different concentrations of Mature Nodal.

A-D

Expression of 3B9 is detected and measured (% of positive expression is indicated in brackets) in NC explants cultured with medium containing Mature Nodal at 50ng/ml, 100ng/ml or 250ng/ml (A-C) or under control conditions (D) for 16 hours. NC treated with 250ng/ml Mature Nodal downregulates 3B9 the most.

E- H

Expression of *Chrd* is detected and measured (% of positive expression is indicated in brackets) in NC explants cultured with medium containing Mature Nodal at 50ng/ml, 100ng/ml or 250ng/ml (E-G) or under control conditions (H) for 16 hours. NC treated with 250ng/ml Mature Nodal downregulates *Chrd* the most. Scale bar = 50 μm

After culture with medium containing 1x ProNodal, NC showed a significant downregulation in 3B9 and *Chrd* compared to the NC cultured with mock-transfected control supernatant (3B9 P value = 0.02 and *Chrd* P value = 0.05) (Figures 5.6 A, B, I and J, 5.7 A and B). Downregulation was observed in all cells in a specific region of the NC (i.e. not in all the cells of the NC). In serial adjacent sections, the downregulation in NC markers was accompanied by a significant upregulation of *Tbx18* (P value = 0.04) compared to controls (Figures 5.6 C and K, 5.7 C). *Gsc* was also significantly upregulated (P value = 0.02) (Figures 5.6 D and L, 5.7 D).

Similarly, NC cultured with Mature Nodal (250 ng/ml) also downregulated 3B9 and *Chrd* from one region of the NC (3B9 P value = 0.05, *Chrd* P value = 0.03) (Figures 5.6 E, F, I and J, 5.7 A and B). Again serial adjacent sections showed a significant upregulation in *Tbx18* in the same region in which 3B9 and *Chrd* were downregulated (P value = 0.01) (Figure 5.6 G and K, 5.7 C). *Gsc* was also upregulated in the same region as *Tbx18* (Figure 5.6 H and L) although unlike ProNodal, the upregulation of *Gsc* by Mature Nodal did not appear to be statistically significant (P value = 0.38) (Figure 5.7 D). However, I am repeating these experiments as variable results observed maybe explained by technical difficulties (see discussion).

5.2.4 Nodal signalling is required for *Tbx18* expression in the PM

These experiments show that ProNodal and Mature Nodal can upregulate *Tbx18* and *Gsc* in NC explants. To directly test if Nodal

Figure 5.6 ProNodal and Mature Nodal downregulate NC markers and upregulate PM markers in NC explants.

A-D
NC explants cultured with medium containing ProNodal at 1x for 16 hours. Post culture NC markers 3B9 and *Chrd* downregulate in most of the explant, whereas, PM markers *Tbx18* and *Gsc* are upregulated.

E- H
NC explants cultured with medium containing Mature Nodal 250 ng/ml for 16 hours. Post culture NC markers 3B9 and *Chrd* downregulate in most of the explant, whereas, PM markers *Tbx18* and *Gsc* are upregulated.

I - L
NC explants cultured under control conditions for 16 hours. Post culture 3B9 and *Chrd* are expressed robustly, additionally, weak expression of *Tbx18* is also detected, however, *Gsc* is not expressed in the explants.

Scale bar = 50 μm

3B9
Chrd
Tbx18
Gsc
ProNodal
Mature Nodal
Control
A
B
C
D
E
F
G
H
I
J
K
L

Figure 5.7 ProNodal and Mature Nodal downregulate NC markers and upregulate PM markers in NC explants

NC explants are scored by measuring the length of the explant and comparing that with the length of the explants with positive expression. Graphs represent results of two tailed t test performed using Prism software.

A
Explants cultured with medium containing ProNodal compared to explants cultured under control conditions show a significant downregulation of 3B9 (P value = 0.02). Those cultured with medium containing Mature Nodal also show a significant downregulation of 3B9 (P value = 0.05).
Control n = 4, ProNodal n = 9 and Mature Nodal n = 10

B
Explants cultured with medium containing ProNodal compared to explants cultured under control conditions show a significant downregulation of *Chrd* (P value = 0.05). Those cultured with medium containing Mature Nodal also show a significant downregulation of *Chrd* (P value = 0.03).
Control n = 8, ProNodal n = 7 and Mature Nodal n = 7

C
Explants cultured with medium containing ProNodal compared to explants cultured under control conditions show a significant upregulation of *Tbx18* (P value = 0.04). Those cultured with medium containing Mature Nodal also show a significant upregulation of *Tbx18* (P value = 0.01).
Control n = 4, ProNodal n = 3 and Mature Nodal n = 6

D
Explants cultured with medium containing ProNodal compared to explants cultured under control conditions show a significant upregulation of *Gsc* (P value = 0.02). However, those cultured with medium containing Mature Nodal compared with control conditions are not significant for *Gsc* upregulation (0.38).
Control n = 4, ProNodal n = 4 and Mature Nodal n = 4

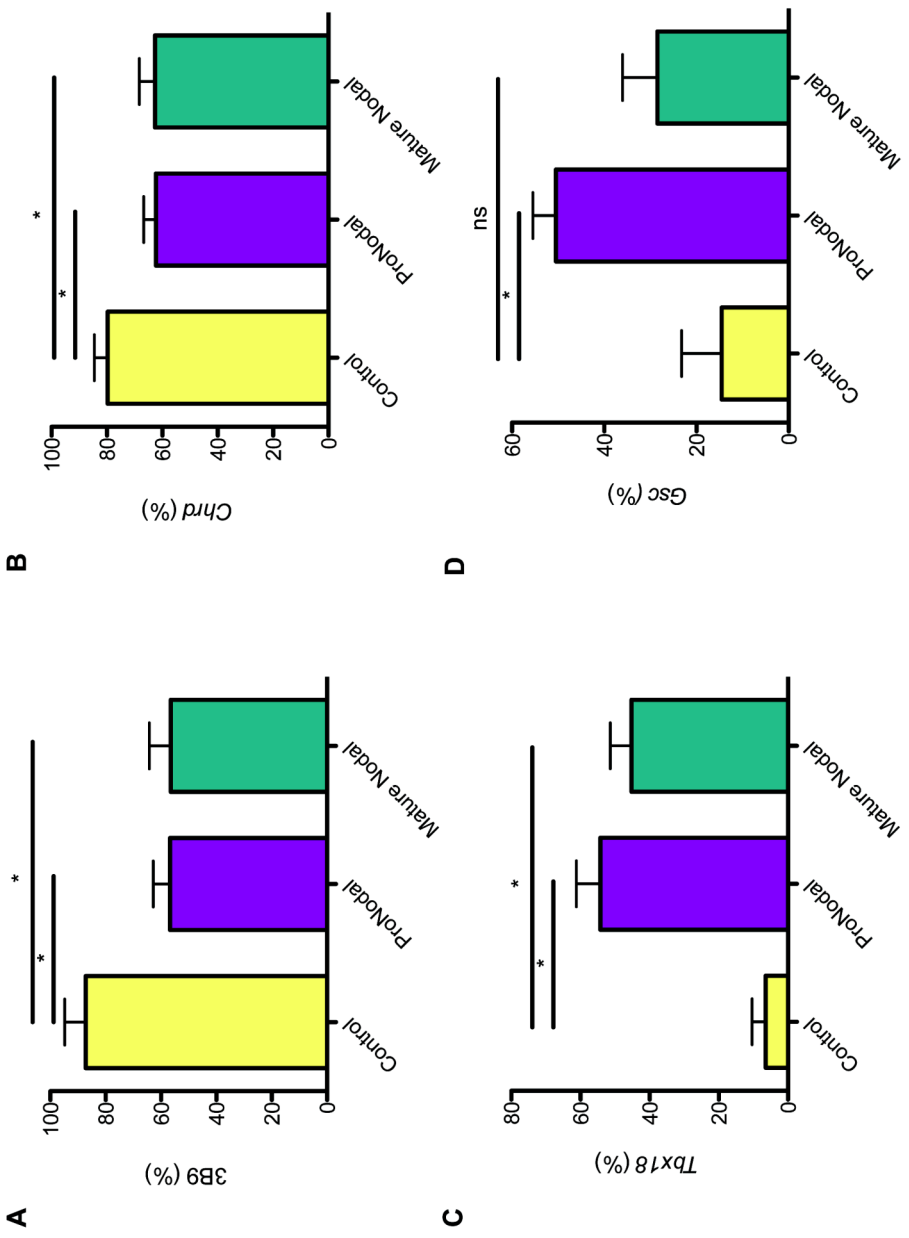
A
3B9 (%)
100
80
60
40
20
0
*
*
Control
ProNodal
Mature Nodal
B
Chrd (%)
100
80
60
40
20
0
*
*
Control
ProNodal
Mature Nodal
C
Tbx18 (%)
80
60
40
20
0
*
*
Control
ProNodal
Mature Nodal
D
Gsc (%)
60
40
20
0
ns
*
Control
ProNodal
Mature Nodal

signalling is required for the maintenance of *Gsc* and the induction of *Tbx18* in the PM, PM was dissected from HH stage 6 chick embryos and cultured for 16 hours in medium containing secreted protein Cerberus Short (CerS) (Figure 5.8 A). CerS is a specific antagonist of Nodal signalling (Piccolo et al., 1999; Belo et al., 2000) and antagonises both ProNodal and Mature Nodal (Ellis et al., in revision).

Previously in the lab it has been shown that CerS downregulates SHH in the PM, so this was used as an independent assay to determine the optimal concentration of CerS for use (Ellis et al., in revision). A concentration range of 0.25x, 0.5x and 1x was chosen based on the concentration used by Ellis et al., in revision. The area of SHH expression then compared in PM explants treated with CerS versus those treated with 1x mock-transfected control supernatant (Figure 5.8 B). Downregulation of SHH was observed at all concentrations but 1x CerS almost completely downregulated SHH (13% SHH expression) (Figure 5.8 C-E). PM explants treated with medium containing mock-transfected control supernatant continued to express SHH (Figure 5.8 F).

Gsc and *Tbx18* were next assessed, to determine if 1x CerS has an effect on their expression. Like SHH, *Gsc* was significantly downregulated in explants cultured with CerS compared to controls (SHH P value = 0.03, Gsc P value 0.008) (Figures 5.9 A, B, F and G, 5.10 A and B). Likewise, *Tbx18* was not detected in explants after culture with CerS, compared to controls (P value = 0.01) (Figures 5.9 C and H, 5.10 C).

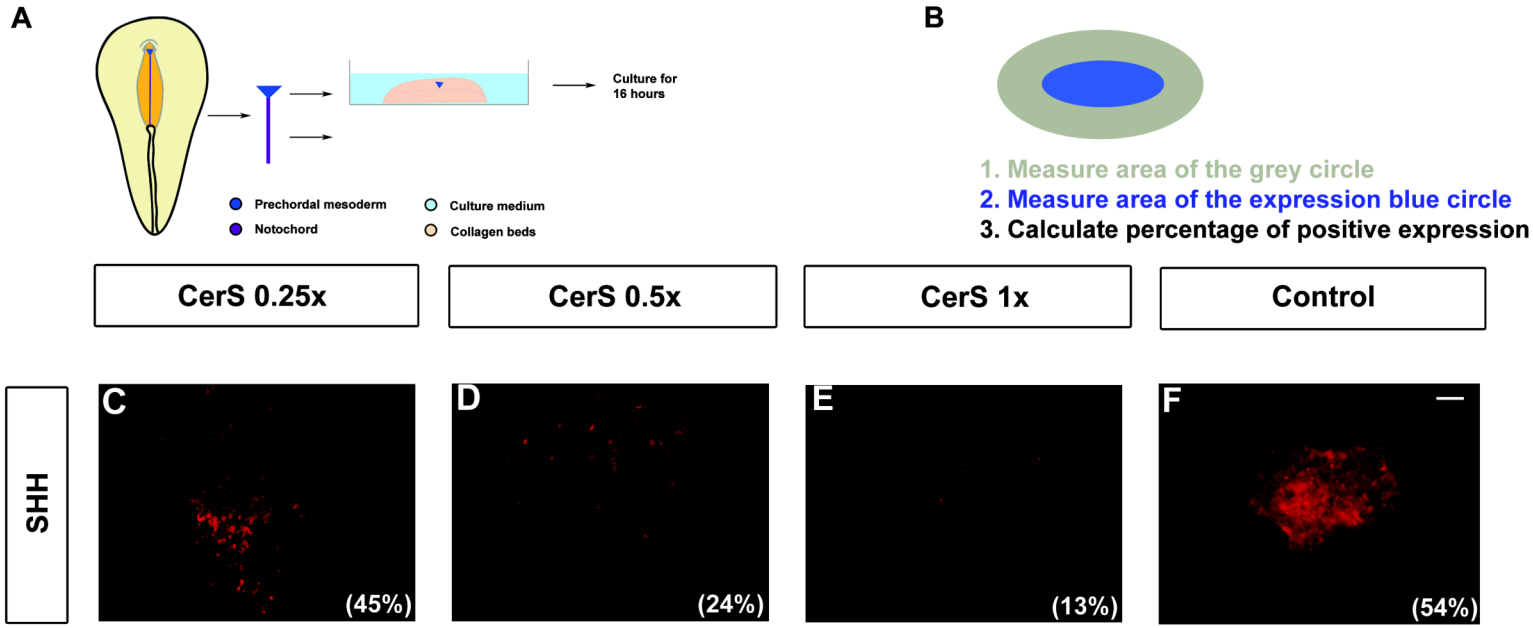

Figure 5.8 Downregulation of SHH in PM explants at different concentrations of CerS.

A
Schematic showing PM explants dissected from stage 6 embryos cultured on collagen beds for 16 hours.
B
Schematic demonstrating the method used to calculate the difference in expression post culture.
C-F
PM explants cultured with medium containing CerS at 0.25x, 0.5x and 1x or under control conditions. SHH is almost completely downregulated in PM explants cultured with medium containing CerS at 1x. Scale bar = 50 μm

Figure 5.9

Inhibition of Nodal signalling results in downregulation of PM markers *Tbx18* and *Gsc.*

A - E
In PM explants cultured with CerS at 1x, PM markers SHH, *Gsc* and *Tbx18* downregulate post culture. Expression of NC markers 3B9 and *Chrd* is not detected.

F - J
PM explants cultured under control conditions continue to express SHH, *Gsc* and *Tbx18.* NC markers 3B9 and *Chrd* are not detected post culture.

For positive control for *Chrd* and 3B9 see Figure 3.8 I and J respectively.

Scale bar = 50 μm

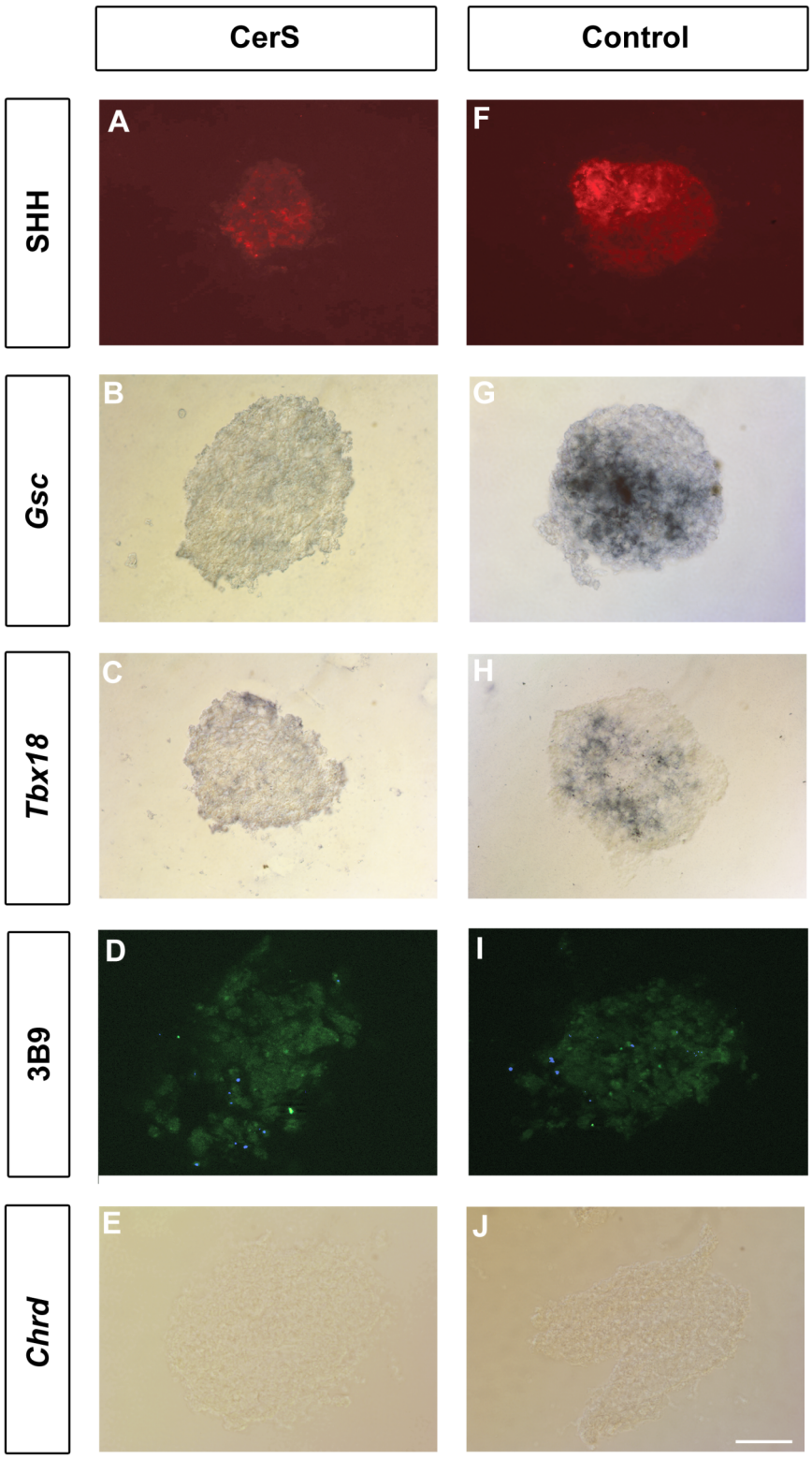
CerS
Control
SHH
Gsc
Tbx18
3B9
Chrd
A
B
C
D
E
F
G
H
I
J

Figure 5.10 Inhibition of Nodal signalling downregulates PM markers.

PM explants are scored by percentage area of the explant with positive expression. Graphs represent results of two tailed t test performed using Prism software.

A
Percentage area of PM explant with positive SHH expression is scored and explants cultured with CerS compared to explants cultured under control conditions show a highly significant downregulation of SHH (P value = 0.03).
Control n = 5
CerS = 8

B
Percentage area of PM explant with positive *Gsc* expression is scored and explants cultured with CerS compared to explants cultured under control conditions show a significant downregulation of *Gsc* (P value = 0.008).
Control n = 3
CerS = 6

C
Percentage area of PM explant with positive *Tbx18* expression is scored and explants cultured with CerS compared to explants cultured under control conditions show a significant downregulation of *Tbx18* (P value = 0.01).
Control n = 4
CerS = 6

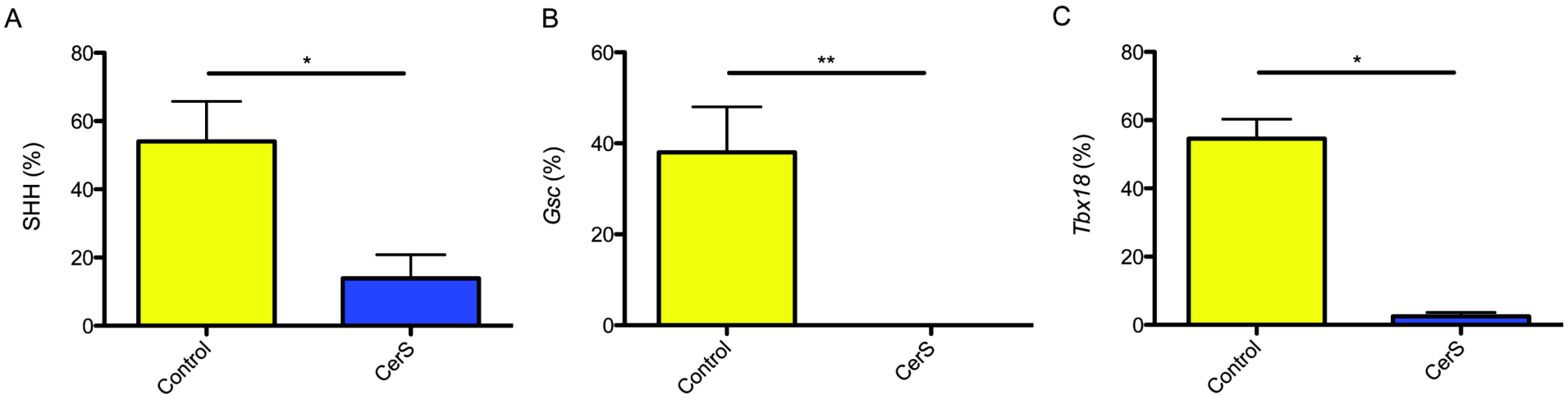
A
SHH (%)
80
60
40
20
0
*
Control
CerS
B
Gsc (%)
60
40
20
0
**
Control
CerS
C
Tbx18 (%)
80
60
40
20
0
*
Control
CerS

As PM explants lost expression of SHH, *Gsc* and *Tbx18* post CerS treatment, expression of *Chrd* and 3B9 was also analysed to see if loss of Nodal signalling was accompanied by a change in fate to NC. I could not detect 3B9 and *Chrd* in PM explant cultured with CerS media or control media (Figure 5.9 D, E, I and J).

5.2.5 Canonical and Non-canonical Nodal pathways may govern expression of *Tbx18* in the PM

As described in the Introduction it is known that Nodal largely acts via ActRII/ALK4/5/7 receptors to initiate *Gsc* expression *in vivo*. Recent work has also shown that ProNodal can bind and act via Fgf receptor 3 (Gu et al., 1998, Ellis et al., in revision). I therefore next set out to test whether the canonical ALK receptor pathway and/or the novel FgfR3 receptor pathway regulate the expression of *Gsc* and *Tbx18* in the post-extended PM.

To test this PM explants were cultured with a widely used inhibitor of ALK receptors, SB-431542 (Inmann et al., 2002) and expression of PM and NC markers analysed. Blocking ALK receptors did not have a statistically significant effect on SHH, consistent with previous studies in the lab (Ellis et al., in revision) (Figures 5.11 A and F, 5.13 A). Weak decrease in *Gsc* expression was observed (Figure 5.11 B and G, 5.13 B) (however, I am repeating these experiments as I am concerned that there are some technical difficulties). Consistent with the finding that Mature Nodal can induce Tbx18 in the NC, a significant reduction of *Tbx18* was

observed in PM with reduced Nodal signalling via ALK receptors (P value = 0.01) (Figures 5.11 C, H and 5.13 C).

I did not detect a change in 3B9 and *Chrd* expression compared to controls (Figure 5.11 D, E, I and J).

To reduce ProNodal signalling acting via FgfR3 in the PM and test if it has a direct role in governing *Gsc* and *Tbx18,* a recombinant protein called FgfR3-fc was used. FgfR3-fc competes with the endogenous FgfR3 receptor for ligand binding and thus decreases signalling downstream of FgfR3. Reduction in FgfR3 led to a significant decrease in SHH and *Tbx18* expression (SHH P value = 0.002, Tbx18 P value = 0.01) but *Gsc* was unaffected (Figures 5.12 A, B, C, F G and H, 5.13 D-F). This confirms previous results obtained in the lab describing the role of ProNodal in the maintenance of SHH in the PM (Ellis et al., in revision). They also show that ProNodal governs the expression of *Tbx18* in the PM but not *Gsc*.

Consistent with PM cultured with CerS and ALK inhibitor loss of PM markers did not lead to a change in fate to NC. 3B9 and *Chrd* could not be detected in the PM cultured with FgfR3-fc (Figure 5.12 D, E, I and J).

After culturing with both SB-431542 and FgfR3-fc expression of SHH and *Gsc* are reduced but *Tbx18* is completely down regulated compared to controls (Figure 5.14 A, B, C, E , F and G). No change was observed in 3B9 (Figure 5.14 D, and H). Due to insufficient numbers (n=2) a statistical test could not be performed.

Taken together these studies suggest that ProNodal and Mature Nodal signalling is important for initiating *Tbx18* expression. Future experiments will determine if both or one is required for maintenance of *Gsc* and/or *Tbx18*.

Figure 5.11

Inhibition of canonical Nodal signalling via ALK receptor results in downregulation of PM markers *Tbx18* and *Gsc.*

A - E
Post culture with ALK inhibitor, SHH is not downregulated, *Gsc* is weakly downregulated and *Tbx18* is completely downregulated in PM explants. NC markers 3B9 and *Chrd* are not expressed post culture.

F - J
In PM explants cultured under control conditions (DMSO), SHH, *Gsc* and *Tbx18* continue to be expressed. NC markers 3B9 and *Chrd* are not expressed post culture.

Scale bar = 50 μm

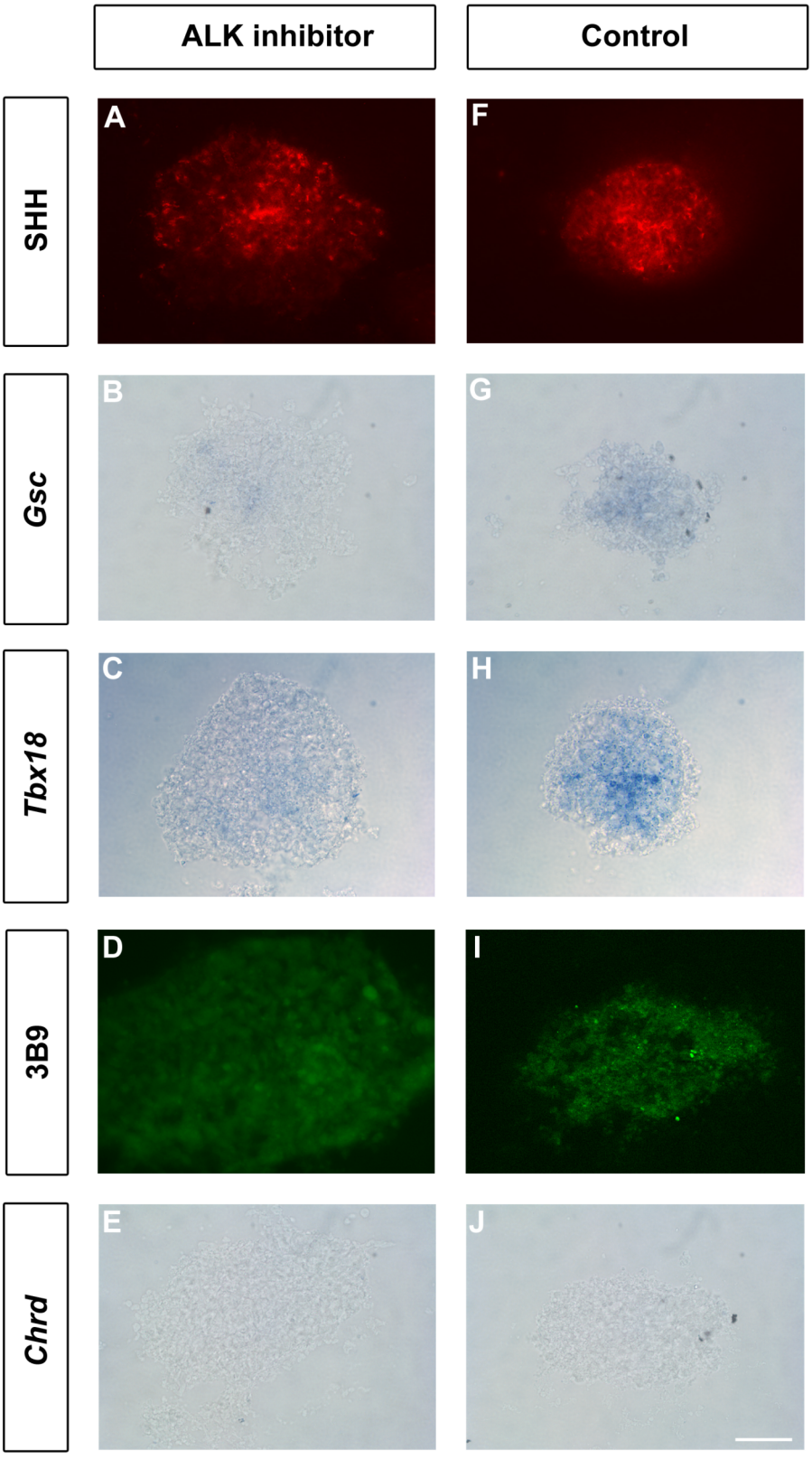
ALK inhibitor
Control
SHH
Gsc
Tbx18
3B9
Chrd
A
B
C
D
E
F
G
H
I
J

Figure 5.12

Inhibition of non canonical Nodal signalling via FgfR3 results in downregulation of PM marker *Tbx18* but not *Gsc.*

A - E
In PM explants cultured with FgfR3-fc SHH and *Tbx18* downregulate but *Gsc* is expressed after culture with FgfR3-fc. NC markers 3B9 and *Chrd* are not detected.

F - J
PM explants cultured under control conditions continue to express SHH, *Gsc* and *Tbx18.* NC markers 3B9 and *Chrd* are not detected

Scale bar = 50 μm

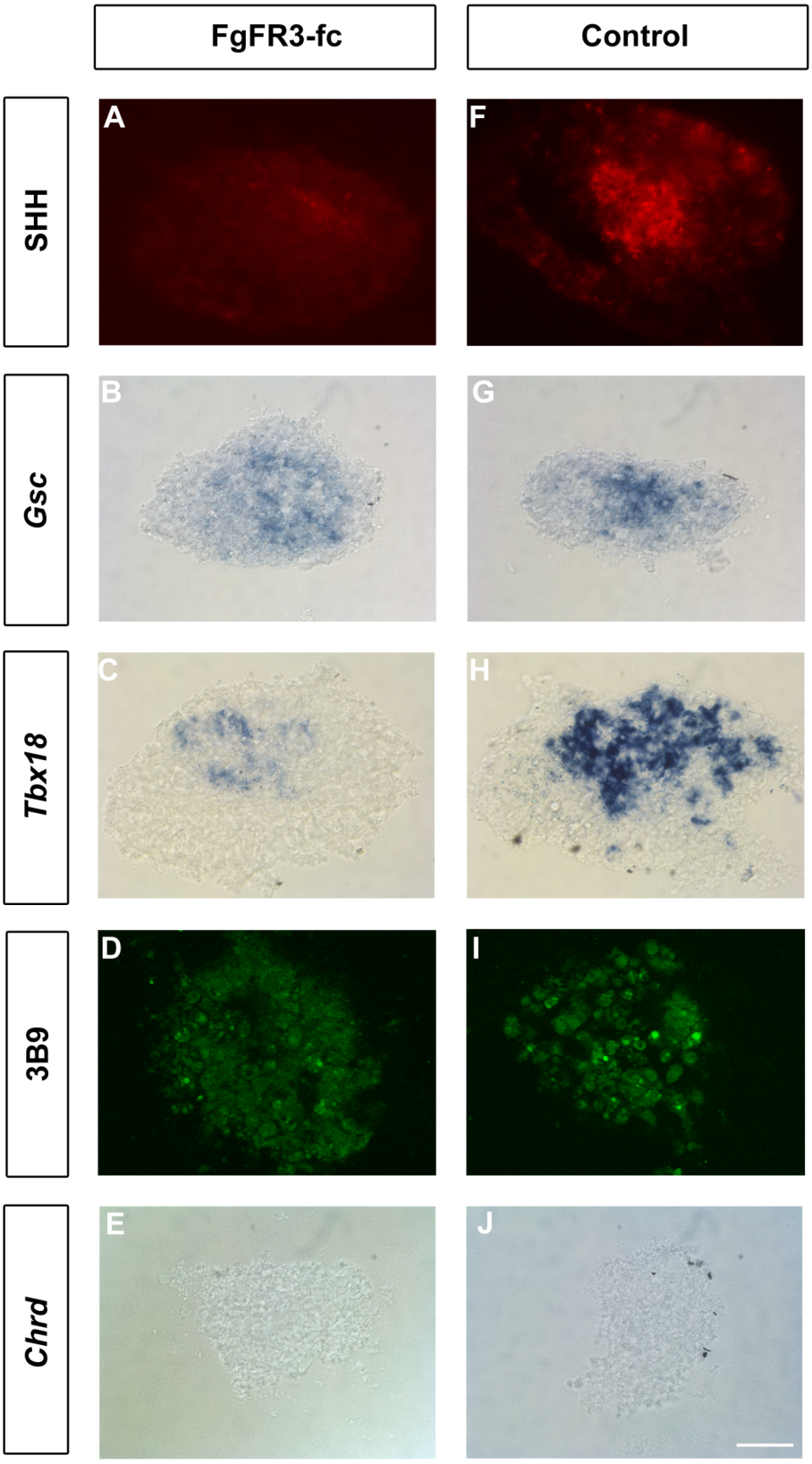
FgFR3-fc
Control
SHH
Gsc
Tbx18
3B9
Chrd
A
B
C
D
E
F
G
H
I
J

Figure 5.13 Inhibition of canonical and non canonical Nodal signalling downregulates Tbx18

PM explants are scored by percentage area of the explant with positive expression. Graphs represent results of two tailed t test performed using Prism software.

A - C
SHH expression in explants cultured with ALK inhibitor compared to explants cultured under control conditions do not show a significant downregulation of SHH. Percentage expression of *Gsc* is also non significant, however, percentage expression of Tbx18 is significantly downregulated (P value = 0.01) in explants cultured with ALK inhibitor compared to controls.
SHH: DMSO control n = 6, ALK inhibitor n = 7
Gsc: DMSO control n = 4, ALK inhibitor n = 7
Tbx18: DMSO control n = 9 , ALK inhibitor n = 14

D - F
SHH expression in explants cultured with FgfR3-fc compared to explants cultured under control conditions show a highly significant downregulation of SHH (P value = 0.002). Percentage expression of *Gsc* is not significant, however, percentage expression of Tbx18 is significantly downregulated (P value = 0.01) in explants cultured with FgfR3-fc compared to controls.
SHH: Control n = 10, FgfR3-fc n = 10
Gsc: Control n = 4, FgfR3-fc n = 3
Tbx18: Control n = 18, FgfR3-fc n = 23

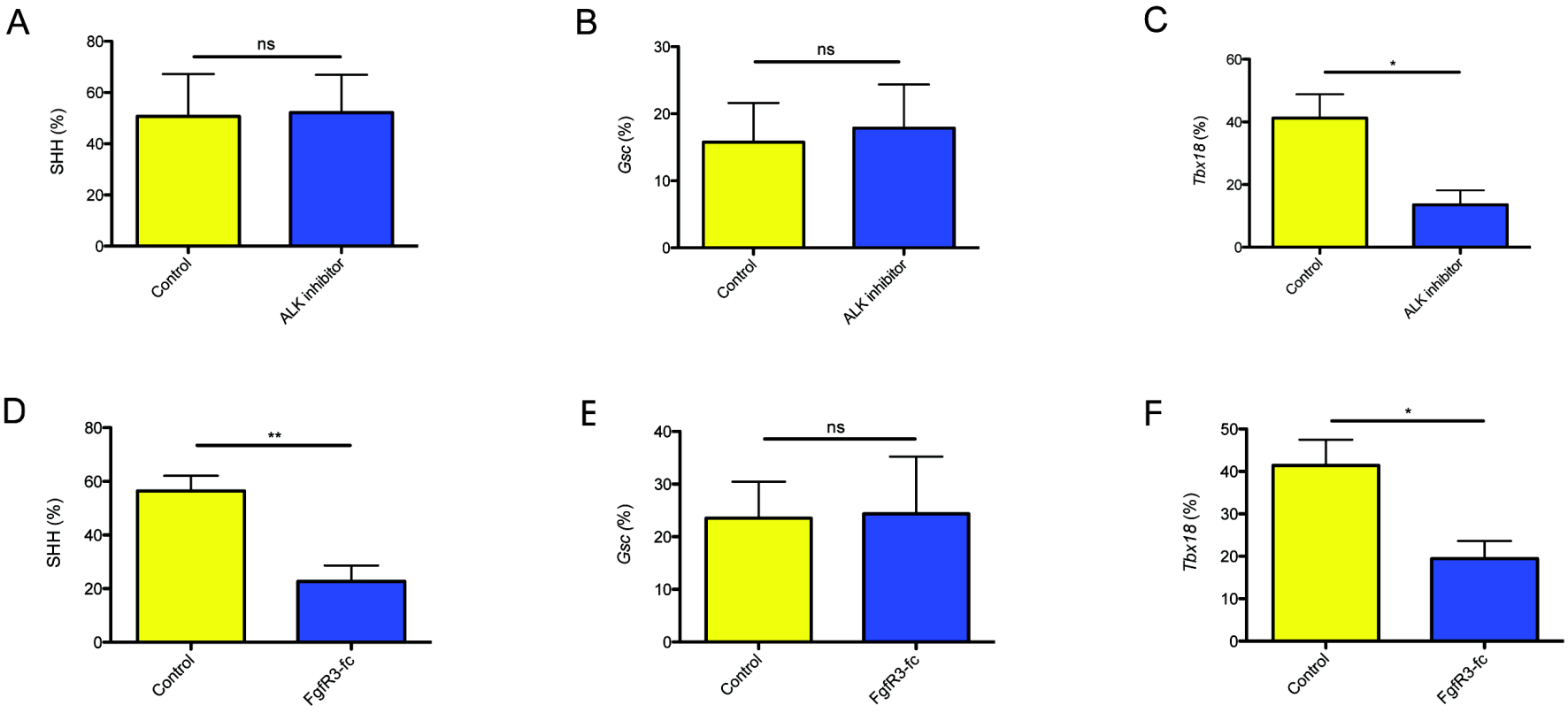
A
SHH (%)
80
60
40
20
0
ns
Control
ALK inhibitor
B
Gsc (%)
30
20
10
0
ns
Control
ALK inhibitor
C
Tbx18 (%)
60
40
20
0
*
Control
ALK inhibitor
D
SHH (%)
80
60
40
20
0
**
Control
FgfR3-fc
E
Gsc (%)
40
30
20
10
0
ns
Control
FgfR3-fc
F
Tbx18 (%)
50
40
30
20
10
0
*
Control
FgfR3-fc

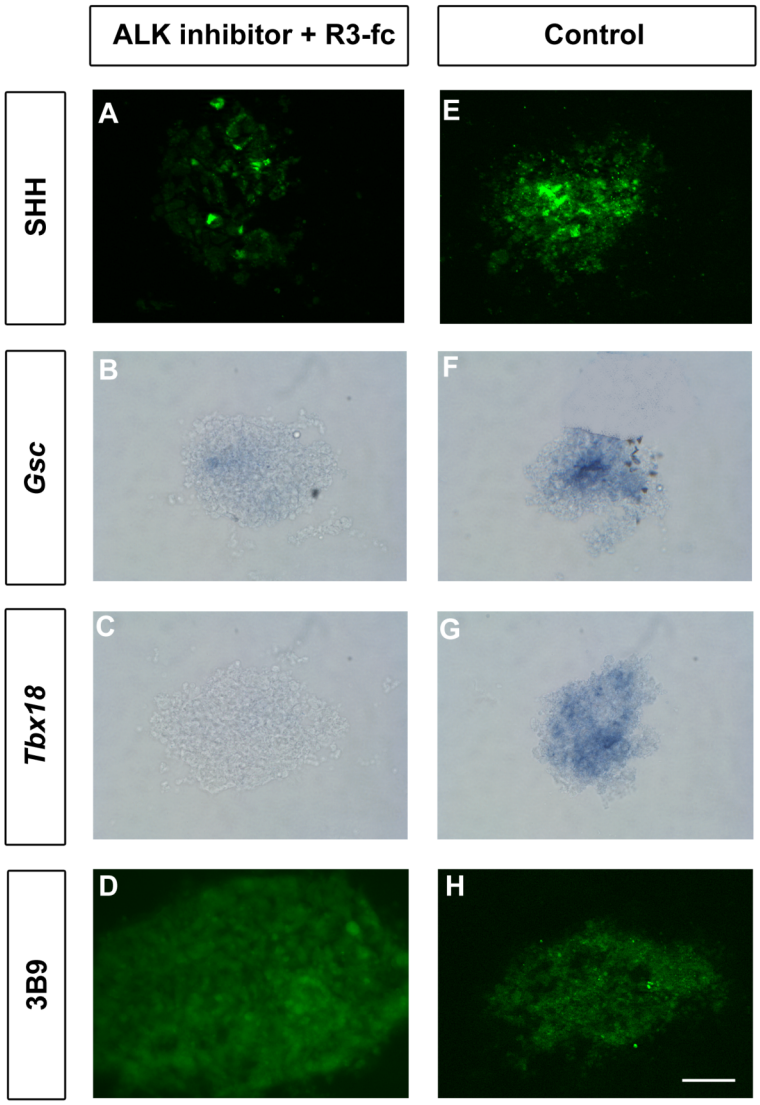

Figure 5.14

Inhibition of canonical and non-canonical Nodal signalling results in downregulation of PM markers *Tbx18* and *Gsc.*

A - D
Weak SHH and *Gsc* expression is detected post culture with ALK inhibitor and FgfR3-fc. *Tbx18* expression is downregulated after culture. NC marker 3B9 is not expressed.

E - H
In PM markers cultured under control conditions SHH, *Gsc* and *Tbx18* continue to be expressed post culture. NC marker 3B9 is not detected. Scale bar = 50 µm

5.3 Discussion

In summary, studies described here demonstrate that the late prechordal mesoderm marker, *Tbx18* behaves like earlier expressed PM markers as it is dependent on Nodal signalling for its expression. Upon inhibition of Nodal signalling by Cerberus Short SHH, *Tbx18* and *Gsc* are downregulated in the PM (Figures 5.9 and 5.10). This also shows that Nodal signalling plays a late role in the PM by continuing to regulate the expression of PM markers.

Further it has recently been found that Nodal can bind and activate FgfR3 and this novel pathway is involved in SHH maintenance in the PM (Figure 5.13, Ellis et al., submitted). Inhibiting Nodal signalling via canonical ALK receptor and/or the novel FgfR3 inhibits *Tbx18,* thus it operates downstream of ALK receptors and FgfR3 (Figures 5.11, 5.12 and 5.13). However, *Gsc* continues to be expressed when FgfR3 is inhibited but its expression though not statistically significant is weak in PM explants cultured with ALK inhibitor (Figures 5.9, 5.10, 5.11, 5.12 and 5.13). Further when both ALK and FgfR3 receptors are inhibited *Gsc* expression appears to be downregulated (Figure 5.14). Thus it would be necessary to confirm this observation by increasing the number of explants analysed. However, interestingly in zebrafish organiser it has been shown that Nodal acting via ALK receptors can regulate *Gsc* expression in a one hour time window post which blocking Nodal signalling no longer downregulates *Gsc* (Hagos and Dougan, 2007). This shows that Nodal can act in a complex temporal manner to maintain *Gsc*. If indeed such a strict time window operates in the PM, this provides a potential reason for a varied result seen in Figure 5.11 B. Explants

were dissected at HH stage 6 which consists of a two hour time window more accurately represented by HH stage 6- and 6+. Thus, potentially Mature Nodal may govern *Gsc* expression at HH stage 6- but not 6+. To test this possibility it would be crucial to block Mature Nodal signalling in PM explants dissected at precise stages.

Where the inhibition of Nodal signalling by CerS led to a loss of PM markers, this effect was not accompanied by an induction of NC markers in the PM (Figure 5.9) Similarly, PM explants cultured with ALK inhibitor or FgfR3-fc also did not induce NC markers (5.11 and 5.12). Thus, although PM loses its character upon Nodal inhibition, it does not acquire other axial mesoderm i.e. NC character by default.

One of the functions of the PM is its ability to induce hypothalamic character in the overlying neural tissue (Dale et al., 1997, 1999; Ohyama et al., 2005, 2008). It would be interesting to test the signalling abilities of PM post Nodal inhibition, by culturing it with neural tissue to see if it is still capable of inducing hypothalamic cell properties. One would predict that it would no longer be able to induce hypothalamic cells as PM requires the activity of both SHH and BMP7 to be able to induce hypothalamic cells and Nodal inhibition suppresses SHH in the PM (Dale et al, 1999).

An interesting observation arising from studies where NC explants were cultured with Pro or Mature Nodal is that Nodal is sufficient to downregulate its own markers and upregulate PM marker *Tbx18* in a particular region of the NC analysed in serial adjacent NC sections. This not only suggests that NC has the ability to respond to a PM signal Nodal and change its fate to PM fate but also that this is true

for only a particular region of the NC. All the cells of the NC are therefore not competent to respond to Nodal signals. These observations raise the question of how Nodal is regulated in the axial mesoderm so that only prechordal mesoderm cells respond to it and not notochord cells despite most of them being competent to be able to do so. Also if the majority of axial mesodermal cells can respond to Nodal and become PM like, why do only a small minority of cells become PM and majority the NC? How is the posterior limit of the PM defined?

CHAPTER 6

Paraxial mesoderm and retinoic acid antagonise Nodal signalling to maintain distinct domains of prechordal mesoderm and notochord

6.1 Introduction

My studies show that Nodal plays a late role in prechordal mesoderm specification and is required for the expression of the PM marker *Tbx18* (Figure 5.9, 5.11 and 5.12). Nodal is sufficient to downregulate notochord markers and upregulate PM markers in notochord explants (Figure 5.6). This shows that notochord cells are competent to respond to Nodal signals and can change their character to prechordal mesoderm. This raises the question of how Nodal is regulated *in vivo* such that only the axial mesoderm becomes prechordal mesoderm. How is the posterior extent of prechordal mesoderm defined? Evidence in other species suggests that the concentration of Nodal signal that an axial mesoderm cell receives is important to determine its fate, such that high concentrations of Nodal are required for prechordal mesoderm fate and lower concentrations for notochord fate (Schier et al., 1997). This raises the possibility that there are mechanisms that restrict high Nodal signalling to anterior-most regions of the axial mesoderm.

Alternatively, it is possible that axial mesoderm is not homogeneous, and that different regions possess different competence to respond to Nodal signalling. In support of this idea, my studies suggested that not all the notochord cells are Nodal responsive: a distinct population of notochord cells clustered at one end of the notochord explants does not respond to Nodal signals (Figure 5.6). This NC population maintains expression of notochord markers and does not upregulate prechordal mesoderm markers. Could this cell population sit anteriorly at the boundary between PM and Nodal-responsive

notochord? If so this would provide a mechanism of how the posterior limit of PM is defined.

A third possibility is that both Nodal signal restriction, and axial mesoderm competence play a role in determining the posterior limit of the prechordal mesoderm. For instance, it is possible to envisage three populations of axial mesoderm:

1. Nodal responsive anterior axial mesoderm that encounters high levels of Nodal signal and forms the PM.
2. Anterior notochord that has the ability to respond to Nodal but does not *in vivo* due to low concentration of Nodal signal or the presence of another factor that inhibits Nodal signaling.
3. Nodal unresponsive posterior notochord.

Thus, my aims in the studies below are to determine the position of Nodal unresponsive notochord cells, and to understand how Nodal signalling is regulated in the notochord such that the posterior limit of the prechordal mesoderm is defined.

6.2 Results

6.2.1 Posterior end of the notochord is ProNodal non-responsive

As described above, cells that are Nodal unresponsive are always clustered at one end of the notochord (Figure 5.6). So, to be able to investigate their relative position in the notochord, cells at the posterior end of notochord explants were labelled with DiI (1,1′-

dioctadecyl-3,3,3′,3′-tetramethylindocarbocyanine perchlorate), a lipophyllic membrane dye that labels the whole cell and emits a red fluorescence. The explants were cultured as described in Figure 6.1A, with medium containing ProNodal. Thus Nodal was presented in a uniform manner to all notochord cells. Figure 6.1 B shows that notochord cells at the posterior end of the NC, marked by DiI, continue to express the notochord marker 3B9 (n=3). Conversely, cells in anterior regions of the notochord explant downregulated 3B9 (Figure 6.1 B). This shows that cells at the posterior end of the notochord are not competent to respond to ProNodal.

6.2.2 Notochord is not responsive to ProNodal *in ovo*

Next I investigated if NC cells can alter their fate *in ovo* if they are exposed to ProNodal. To be able to establish this I used the hanging drop method to create pellets of pCS2 CMN-transfected 293T cells that could be used as a source of ProNodal protein (see materials and methods) (Ben-Haim et al., 2006). Cells were co-transfected with a pCAGGS-RFP vector to distinguish transfected cell pellets from other tissue upon transplantion *in vivo*. Figure 6.2 shows an example of a pellet, successfully transfected with pCAGGS-RFP vector with cells fluorescing red. An empty pCS2+ vector and pCAGGS-RFP were co-transfected into 293T for control cell pellets.

Next, I determined that the pellets were secreting sufficient ProNodal protein to downregulate the notochord marker 3B9, i.e. with an efficiency similar to that observed with the soluble protein (shown in Figure 5.6). I cultured notochord explants with either ProNodal-

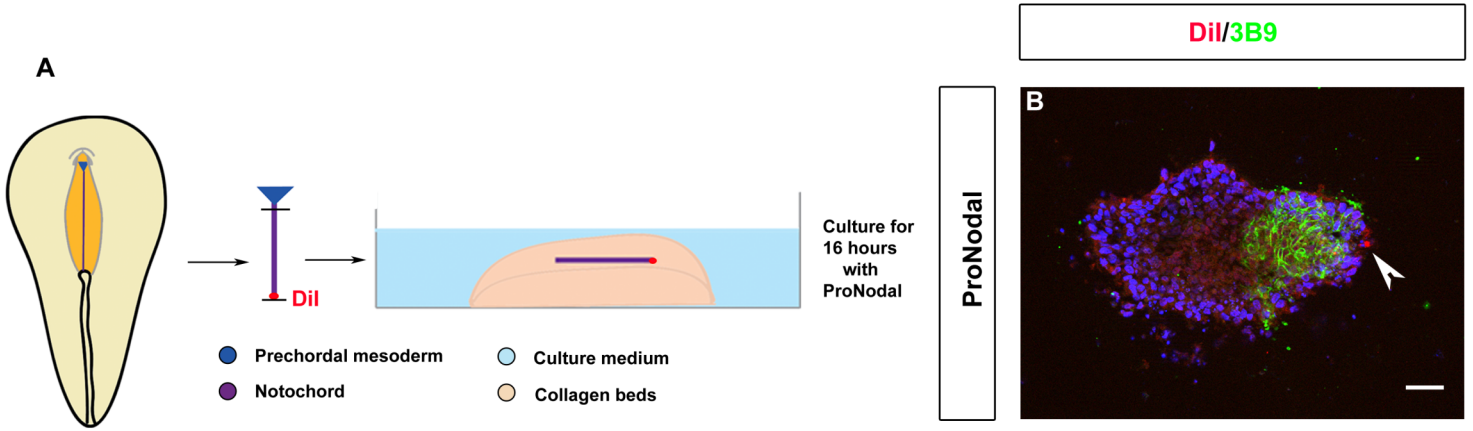

Figure 6.1 Cells at the posterior end of the notochord are Nodal unresponsive.

A Schematic showing HH stage 6 NC marked with DiI at its posterior end and then cultured with medium containing ProNodal.

B NC cells labelled with DiI at the posterior end (marked by arrowhead) continue to express 3B9 whereas anterior cells downregulate 3B9 post culture with ProNodal.

Scale bar = 50 μm

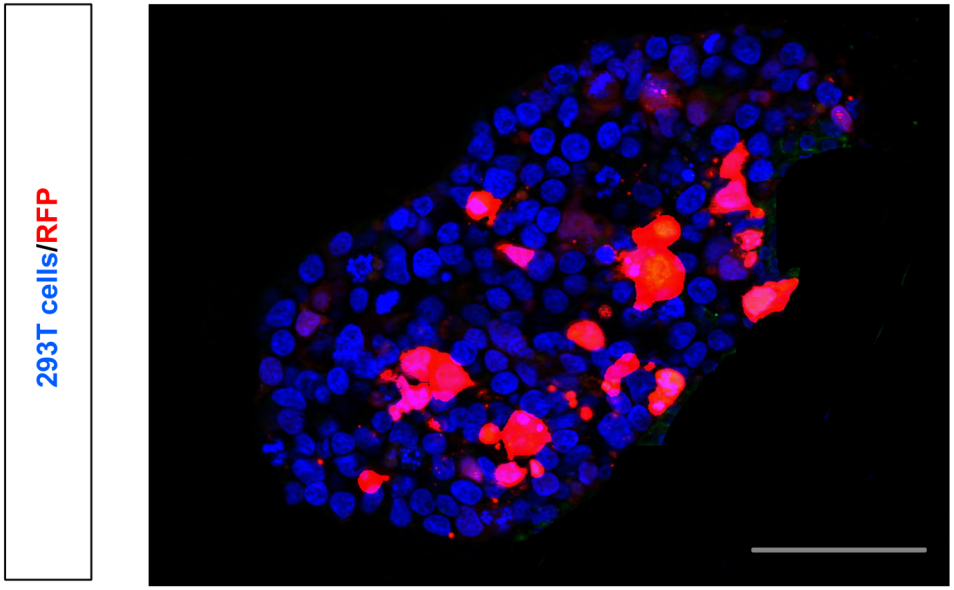

Figure 6.2 Expression of RFP in 293T cell pellet transfected with pCAGGS-RFP.

293T cells transfected with pCAGGS-RFP and aggregated together to create pellets by the hanging drop method. The example pellet here shows successful transfection, indicated by many cells expressing RFP. Scale bar = 50 μm

transfected or control vector-transfected pellets and found that the notochord marker 3B9 was downregulated in much of the notochord cultured with the ProNodal transfected pellet (n=3), whereas explants cultured with control vector pellet expressed 3B9 in all cells (n=3) (Figure 6.3). This shows that the pellets behave in the same way to the soluble proteins and can be used for *in ovo* transplantations.

To examine if ProNodal can alter the fate of the notochord *in ovo,* I transplanted ProNodal pellets into HH stage 10 embryos. HH stage 10 embryos were chosen initially due their ease of manipulation. A small incision was made immediately lateral to the neural tube and the pellet was transplanted into the pore created (Figure 6.4). The embryos were analysed after 24 hours at HH stage 14 and only those embryos in which RFP-expressing pellets could be seen were analysed (Table 6.1) (Figure 6.5 A and F). Expression analysis of 3B9 did not reveal a downregulation in embryos transplanted with ProNodal transfected pellet (n=6/6) (Figure 6.5 B). *Chrd* was not detected in the notochord, as it is normally downregulated in the notochord at HH stage 14 (Figure 6.5 C). The PM markers *Gsc* and *Tbx18* were not upregulated in embryos transplanted with ProNodal transfected pellet (n=6/6) (Figure 6.5 D and E). Embryos transplanted with control vector pellet continued to express 3B9 and did not express *Chrd, Gsc* and *Tbx18* (n=1/1) (Figure 6.5 G - J). This shows that NC does not respond to ProNodal and change its fate to prechordal mesoderm *in ovo.* However, noticeably, in a number of embryos (n=5/6) with a transfected Nodal pellet, a small group of notochord cells appeared to 'pinch off' from the main endogenous notochord (Figure 6.5B, yellow arrowhead). This was never detected with control-transfected pellets.

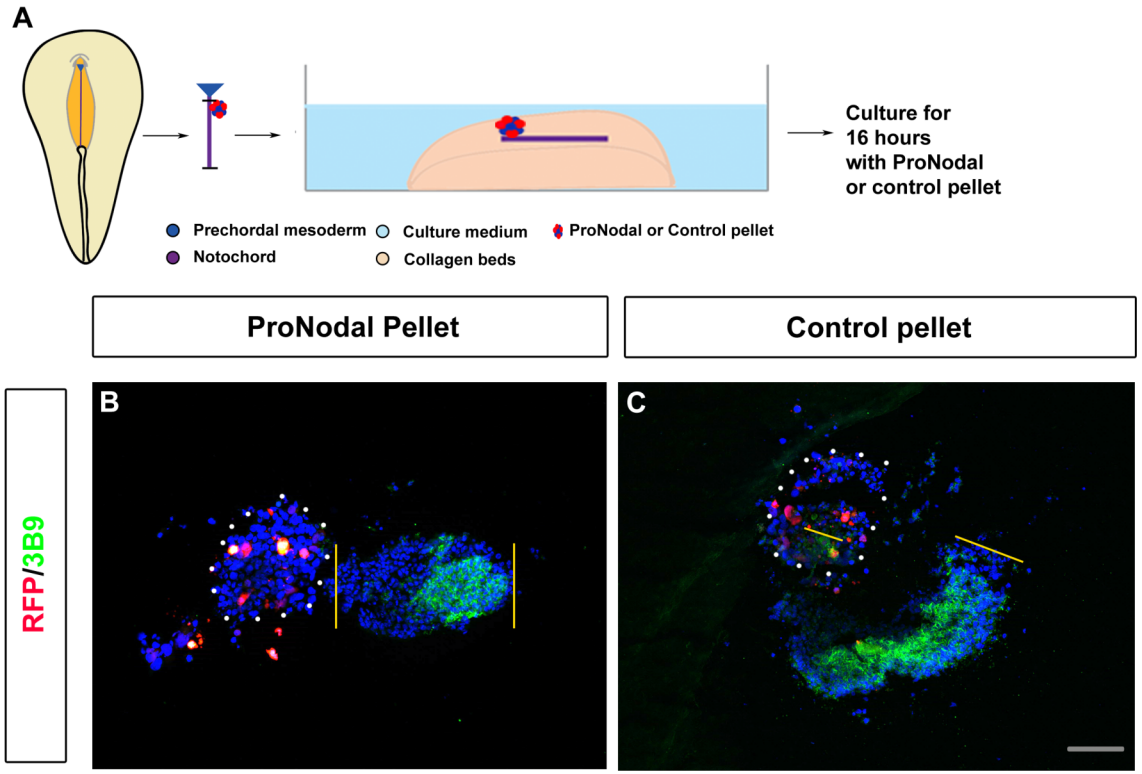

Figure 6.3 Anterior notochord is ProNodal responsive when cultured with ProNodal pellet *in vitro*.

A Schematic shows set up of NC explants cultured with ProNodal secreting or Control pellet for 16 hours.
B NC explants cultured with ProNodal secreting cells (marked by dotted line) downregulate 3B9 expression in the anterior NC.
C NC explants cultured with Control cell pellet (marked by dotted line) continue to express 3B9 throughout the NC. Scale bar = 50 μm

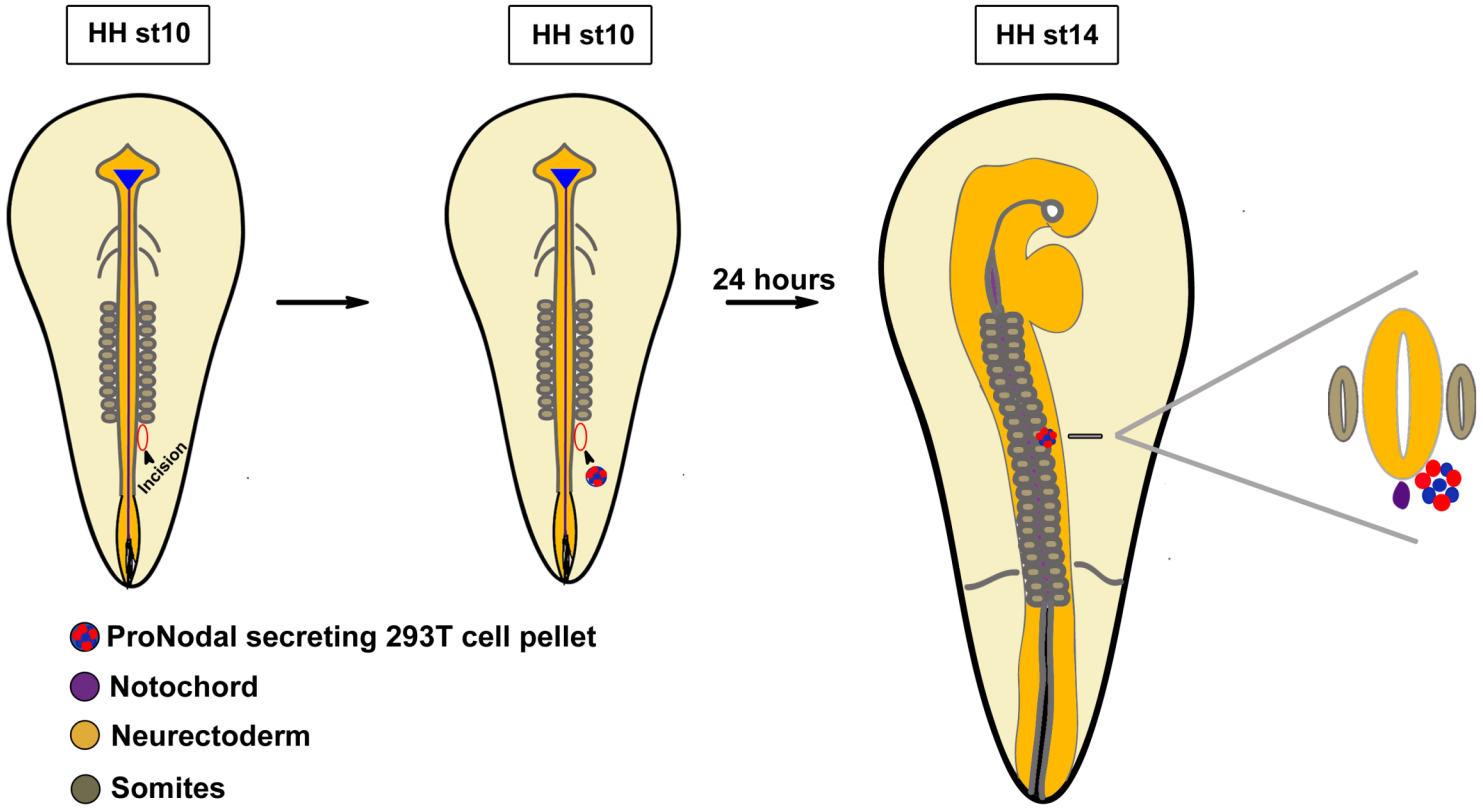

Figure 6.4 Schematic illustrating transplantation of cell pellets *in ovo.*

A small incision is made as indicated in A using a sharp knife, a cell pellet is then inserted in and gentle pressure is applied to place the pellet close to the notochord. The embryos are then sealed and incubated for 24 hours.

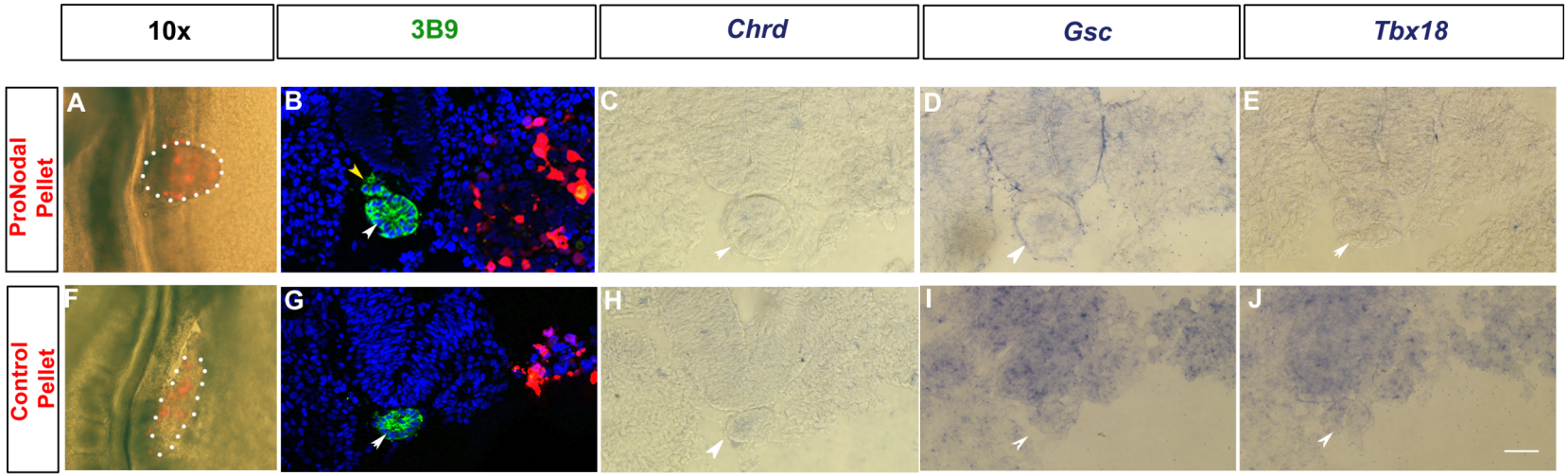

Figure 6.5 Notochord is unresponsive to ProNodal over the period HH stage 10-14.

A Wholemount view shows position of the ProNodal pellet post development.

B-E Serial adjacent sections show that the NC (marked by white arrowhead) continues to express 3B9, does not express *Chrd*, *Gsc* and *Tbx18* in embryos with ProNodal pellet. However, a small set of 3B9+ NC cells appear to pinch off (yellow arrowhead).

F Wholemount view shows position of the Control pellet post development.

G-J NC continues to express 3B9 and does not express *Chrd*, *Gsc* and *Tbx18* in embryos with Control pellet.
Scale bar = 50 μm

The lack of clear effect in ovo after transplanting beads to HH stage 10 embryos prompted me to attempt to perform the more difficult transplants into HH stage 6 embryos, to more closely mimic the *in vitro* NC explants (which were all isolated from HH stage 6 embryos) (Table 6.1). Again no obvious change in 3B9 or *Chrd* expression was detected and the endogenous intact NC did not express *Gsc* and *Tbx18* (n=1/1) (Figure 6.6). At first glance, this suggests that NC might not alter its fate to PM in response to ProNodal signal. However, interestingly I observed an ectopic structure was observed (marked by dotted lines in Figure 6.6), which did not express 3B9 and *Chrd* but expressed *Gsc* and *Tbx18.* The cells of this ectopic structure might be notochord cells, which have changed their fate in response to ProNodal signal to PM and then pinched off. Work is currently ongoing to confirm this observation by repeating this experiment and comparing the results to control pellet transplanted embryos.

Table 6.1 Summary of in ovo transplantations

	Transplanted at HH stage	Number of embryos transplanted	Number of embryos surviving	Embryos with RFP+ pellets
ProNodal	10	36	15	6
Control	10	24	7	1
ProNodal	6	24	17	1
Control	6	18	1	0

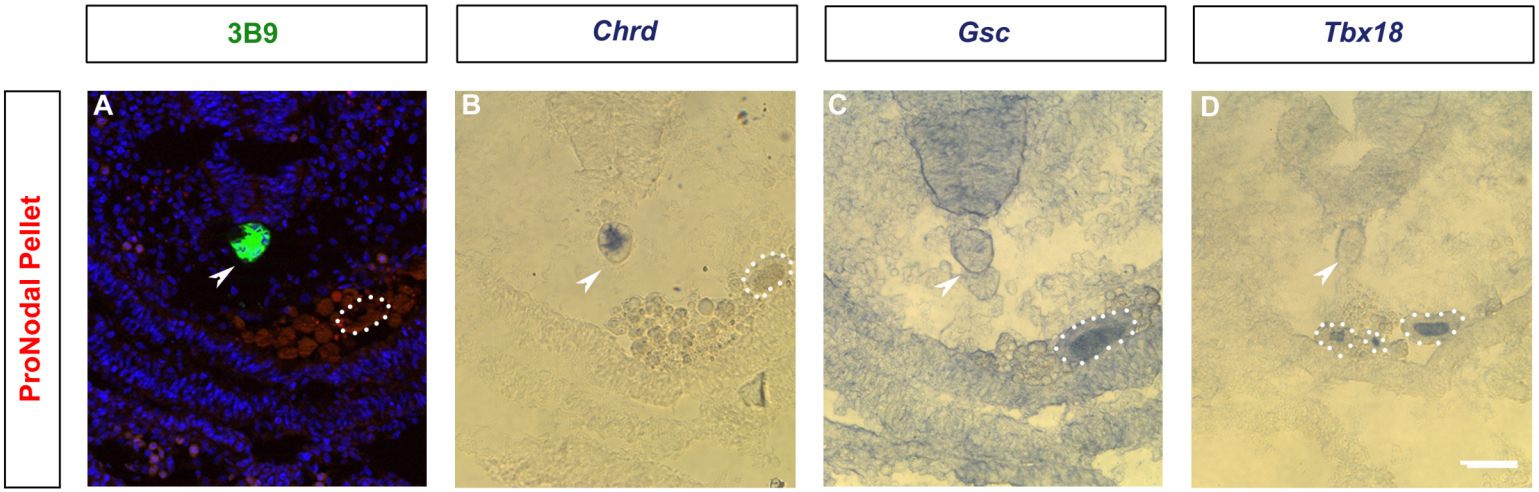

Figure 6.6 Notochord is unresponsive to ProNodal over the period HH stage 6-10.

A & B Notochord (marked by arrow) robustly expresses 3B9 and *Chrd.* Ectopic structure (marked by dotted line) did not express 3B9 or *Chrd.*

C & D Prechordal mesoderm markers *Tbx18 and Gsc* are not detected in notochord (marked by arrow) in serial adjacent sections. However, ectopic structure (marked by dotted line) expresses *Gsc* and *Tbx18.*

Scale bar = 50 μm

6.2.3 Paraxial mesoderm counteracts ProNodal signalling and maintains notochord fate

The observation that NC cannot alter its fate to PM in response to ProNodal *in ovo* suggests that perhaps an external factor operates to inhibit ProNodal (or ProNodal signalling) *in ovo* and maintain the fate of notochord. The source of such a posteriorising factor could be paraxial mesoderm lying parallel to the notochord. Signals such as Wnts, FGFs and retinoic acid from the presomitic mesoderm and paraxial mesoderm are crucial to posteriorise neuroectoderm and transform it into hindbrain and spinal cord (Aulehla and Pourquie, 2010), and potentially, could play a role in anterior-posterior character of the axial mesoderm, i.e. restricting Nodal, or its signalling effect.

To investigate if paraxial mesoderm can inhibit ProNodal/ProNodal signalling from altering NC fate and downregulating 3B9, notochord explants was cultured with the adjacent paraxial mesoderm intact, in the presence of a ProNodal pellet (Figure 6.7 A). Analysis of 3B9 expression shows that 3B9 expression was maintained in the notochord cultured with paraxial mesoderm and the ProNodal secreting pellet (n=9) (Figure 6.7 B). This contrasts with the situation in which notochord explants are cultured alone, in which case ProNodal downregulates 3B9 expression anteriorly and maintains it only posteriorly (n=3) (Figure 6.7 C; see also Figure 6.3).

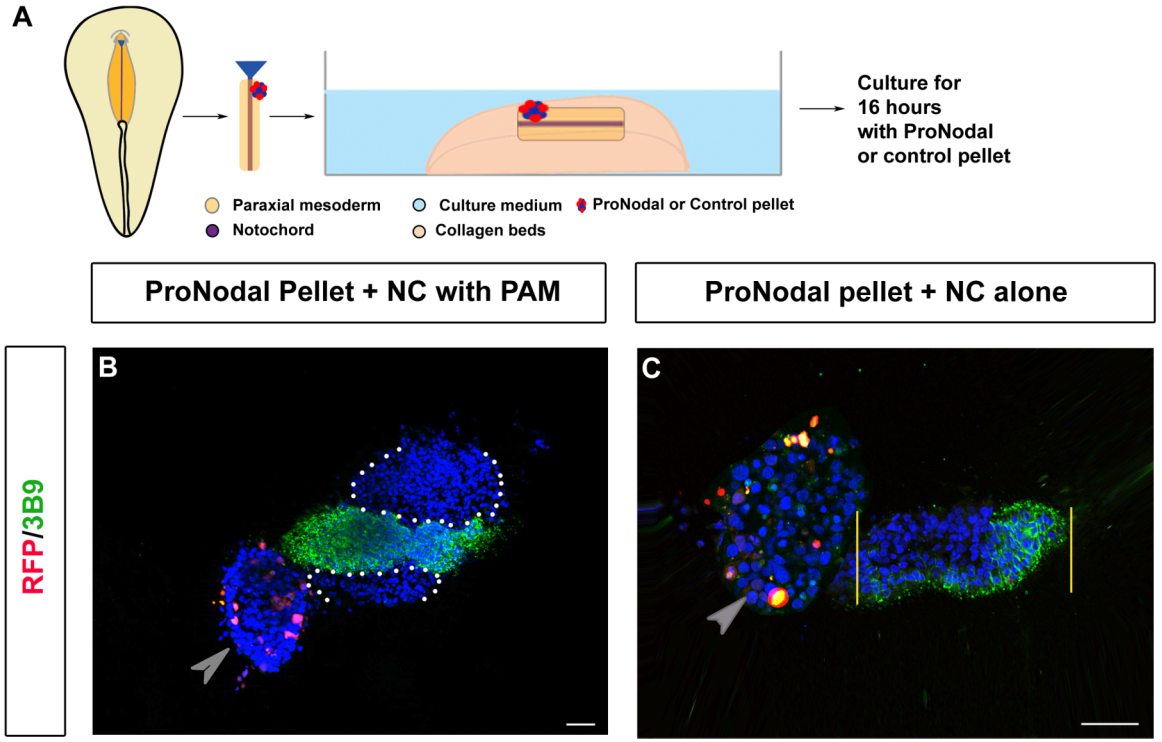

Figure 6.7 Paraxial mesoderm counteracts the effects of ProNodal.

A Schematic showing intact NC and paraxial mesoderm (PAM) explant cultured with ProNodal secreting pellet for 16 hours.
B NC and paraxial mesoderm (marked by dotted line) explants cultured with ProNodal secreting cells (marked by arrowhead) express 3B9 throughout the NC.
C NC cultured alone with ProNodal pellet (marked by arrow) downregulates 3B9 anteriorly. Scale bar = 50 μm

6.2.4 Retinoic acid counteracts ProNodal signalling to maintain prechordal mesoderm and notochord fate

Paraxial mesoderm flanking the notochord is arranged in segmented somites, which are a source of retinoic acid (Rossant et al., 1991; Niederreither et al., 1997). As mentioned earlier retinoic acid is a key posteriorising signalling molecule and its activity is highest in the newly formed somites posteriorly and decreases anteriorly (Niederreither et al., 1997). This posterior to anterior gradient of retinoic acid makes it an ideal candidate to oppose the anterior to posterior Nodal gradient. Additionally, the observation that newly formed posterior notochord is completely resistant to Nodal signals also supports this fact as it receives the highest retinoic acid signalling.

Thus, to investigate if retinoic acid counteracts Nodal signalling, notochord explants were cultured with ProNodal and retinoic acid and the expression of 3B9 was analysed (Figure 6.8 A). As a positive control all-trans retinoic acid was tested and successfully differentiated ES cells into neurons (data not shown). It was used at 10^{-6} M as previously described for other chick explants (Osmond et al., 1991; Kramer and Penny, 2003). Notochord explants maintain the expression of 3B9 throughout the notochord when cultured with medium containing both ProNodal and retinoic acid (n=4) (Figure 6.8 B). However, consistent with previous results (Figure 6.1), when cultured with medium containing ProNodal and DMSO, the anterior NC downregulates 3B9 (n=3) (Figure 6.8 C). This suggests that retinoic acid inhibits ProNodal signalling, suggesting a mechanism

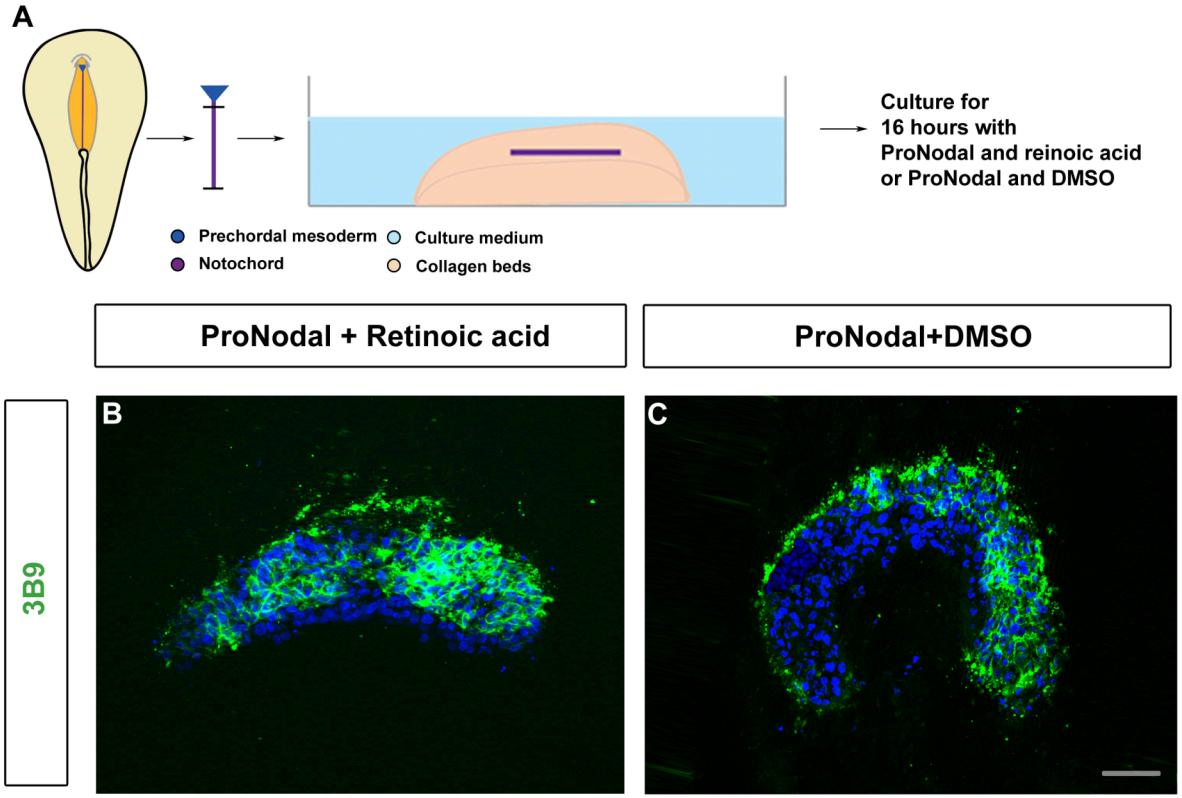

Figure 6.8 Retinoic acid counteracts ProNodal signalling in the notochord *in vitro*.

A Schematic showing NC explants cultured with ProNodal and retinoic acid or ProNodal and DMSO for 16 hours.
B NC explant cultured with ProNodal and retinoic acid expresses 3B9 throughout.
C NC explant cultured with ProNodal and DMSO downregulates the expression of 3B9. Scale bar = 50 μm

for the normal restriction of prechordal mesoderm to anterior-most parts of the axial mesoderm.

6.3 Discussion

As described in the main introduction, a plethora of studies have indicated that Nodal/Nodal related signals act in a dose-dependent way to induce prechordal mesoderm and notochord (Jones et al., 1995; Lustig et al., 1996; Erter et al., 1998; Schier et al., 1997; Chen and Schier, 2001; Dougan et al., 2003). However, the mechanisms that lead to the formation and maintenance of these two distinct cell populations remain unclear.

Studies described here provide a mechanism through which Nodal signals are regulated in a way that induces and then maintains the distinct fates of prechordal mesoderm and notochord. My *in vitro* studies show that notochord can be further classified into two sub-populations: Nodal-responsive anterior notochord and Nodal-unresponsive posterior notochord (Figure 5.6 and Figure 6.1). My *in vivo* experiments, while incomplete, support this conclusion, showing that posterior notochord does not appear to respond to Nodal signals and change its fate to prechordal mesoderm (Figure 6.5). My studies provide evidence that the failure of posterior notochord to respond to Nodal maybe due to paraxial mesoderm-derived retinoic acid, which inhibits Nodal signaling, thus maintaining the posterior character of notochord (Figure 6.7 and 6.8). Thus, retinoic acid exerts its effects by restricting the effects of Nodal signalling to the anterior regions and therefore potentially defining the posterior limit of the prechordal mesoderm. It would be crucial to confirm this observation by

increasing the number of experiments performed as well as culturing NC and paraxial mesoderm with retinoic acid receptor inhibitor BMS 453. Additionally, to prove this process occurs *in ovo*, it would be crucial to repeat the transplant experiments with ProNodal cell pellets and BMS 453 soaked beads and see if PM domain expands into the anterior NC.

Interestingly, another study shows that retinoic acid can limit the posterior extent of PM *in ovo* (Halilagic et al., 2003). They show that RA maybe synthesised in the PM, as one of the enzymes required for its synthesis, *Raldh2*, is expressed in the head process mesoderm and the prechordal mesoderm at HH stages 5 and 6. Using the vitamin A-deficient quail model, which resembles RA knockout model, they show that PM domain marked by *Gsc* and *BMP7* expands into the anterior NC, which downregulates the expression of *Chordin,* similar to my observations described in this chapter (Halilagic et al., 2003). The authors propose that RA may refine the extent of the PM by controlling BMP signalling, which is required in the anterior endoderm to upregulate PM characteristics in the head process mesoderm (Halilagic et al., 2003; Vesque et al., 2000). However, since this study another study has shown that RA catabolising enzyme *Cyp26C1* is expressed in the anterior head mesoderm and the anterior paraxial mesoderm at HH stage 4-9 (Reijntjes et al., 2004). However, *Cyp26C1* is not detected in the notochord and the posterior paraxial mesoderm, anterior to the *Raldh2* expressing presomitic mesoderm (Reijntjes et al., 2004). Thus, even though RA might be synthesised in the PM indicated by the expression of *Raldh2*, it is potentially catabolised due to the presence of *Cyp26C1*. The observation that PM expands into the anterior NC, which

downregulates its characteristics in the vitamin A-deficient model as well as my studies can potentially be explained by the lack of posterior gradient of RA. According to my revised model, RA from the posterior paraxial mesoderm and not the prechordal mesoderm may antagonise the anterior Nodal gradient to limit the PM domain.

CHAPTER 7

Discussion

7.1 Discussion

My studies provide insights into the late specification of axial mesoderm. I identify an exclusive marker of the PM, *Tbx18*, which may play a key role in establishing the boundary between PM and NC. I also show that ProNodal and Mature Nodal signalling plays a late role in PM specification by inducing *Tbx18*, post-extension. Taking these observations together, in this chapter I suggest a model (Figure 7.1) for how PM and NC domains might be established and how the boundary between them could be further refined. I also discuss other findings, future perspectives and the significance of these studies.

7.2 Model for axial mesoderm development

One of the outstanding questions in axial mesoderm development is that of how the discrete domains of PM and NC are set up. It has been shown that head process mesoderm cells extending out of Hensen's node are initially specified by TGFβ signals from the anterior endoderm, which upregulate PM character and downregulate NC character (Vesque et al., 2000). My studies imply that once the axial mesoderm is fully extended, the opposing actions of ProNodal and retinoic acid may further establish notochord and prechordal mesoderm, potentially defining the posterior limit of the prechordal mesoderm and the anterior limit of the notochord (Figure 6.8, Figure 7.1). Prechordal mesoderm does not receive the posterior-derived retinoic acid signals: thus ProNodal specifies prechordal mesoderm

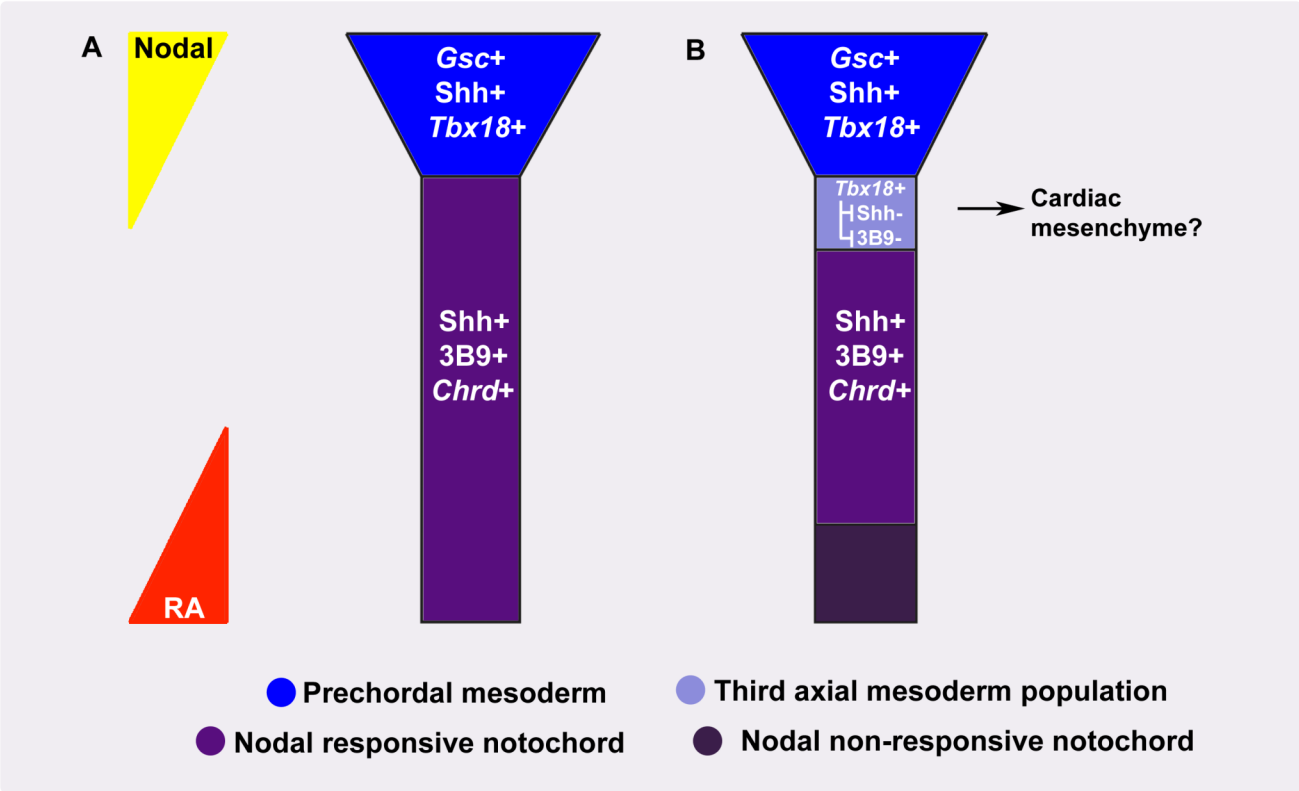

Figure 7.1 Model for establishing prechordal mesoderm and notochord domains.

A The opposing gradients of Nodal and retinoic acid begin to establish the PM and NC domains.
B Nodal specifies the PM by inducing Tbx18, which sharpens the PM-NC boundary by downregulating 3B9 and establishing a SHH- third subpopulation of axial mesoderm, which might contribute to the heart tube forming cardiac mesenchyme.

character further by inducing *Tbx18* (Figure 5.9). Once induced, *Tbx18* downregulates the notochord marker, 3B9 and potentially is involved in refining the boundary between PM and NC cells through the formation of a third type of SHH negative axial mesoderm (Figure 4.5 and 4.9, discussed further in 7.3). Anterior notochord, though competent to respond to ProNodal signals and become prechordal mesoderm, maintains its fate due to the presence of retinoic acid, which inhibits ProNodal signals (Figure 5.6 and 6.8). The caudorostral wave of retinoic acid means that the newly formed notochord receives the highest retinoic acid concentration from the posterior paraxial mesoderm, presomitic mesoderm and Hensen's node and thus is completely resistant to ProNodal.

This model is consistent with the observations made using the vitamin A-deficient quail model where the PM domain marked by *Gsc* expands into the anterior NC (Halilagic et al., 2003). Anterior, and not posterior, NC changes its fate to PM fate by downregulating the NC marker *Chrd.* Further, consistent with my studies, the authors also note that *Shh* is weaker in the region corresponding to the PM-NC interface. Thus, I hypothesise that in vitamin A-deficient quail model, the domain of *Tbx18,* like *Gsc* would expand. As a result of this, the SHH- region would also expand as *Tbx18* downregulates NC marker 3B9 and creates an expanded third subpopulation of axial mesoderm by downregulating SHH.

7.3 Role of the third subpopulation of axial mesoderm

What could be the destiny of this third subpopulation of axial mesoderm, that lies at the interface of the notochord and prechordal

mesoderm? Intriguingly, preliminary data shown in Figure 6.6 shows that although the NC does not appear to downregulate its markers nor upregulate PM markers in response to ProNodal signals *in ovo*, an ectopic structure can be clearly seen expressing PM markers *Gsc* and *Tbx18*. This structure could be derived either from the notochord – i.e. tissue that has pinched off from the notochord, downregulated NC markers and upregulated PM markers, or could be derived from other mesenchymal tissue that has responded to ProNodal signals by upregulating PM markers. While further experiments are needed to distinguish these, I do see an apparent pinching off of notochord cells in response to ProNodal (Figure 6.5), potentially supporting the former interpretation.

Intriguingly, this observation is similar to the phenotypes described in embryos misexpressing *Tbx18* in the notochord (Figure 4.4). As discussed in chapter 4, *Tbx18*- misexpressing notochord cells potentially behave like the third subtype (3B9- SHH- Tbx18+) of axial mesoderm that is situated at the boundary between PM and NC (Figure 4.5 and 4.9). This is a transient population of cells only seen over the period HH stage 8 – 9. Their transient appearance means they could have the following potential fates: to die, to transform into either PM or NC or to migrate away from that region. My studies suggest that these cells are not undergoing apoptosis and they also do not express full PM or NC characteristics (Figure 4.6 and 4.7). One hypothesis could be that perhaps these cells migrate away from this region. In support of this, *Tbx18*-misexpressing embryos have a high number of RFP+ cells, not only in the notochord, but also in the heart compared to controls (Figure 4.4). Also, Figure 6.6 described here shows that post-ProNodal exposure, ectopic *Tbx18*+ *Gsc*+ cells are

observed. I hypothesise that this third subtype of axial mesoderm is composed of cells that migrate away from the axial mesoderm and potentially contribute to the cardiac mesenchyme.

Cardiac precursors are, in fact, known to migrate in an anterior and lateral direction post-gastrulation and come to lie in the anterior lateral plate mesoderm either side of the anterior notochord forming bilateral heart fields (Olsen and Srivastava, 1996; Garcia-Martinez and Schoenwolf, 1993). They will then contribute to a single primary heart tube, which starts beating by HH stage 10 (Song et al., 2011). In zebrafish it has been shown that cardiac precursors lie adjacent to the border of the prechordal-notochord interface and are marked by the homeodomain transcription factor *Nkx2.5* (Goldstein and Fishman, 1998). Ablating the anterior notochord leads to the expansion of *Nkx2.5*+ territory as lateral cells lying adjacent to the notochord are redirected to form the cardiac mesenchyme (Goldstein and Fishman, 1998). However, it remains to be seen whether the anterior notochord or indeed the prechordal-notochord interface itself contributes to the cardiac mesenchyme. In chick we know that the prechordal-notochord interface is SHH-. A further full marker profile including analysis of the prechordal mesoderm markers *Tbx18*, *Gsc* and the cardiac mesenchyme markers, *Nkx2.5* and Islet1, along with fate mapping studies of this region, are required, in future studies, to identify if this region does indeed contribute to the cardiac mesenchyme over the period HH stage 8 – 9. The fact that, post-HH stage 9, the Shh negative territory is no longer observed in the axial mesoderm would support this hypothesis, as by this stage, the cardiac mesenchyme has migrated to form bilateral heart fields which will contribute to form the heart tube.

Intriguingly, the vitamin-A deficient quail embryos die due to cardiovascular defects (Twal et al., 1995; Zile et al., 2004). Instead of a looped heart tube, these embryos have an enlarged non-compartmentalised heart (Twal et al., 1995). This observation supports my observation that embryos misexpressing *Tbx18* also have enlarged hearts (Figure 4.4). Thus, based on my model I hypothesise that lack of RA would allow Nodal to act on anterior NC and change its fate to *Tbx18*+ PM. This expanded *Tbx18*+ region would then create an expanded SHH- population potentially giving rise to an enlarged heart domain.

7.4 Future direction

In future it will be important to investigate if the expression of *Tbx18* is conserved across species. Expression of *Tbx18* has been described in the mouse, zebrafish and Xenopus in other tissues but its expression in the PM has not been especially investigated (Kraus et al., 2001; Begemann et al., 2002 and Jahr et al., 2008). The lack of phenotype associated with the PM in *Tbx18* knockout studies suggests that perhaps another gene may compensate for its loss. A candidate gene could be *Tbx15*, which is closely related to *Tbx18* due to highly conserved sequences between them (Farin et al., 2007; Begemann et al., 2002). It has been shown that both proteins can heterodimerise, further suggesting that they can be capable of controlling the same target genes if expressed in the same tissue (Farin et al., 2007). Examples of such a tissue include the proximal limb bud region and the somites where it has been shown that *Tbx15*

replaces *Tbx18* expression in zebrafish (Farin et al., 2008; Begemann et al., 2002). Thus, it would be crucial to further characterise the expression of both these genes in the PM. Further using Nodal and *Tbx18*/*Tbx15* conditional knockdown mouse and zebrafish models it would be important to show that they play a conserved role in the process axial mesoderm regionalisation across all species.

It would be crucial to confirm the observations presented in Chapter 4 by analysing a larger sample of electroporated embryos. One of the main challenges of this experiment has been targeting the notochord and prechordal mesoderm specifically. To be able to achieve both the specificity and a larger sample to analyse, an early chick embryo culture (EC culture) technique would be useful to establish. The advantages of this technique include being able to dissect the embryo and maintaining it *in vitro* allowing to specifically target the prechordal mesoderm and notochord by accessing them directly on the ventral side (Chapman et al., 2001). Also, the embryos can then be imaged as they develop, this will have the further advantage of revealing what structures the cells contribute to post electroporation with transgene compared to controls. This will allow me to test the hypothesis that *Tbx18* expressed in the anterior notochord directs these cells to the contribute to the heart fields by changing its fate to the third type of axial mesoderm cell population.

7.5 Conclusion

The data presented in this thesis suggests a model for axial mesoderm regionalisation in the chick embryo. Axial mesoderm regionalisation into prechordal mesoderm and notochord is crucial for the

regionalisation of the overlying neural tissue. As described in the Introduction a plethora of studies have shown that differential signalling from the prechordal mesoderm and notochord compartmentalises the overlying neural tissue, which is key for the different functions performed by the different regions of the resulting fore-, mid-, hindbrain and spinal cord. Further, my data also suggests that the maintenance of a sharp boundary between prechordal mesoderm and notochord may also be crucial for the correct specification of the developing heart. Thus, for the correct regionalisation of the central nervous system and the heart it is important that prechordal mesoderm and notochord maintain their separate domains.

References

Adelman, H. B. (1922). The significance of the prechordal plate: an interpretative study. Am. J. Anat. 31, 55-101.

Adelman, H. B. (1927). The development of the eye muscles of the chick. J. Morph. Physiol. 44, 29-87.

Adelman, H. B. (1930). Experimental studies on the development of the eye. III. The effect of the substrate ('Unterlagerung') on the heterotopic development of median and lateral strips of the anterior end of the neural plate of amblystoma. Journal of Experimental Zoology 57, 223-281.

Agathon, A., Thisse, B. and Thisse, C. (2001). Morpholino knock-down of antivin1 and antivin2 upregulates nodal signaling. Genesis 30, 178-182.

Agius, E., Oelgeschlager, M., Wessely, O., Kemp, C. and De Robertis, E. M. (2000). Endodermal Nodal-related signals and mesoderm induction in Xenopus. Development 127, 1173-1183.

Airik, R., Bussen, M., Singh, M. K., Petry, M. and Kispert, A. (2006). Tbx18 regulates the development of the ureteral mesenchyme. J. Clin. Invest. 116, 663-674.

Aulehla, A. and Pourquie, O. (2010). Signalling gradients during paraxial mesoderm development. Cold Spring Harbour Perspectives in Biology 2, a000869.

Ang, S. L., Jin, O., Rhinn, M., Daigle, N., Stevenson, L., and Rossant, J. (1996). A targeted mouse Otx2 mutation leads to severe defects in gastrulation and formation of axial mesoderm and to deletion of rostral brain. Development 122, 243–25.

Ang, S. L. and Rossant, J. (1994). HNF-3β is essential for node and notochord formation in mouse development. Cell 78 (4) 561-574.

Armes, N. A., and Smith, J. C. (1997). The ALK-2 and ALK-4 activin receptors transduce distinct mesoderm-inducing signals during early Xenopus development but do not co-operate to establish thresholds. Development 124, 3797-3804.

Arnold, S. J., Hofmann, U. K., Bikoff, E. K. and Robertson, E. J. (2008). Pivotal roles for eomesodermin during axis formation, epithelium-to-mesenchyme transition and endoderm specification in the mouse. Development 135, 501–511.

Bae, S., Reid, C. D. and Kessler, D. S. (2011). Siamois and Twin are redundant and essential in formation of the Spemann organizer. Developmental Biology 352, 367-381.

Bachiller, D., Klingensmith, J., Kemp, C., Belo, J. A., Anderson, R. M., May, S. R., McMahon, J. A., McMahon, A. P., Harland, R. M., Rossant, J. et al. (2000). The organizer factors Chordin and Noggin are required for mouse forebrain development. Nature 403, 658-661.

Beck, S., Le Good, J. A., Guzman, M., Ben Haim, N., Roy, K., Beemann, F. and Constam, D. B. (2002). Extraembryonic proteases regulate Nodal signalling during gastrulation. Nature Cell Biology 4, 981-985

Baker, R. K. and Antin, P. B. (2003). Ephs and ephrins during early stages of chick embryogenesis. Developmental Dynamics 228, 128-142.

Barresi, M. J., Stickney, H. L. and Devoto, S. H. (2000). The zebrafish slowmuscle-omitted gene product is required for Hedgehog signal transduction and the development of slow muscle identity. Development 127, 2189-2199.

Beddington, R. S. (1994). Induction of a second neural axis by the mouse node. Development 120, 613-620.

Begemann, G., Gilbert, Y., Meyer, A. and Ingham, P. W. (2002). Cloning of zebrafish T-box genes tbx15 and tbx18 and their expression during embryonic development. Mechanisms of Development 114, 137-141.

Bellairs, R. (1986). The primitive streak. Anat. Embryol. 174, 1-14.

Belo, J. A., Bouwmeester, T., Leyns, L., Kertesz, N., Gallo, M., Follettie, M. and De Robertis E. M. (1997). Cerberus-like is a secreted factor with neutralizing activity expressed in the anterior primitive endoderm of the mouse gastrula. Mechanisms of Development 68, 45-57.

Bertocchini, F. and Stern C. D. (2002). The hypoblast of the chick embryo positions the primitive streak by antagonizing nodal signaling. Developmental Cell 3, 735–744.

Bertocchini, F., Skromne, I., Wolpert, L. and Stern, C. D. (2004). Determination of embryonic polarity in a regulative system: evidence for endogenous inhibitors acting sequentially during primitive streak formation in the chick embryo.

Bisgrove, B. W., Essner, J. J. and Yost, H. J. (1999). Regulation of midline development by antagonism of lefty and nodal signaling. Development 126, 3253–3262.

Borycki, A.-G., Mendham, L. and Emerson, C. P., Jr. (1998). Control of somite patterning by Sonic hedgehog and its downstream signal response genes. Development 125, 777-790.

Boterenbrood, E. C. and Nieuwkoop, P. D. (1973). The formation of the mesoderm in urodelean amphibians. V. Its regional induction by the endoderm. Wilhelm Roux' Arch, Dev. Biol. 173, 319-332.

Bouwmeester, T. (2001). The Spemann-Mangold organizer: the control of fate specification and morphogenetic rearrangements during gastrulation in Xenopus. Int. J. Dev. Biol 45, 251-258.

Bouwmeester, T., Kim, S., Sasai, Y., Lu, B. and De Robertis, E. M. (1996). Cerberus is a head-inducing secreted factor expressed in the anterior endoderm of Spemann's organizer. Nature 382, 595–601.

Brand-Saberi, B., Ebensperger, C., Wilting, J., Balling, R. and Christ, B. (1993). The ventralizing effect of the notochord on somite differentiation in chick embryos. Anatomy and Embryology 188, 239–245.

Brannon, M., Gomperts, M., Sumoy, L., Moon R. T. and Kimelman, D. (1997). A beta-catenin/XTcf-3 complex binds to the siamois promoter to regulate dorsal axis specification in Xenopus. Genes and Development 11, 2359–2370.

Brickman, J. M., Jones, C. M., Clements, M., Smith, J. C. and Beddington, R. S. (2000). Hex is a transcriptional repressor that contributes to anterior identity and suppresses Spemann organiser function. Development 127, 2303–2315.

Briscoe, J. and Ericson, J. (2001). Specification of neuronal fates in the ventral neural tube. Current Opinion in Neurobiology 11, 43–49.

Briscoe. J., Pierani, A., Jessell, T. M. and Ericson, J. (2000). A homeodomain protein code specifies progenitor cell identity and neuronal fate in the ventral neural tube. Cell 101, 435-445.

Bussen, M., Petry, M., Schuster-Gossler, K., Leitges, M., Gossler, A. and Kispert, A. (2004). The T-box transcription factor Tbx18 maintains the separation of anterior and posterior somite compartments. Genes and Development 18, 1209–1221.

Carnac, G., Kodjabachian, L., Gurdon, J. B. and Lemaire, P. (1996). The homeobox gene Siamois is a target of the Wnt dorsalisation pathway and triggers organiser activity in the absence of mesoderm. Development 122, 3055-3065.

Casey, E. S., O'Reilly, M. A., Conlon, F. L. and Smith, J. C. (1998). The Tbox transcription factor Brachyury regulates expression of eFGF through binding to a non-palindromic response element. Development 125, 3887-3894.

Catala, M., Teillet, M. -A., De Robertis, E. M. and LE Douarin, N. M. (1996). A spinal cord fate map in the avian embryo: while regressing, Hensen's node lays down the notochord and floor plate thus joining the spinal cord lateral walls. Development 122, 2599-2610.

Chan, J., Malby, J. D., Serluca, F. C., Chen, J. N., Goldstein, N. B., Thomas, M. C., Cleary, J. A., Brennan, C., Fishman, M. C. and Roberts, T. M. (2001). Morphogenesis of prechordal plate and notochord requires intact Eph/ephrin B signaling. Developmental Biology 234, 470-482.

Chang, C., Wilson, P. A., Mathews, L. S. and Hemmat-Brivanlou, A. (1997). A Xenopus type I activin receptor mediates mesodermal but not neural specification during embryogenesis. Development 124, 827-837.

Chapman, D. L., Agulnik, I., Hancock, S., Silver, L. M. and Papaioannou, V. E. (1996). Tbx6, a mouse T-box gene implicated in paraxial mesoderm formation at gastrulation. Developmental Biology 180, 534–542.

Chapman, D. L. and Papaioannou, V. E. (1998). Three neural tubes in mouse embryos with mutations in the T-box gene, Tbx6. Nature 39, 695–697.

Chapman S. C., Collignon J., Schoenwolf G. C., Lumsden A. (2001). Improved method for chick whole-embryo culture using a filter paper carrier. Dev. Dyn. **220**, 284-289.

Chapman, D. L., Cooper-Morgan, A., Harrelson, Z. and Papaioannou, V. E. (2003). Critical role for Tbx6 in mesoderm specification in the mouse embryo. Mechanisms of Development 120, 837–847.

Chapman, S. C., Brown, R., Lees, L., Schoenwolf, G. C. and Lumsden, A. (2004). Expression analysis of chick Wnt and frizzled genes and selected inhibitors in early chick patterning. Developmental Dynamics 229, 668-676.

Chen, Y. and Schier, A. F. (2001). The zebrafish Nodal signal Squint functions as a morphogen. Nature 411, 607–610.

Chen, Y. and Schier, A. F. (2002). Lefty proteins are long-range inhibitors of squint-mediated nodal signaling. Current Biology 12, 2124–2128.

Chen, Y., Whitaker, L. L. and Ramsdell, A. F. (2005). Developmental analysis of Activin-Like kinase receptor-4 (ALK4) expression in Xenopus laevis. Developmental Dynamics 232, 393–398.

Christian, J. L. and Moon. R.T. (1993). Interactions between Xwnt-8 and Spemann organizer signaling pathways generate dorsoventral pattern in the embryonic mesoderm of Xenopus. Genes and Development 7, 13–28.

Christian, J. L., McMahon, J. A., McMahon, A.P. and Moon. R.T. (1991). Xwnt-8, a Xenopus Wnt-1/int-1-related gene responsive to mesoderm-inducing growth factors, may play a role in ventral mesodermal patterning during embryogenesis. Development 111, 1045–1055.

Chu, G. C., Dunn, N. R., Anderson, D. C., Oxburgh, L. and Robertson, E. J. (2004). Differential requirements for Smad4 in TGFβ-dependent patterning of the early mouse embryo. Development 131, 3501-3512.

Chu, J., Ding, J., Jeays-Ward, K., Price, S. M., Placzek, M. and Shen, M. M. (2005). Non-cell-autonomous role for Cripto in axial midline formation during vertebrate embryogenesis. Development 132, 5539–5551.

Clements, D., Friday, R. V. and Woodland, H. R. (1999) Mode of action of VegT in mesoderm and endoderm formation. Development 126, 4903–4911.

Cleaver, O. and Krieg, P. A. (2001) Notochord patterning of the endoderm. Developmental Biology 234, 1-12.

Colas, J-F., Schoenwolf, G. C. (2000). Subtractive hybridization identifies chick-cripto, a novel EGF–CFC ortholog expressed during gastrulation, neurulation and early cardiogenesis. Gene 225, 205-217.

Conlon, F. L., Barth, K. S. and Robertson, E. J. (1991). A novel retrovirally-induced embryonic lethal mutation in the mouse; assessment of the developmental fate of ES cells homozygous for the 413.d proviral integration. Development 111, 969–981.

Conlon, F. L., Lyons, K. M., Takaesu, N., Barth, K. S., Kispert, A., Herrmann, B. and Robertson, E. J. (1994). A primary requirement for nodal in the formation and maintenance of the primitive streak in the mouse. Development 120, 1919–1928.

Croteau, L. P. and Kania, A. (2011). Optimisation of in ovo electroporation of the chick neural tube. Journal of Neuroscience Methods 201, 381-384.

Cunliffe, V. and Smith, J. C. (1992). Ectopic mesoderm formation in Xenopus embryos caused by widespread expression of a Brachyury homologue. Nature 358, 427-430.

Dale, J. K., Vesque, C., Lints, T. J., Sampath, T. K., Furley, A., Dodd, J. and Placzek, M. (1997). Cooperation of BMP7 & SHH in the induction of forebrain ventral midline cells by prechordal mesoderm. Cell 90, 257-69.

Dale, K., Sattar, N., Heemskerk, J., Clarke, J. D., Placzek, M. and Dodd, J. (1999). Differential patterning of ventral midline cells by axial mesoderm is regulated by BMP7 and chordin. Development 126, 397-408.

Dale, L. and Slack, J. M. W. (1987a). Fate map for the 32-cell stage of Xenopus laevis. Development 99, 527-551.

Dale, L. and Slack, J. M. W. (1987b). Regional specification within the mesoderm of early embryos of Xenopus laevis. Development 100, 279-295.

Dale, L., Smith, J. C. and Slack, J. M. W. (1985). Mesoderm induction in Xenopus laevis: a quantitative study using a cell lineage label and tissue-specific antibodies. J. Embryol. Exp. Morph. 89, 289-312.

Danos, M. C. and Yost, H. J. (1995). Linkage of cardiac left-right asymmetry and dorsal-anterior development in Xenopus. Development 121, 1467-1474.

Das, R. M., Van Hateren, N. J., Howell, G. R., Farrell, E. R., Bangs, F. K., Porteous, V. C., Manning, E. M., McGrew, M. J., Ohyama, K., Sacco, M. A., Halley. P. A., Sang, H. M., Storey, K. G., Placzek, M., Tickle, C., Nair, V. K., Wilson, S. A. (2006). A robust system for RNA interference in the chicken using a modified microRNA operon. Developmental Biology 294, 554-63.

De Robertis, E. M. (2006). Spemann's organiser and self regulation in amphibian embryos. Nature reviews molecular cell biology. 7, 296-302.

De Souza, F. S., Gawantka, V., Gomez, A. P., Delius, H., Ang, S. L. and Niehrs, C. (1999). The zinc finger gene Xblimp1 controls anterior endomesodermal cell fate in Spemann's organizer. EMBO J. 18, 6062–6072.

Dessaud, E., McMahon, A. P. and Briscoe, J. (2008). Pattern formation in the vertebrate neural tube: a sonic hedgehog morphogen-regulated transcriptional network. Development 135, 2489-2503.

Dias, M. and Schoenwolf, G. C. (1990). Formation of ectopic neuroepithelium in chick blastoderms:age-related capacities for induction and self-differentiation following transplant of quail Hensen's nodes. Anat. Embryol. 229, 437-448.

Ding, J., Yang, L., Yan, Y. T., Chen, A., Desai, N., Wynshaw-Boris, A. and Shen, M. M. (1998). Cripto is required for correct orientation of the anterior–posterior axis in the mouse embryo. Nature 395, 702-707.

Dobrovolskaia-Zavadskaia, N. C. R. (1927). Sur la mortification spontanée dela que chez la souris nouveau-née sur l'existence d'un caractere (facteur) héréditaire, non viable. Seanc. Soc. Biol. 97, 114-116.

Doniach, T. (1992). Induction of anteroposterior neural pattern in Xenopus by planar signals. Development supplement 183-193.

Doniach, T. (1995). Press basic FGF as an inducer of anteroposterior neural pattern. Cell 63, 1067-1070.

Dougan, S. T., Warga, R. M. , Kane, D. A., Schier, A. F. and Talbot, W. S. (2003). The role of the zebrafish nodal-related genes squint and cyclops in patterning of mesendoderm. Development 130 (9) 1837-1851.

Dunn, N. R., Vincent, S. D., Oxburgh, L., Robertson, E. J. and Bikoff, E. K. (2004). Combinatorial activities of Smad2 and Smad3 regulate mesoderm formation and patterning in the mouse embryo. Development 131, 1717-1728.

Echelard, Y., Epstein, D. J., St-Jacques, B., Shen, L., Mohler, J., McMahon, J. A. and McMahon, A. P. (1993). Sonic hedgehog, a member of a family of putative signaling molecules, is implicated in the regulation of CNS polarity. Cell 75, 1417-1430.

Ellis, P., Soubes, S., Ohyama, K., Burbridge, S., Ben-Haim, N., Chen, C., Shen, M. M., Constam, D. and Placzek, M. (*in revision*)

Engleka, M. J. and Kessler, D. S. (2001). Siamois cooperates with TGFβ signals to induce the complete function of the Spemann-Mangold organizer. Int. J. Dev. Biol. 45, 241–250.

Erter, C. E., Solnica-Krezel, L. and Wright, C. V. E. (1998). Zebrafish nodal related 2 encodes an early mesendodermal inducer signaling from the extraembryonic yolk syncytial layer. Developmental Biology 204, 361-372.

Fainsod, A., Deissler, K., Yelin, R., Marom, K., Epstein, M., Pillemer, G., Steinbeisser, H. and Blum M. (1997). The dorsalizing and neural inducing gene follistatin is an antagonist of BMP-4. Mechanisms of Development 63, 39–50.

Fainsod, A., Steinbeisser, H. and De Robertis, E. M. (1994) On the function of BMP-4 in patterning the marginal zone of the Xenopus embryo. EMBO J. 13, 5015–5025.

Fan, C. M. and Tessier Lavigne, M. (1994). Patterning of mammalian somites by surface ectoderm and notochord: evidence for sclerotome induction by a hedgehog homolog. Cell 79, 1175–1186.

Fan, M. J. and Sokol, S. Y. (1997). A role for Siamois in Spemann organizer formation. Development 124, 2581–2589.

Fan, M. J., Gruning, W., Walz, G. and Sokol, S. Y. Wnt signaling and transcriptional control of Siamois in Xenopus embryos. (1998). PNAS 95, 5626–5631.

Farin, H. F., Bussen, M., Schmidt, M. K., Singh M. K., Schuster-Gossler, K. and Kispert, A. (2007). Transcriptional repression by the T-box proteins Tbx18 and Tbx15 depends on Groucho corepressors. Journal of Biological Chemistry 282, 25748-59.

Farin, H. F., Mansouri, A., Petry, M. and Kispert, A. (2008). T-box protein Tbx18 interacts with the paired protein pax3 in the development of the paraxial mesoderm. Journal of Biological Chemistry 283, 25372-80.

Feldman, B., Gates, M. A., Egan, E. S., Dougan, S. T., Rennebeck, G., Sirotkin, H. I., Schier, A. F. and Talbot, W. S. (1998). Zebrafish organiser development and germ layer formation require nodal-related signals. Nature 395, 181–184.

Filosa, S., Rivera-Perez, J. A., Gomez, A. P., Gansmuller, A., Sasaki, H., Behringer, R. R. and Ang, S. L. (1997). Goosecoid and HNF-3beta genetically interact to regulate neural tube patterning during mouse embryogenesis. Development 124, 2843-2854.

Foley, A. C., Storey, K. G. and Stern, C. D. (1997). The prechordal region lacks neural inducing ability, but can confer anterior character to more posterior neuroepithelium. Development 124, 2983-2996.

Fouquet, B., Weinstein, B. M., Serluca, F. C. and Fishman, M. C. (1997). Vessel patterning in the embryo of the zebrafish: Guidance by notochord. Developmental Biology 183, 37-48.

Games, J. and Sive, H. (2000). Vertebrate anteroposterior patterning: the Xenopus neurectoderm as a paradigm. BioEssays 22, 976-986.

Garcia-Martinez, V. and Schoenwolf, G. (1993). Primitive-streak origin of the cardiovascular system in avian embryos. Developmental Biology 159, 706–719.

Gerhart, J., Danilchik, M., Doniach, T., Roberts, S., Rowing, B. and Steward, R. (1989). Cortical rotation of the Xenopus egg: Consequences for the anteroposterior pattern of embryonic dorsal development. Development 107, 37-51.

Germain, S., Howell, M., Esslemont, G. M. and Hill, C. S. (2000). Homeodomain and winged-helix transcription factors recruit activated Smads to distinct promoter elements via a common Smad interaction motif. Genes and Development14, 435-451.

Gimlich, R. L. (1986). Acquisition of developmental autonomy in the equatorial region of the Xenopus embryo. Developmental Biology 115, 340-352.

Glinka, A., Wu, W., Delius, H., Monaghan, A. P., Blumenstock, C. and Niehrs, C. Dickkopf-1 is amember of a new family of secreted proteins and functions in head induction. Nature, 391, 357-362.

Gluecksohn-Schoenheimer, S. (1938). The development of two tailless mutants in the house mouse. Genetics, 23, 573-84.

Goldstein, A. M. and Fishman, M. C. (1998). Notochord regulates cardiac lineage in zebrafish embryos. Developmental Biology 201, 247–252.

Goriely, A., Stella, M., Coffinier, C., Kessler, D., Mailhos, C., Dessain, S. and Desplan, C. (1996). A functional homologue of goosecoid in Drosophila. Development 122, 1641–1650.

Grabowski, C. T. (1956). The effects of the excision of Hensen's node on the development of the chick embryo. J. Exp. Zool. 133, 301-344.

Graff, J. M., Thies, R. S., Song, J. J., Celeste, A. J. and Melton, D. A. (1994). Studies with a Xenopus BMP receptor suggest that ventral mesoderm–inducing signals override dorsal signals in vivo. Cell 79, 169-179.

Gray, S. and Dale, J. K. (2010). Notch signalling regulates contribution of progenitor cells from chick Hensen's node to the floor plate and notochord. Development 137, 561-568.

Green, J. B. A., New, H. V. and Smith, J. C. (1992). Responses of embryonic Xenopus cells to activin and FGF are separated my multiple dose thresholds and correspond to distinct axes of the mesoderm. Cell 71, 731-739.

Green, J. B., Cook, T. L., Smith, J. C. and Grainger, R. M. (1997). Anteroposterior neural tissue specification by activin-induced mesoderm. PNAS 94, 8596-8601.

Gritsman, K., Zhang, J., Cheng, S., Heckscher, E., Talbot, W. S. and Schier, A. F. (1999). The EGF-CFC protein one-eyed pinhead is essential for nodal signaling. Cell 97, 121-132.

Gritsman, K., Talbot, S. and Shier, F. (2000). Nodal signalling patterns the organizer. Development 127, 921-932.

Greulich, F., Rudat, C. and Kispert, A. (2011) Mechanisms of T-box gene function in the developing heart. Cardiovascular Research 91 (2) 212-222.

Gu, Z., Nomura, M., Simpson, B. B., Lei, H., Feijen, A., Raaiji, J. V. D. E. V., Donahoe, P. K. and Li, E. (1998). The type I activin receptor ActRIB is required for egg cylinder organization and gastrulation in the mouse. Genes and Development 12, 844-857.

Gurdon, J. B., Mitchell, A. and Ryan, K. (1996). An experimental system for analyzing response to a morphogen gradient. PNAS 93, 9334-9338.

Hagos, E. G. and Dougan, S. T. (2007). Time-dependent patterning of the mesoderm and endoderm by Nodal signals in zebrafish. BMC Developmetal Biology 7, 22.

Hahn, M. and Jaeckle, H. (1996) Drosophila goosecoid participates in neural development but not in body axis formation. EMBO J. 15, 3077–3084.

Haenig, B. and Kispert, A. (2004). Analysis of TBX18 expression in chick embryos. Dev. Genes. Evol. 214, 407–411.

Halilagic, A., Zile, M. H. and Studer, M. (2003). A novel role for retinoids in patterning the avian forebrain during presomite stages. Development 130, 2039-2050.

Halpern, M. E., Ho, R. K., Walker, C. and Kimmel, C. B. (1993). Induction of muscle pioneers and floor plate is distinguished by the zebrafish no tail mutation. Cell 75, 99–111.

Hamburger, V. and Hamilton, H. L. (1951). A series of normal stages in the development of the chick embryo. Journal of Morphology 88 (1) 49–92.

Harland, R. and Gerhart, J. (1997). Formation and function of Spemann's organizer. Annual Review Cell Devevelopment Biology 13, 611-667.

Hashimoto, H., Itoh, M., Yamanaka, Y., Yamashita, S., Shimizu, T., Solnica-Krezel, L., Hibi, M. and Hirano, T. (2000). Zebrafish Dkk1 functions in forebrain specification and axial mesendoderm formation. Dev elopmental Biology. 217, 138-152.

Hatta, K., Kimmel, C. B., Ho, R. K. and Walker, C. (1991). The cyclops mutation blocks specification of the floor plate of the zebrafish central nervous system. Nature 350, 339–341.

Heasman, J., Crawford, A., Goldstone, K., Garner-Hamrick, P., Gumbiner, B., McCrea, P., Kintner, C., Noro, C. Y. and Wylie, C. (1994). Overexpression of cadherins and underexpression of beta-catenin inhibit dorsal mesoderm induction in early Xenopus embryos. Cell 79, 791-803.

Heisenberg, C. P. and Nusslein-Volhard, C. (1997). The function of silberblick in the positioning of the eye anlage in the zebrafish embryo. Developmental Biology 184, 85–94.

Hemmati-Brivanlou, A. and Melton, D.A. (1994). Inhibition of activin receptor signaling promotes neuralization in Xenopus. Cell 77, 273–281.

Hemmati-Brivanlou. A. and Thomsen, G. H. (1995). Ventral mesodermal patterning in Xenopus embryos: expression patterns and activities of BMP-2 and BMP-4. Developmental Genetics 17, 78-89.

Henry, G. L., Brivanlou, I. H., Kessler, D. S., Hemmati-Brivanlou, A., Melton, D.A., (1996). TGF-beta signals and a pattern in Xenopus laevis endodermal development. Development 122, 1007–1015.

Hoodless, P. A., Pye, M., Chazaud, C., Labbe, E., Attisano, L., Rossant, J. and Wrana, J. L. (2001). FoxH1 (Fast) functions to specify the anterior primitive streak in the mouse. Genes and Development 15, 1257-1271.

Hsu, D. R., Economides, A. N., Wang, X., Eimon, P. M. and Harland, R. M. (1998). The Xenopus dorsalizing factor Gremlin identifies a novel family of secreted proteins that antagonize BMP activities. Molecular Cell 1, 673–683.

Hume, C. R. and Dodd, J. (1993). Cwnt-8C: a novel Wnt gene with a potential role in primitive streak formation and hindbrain organization. Development119, 1147-1160.

Hug, B., Walter, V. and Grunwald, D. J. (1997). tbx6, a Brachyury-related gene expressed by ventral mesendodermal precursors in the zebrafish embryo. Developmental Biology 183, 61-73.

Hynes, M., Poulsen, K., Tessier-Lavigne, M. and Rosenthal A. (1995). Control of neuronal diversity by the floor plate: contact-mediated induction of midbrain dopaminergic neurons. Cell 80, 95-101.

Inman, G. J., Nicolas, F. J., Callahan, J. F., Harling, J. D., Gaster, L. M., Reith, A. D., Laping, N. J. and Hill, C. S. (2002). SB-431542 is a potent and specific inhibitor of transforming growth factor-beta superfamily type I activin receptor-like kinase (ALK) receptors ALK4, ALK5, and ALK7. Molecular Pharmacology 62, 65-74.

Izpisua-Belmonte, J. C., De Robertis, E. M., Storey, K. G. and Stern, C. D. (1993). The homeobox gene goosecoid and the origin of organiser cells in the early chick blastoderm. Cell 74, 645-659.

Jacob, J. and Briscoe, J. (2003). Gli proteins and the control of spinal cord patterning. EMBO reports 4, 761-765.

Joubin, K. and Stern, C. D. (1999). Molecular interactions continuously define the organiser during the cell movements of gastrulation. Cell 98, 559-571.

Jahr, M., Schlueter, J., Brand, T. and Manner, J. (2008). Development of the proepicardium in Xenopus laevis. Developmental Dynamics 237, 3088-3096.

Jia, S., Ren, Z., Li, X., Zheng, Y. and Meng, A. (2008). Smad2 and smad3 are required for mesendoderm induction by transforming growth factor-beta/nodal signals in zebrafish. Journal of Biological Chemistry 283, 2418-2426.

Johnson, R. L., Laufer, E., Riddle, R. D. and Tabin, C. (1994). Ectopic expression of Sonic hedgehog alters dorsal-ventral patterning of somites. Cell 79, 1165-1173.

Jones, C. M., Broadbent, J., Thomas, P. Q., Smith, J. C. and Beddington, R. S. (1999). An anterior signaling centre in Xenopus revealed by the homeobox gene Xhex. Current Biology 9, 946–954.

Jones, C. M., Kuehn, M. R., Hogan, B. L. M., Smith, J. C. and Wright, C. V. E. (1995). Nodal-related signals induce axial mesoderm and dorsalize mesoderm during gastrulation. Development 121, 3651-3662.

Jurand, A. (1962). The development of the notochord in chick embryos. J. Embryol. exp. Morpb. 10, 602-621.

Kapoor, N., Galang, G., Marban, E. and Cho, H. C. (2011). Transcriptional suppression of connexin43 by Tbx18 undermines cell-cell electrical coupling in postnatal cardiomyocytes. Journal of Biological Chemistry 286, 14073-9.

Kessler, D. S. (1997). Siamois is required for Spemann's organiser. PNAS 94, 13017-13022.

Keller, R. E. (1976). Vital dye mapping of the gastrula and neurula of Xenopus laevis. II. Prospective areas and morphogenetic movements of the deep layer. Developmental Biology 51, 118-137.

Khaner, O. and Eyal-Giladi, H. (1989). The chick's marginal zone and primitive streak formation. I. Coordinative effect of induction and inhibition. Developmental Biology 134, 206-14.

Kim, S. K., Hebrok, M. and Melton, D. A. (1997). Notochord to endoderm signaling is required for pancreas development. Development 124, 4243-4252.

Kispert, A. (1995). The Brachyury protein: a T-domain transcription factor. Semin. Dev. Biol. 6, 395–403.

Kochav, S. and Eyal-Giladi, H. (1971). Bilateral Symmetry in Chick Embryo Determination by Gravity. Science 171 (3975) 1027-1029.

Kofron. M., Demel, T., Xanthos, J., Lohr, J., Sun, B., Sive, H., Osada, S., Wright, C., Wylie, C. and Heasman J. (1999) Mesoderm induction in Xenopus is a zygotic event regulated by maternal VegT via TGF growth factors. Development 126, 5759–5770.

Kramer, B. & Penny, C. (2001). Regulation of embryonic chick insulin cells: effect of retinoic acid and insulin-like growth factor 1. Cells Tissues Organs 169, 42–48.

Kraus, F., Haenig, B. and Kispert, A. (2001). Cloning and expression analysis of the mouse T-box gene Tbx18. Mechanisms of Development 100, 83-86.

Krauss, S., Concordet, J. P. and Ingham, P. W. (1993). A functionally conserved homolog of the Drosophila segment polarity gene hh is expressed in tissues with polarizing activity in zebrafish embryos. Cell 75, 1431-1444.

Kuhl, M., Geis, K., Sheldahl, L. C., Pukrop, T., Moon, R. T. and Wedlich, D. (2001). Antagonistic regulation of convergent extension movements in Xenopus by Wnt/b-catenin and Wnt/Ca2+ signaling. Mechanisms of Development 106, 61 -76.

Labbe, E., Silvestri, C., Hoodless, P. A., Wrana, J. L. and Attisano, L. (1998). Smad2 and Smad3 positively and negatively regulate TGF beta-dependent transcription through the forkhead DNA-binding protein FAST2. Molecular Cell 2, 109-120.

Ladher, R. K., Church, V. L., Allen, S., Robson, L., Abdelfattah, A., Brown, N. A., Hattersley, G., Rosen, V., Luyten, F. P., Dale, L. and FrancisWest, P. H. (2000). Cloning and expression of the Wnt antagonists Sfrp-2 and Frzb during chickdevelopment. Developmental Biology 218, 183–198.

Lamb, T. M., Knecht, A. K., Smith, W. C., Stachel, S. E., Economides, A. N., Stahl, N., Yancopolous, G. D. and Harland, R. M. (1993). Neural induction by the secreted polypeptide noggin. Science 262, 713–718.

Laurent, M. N., Blitz, I. L., Hashimoto, C., Rothbacher, U., and Cho, K. W. (1997) The Xenopus homeobox gene twin mediates Wnt induction of goosecoid in establishment of Spemann's organizer. Development 124, 4905-4916.

Lawson, A., Colas, J. F. and Schoenwolf, G. C. (2001). Classification scheme for genes expressed during formation and progression of the avian primitive streak. Anatomical Record 262, 221–226.

Le Douarin, N. M., Teillet, M. A. and Catala, M. (1998). Neurulation in amniote vertebrates: a novel view deduced from the use of quail-chick chimeras. Int. J. Dev. Biol. 42, 909-916.

Le Douarin, N. M. and Halpern, M. E. (2000). Discussion point. Origin and specification of the neural tube floor plate: insights from the chick and zebrafish. Current Opinion in Neurobiology 10, 23-30.

Lee, M. A., Heasman, J. and Whitman, M. (2001). Timing of endogenous activin-like signals and regional specification of the Xenopus embryo. Development 128, 2939–2952.

Lemaire, P., Garrett, N. and Gurdon, J. B. (1995). Expression cloning of Siamois, a Xenopus homeobox gene expressed in dorsal-vegetal cells of blastulae and able to induce a complete secondary axis. Cell 81, 85–94.

Lemaire, P. and Kodjabachian, L. (1996). The vertebrate organizer: structure and molecules. Trends in Genetics 12, 525–531.

Leyns, L., Bouwmeester, T., Kim, S. H., Piccolo, S. and De Robertis, E. M. (1997). Frzb-1 is a secreted antagonist of Wnt signaling expressed in theSpemann organizer. Cell 88, 747–756.

Lowe, L. A., Yamada, S. and Kuehn, M. R. (2001). Genetic dissection of nodal function in patterning the mouse embryo. Development 128, 1831–43.

Lustig, K. D., Kroll, K., Sun, E., Ramos, R., Elmendorf, H. and Kirschner, M. W. (1996). A Xenopus nodal-related gene that acts in synergy with noggin to induce complete secondary axis and notochord formation. Development 122, 3275-3282.

Mangold, O. (1933). liber die InducktionsfShigkeit der verschiedenen Bezirke der Neurula von Urodelen. Naturwissenschaften 43, 761 -766.

Manning, L., Ohyama, K., Saeger, B., Hatano, O., Wilson, S. A., Logan, M. and Placzek, M. (2006). Regional morphogenesis in the hypothalamus: a BMP Tbx2 pathway coordinates fate and proliferation through Shh downregulation. Developmental Cell 11, 873–885.

Marti, E., Takada, R., Bumcroft, D. A., Sasaki, H. and McMahon, A. P. (1995). Distribution of Sonic hedgehog peptides in the developing chick and mouse embryo. Development 121, 2537-2547.

Martinez Barbera, J. P., Clements, M., Thomas, P., Rodriguez, T., Meloy, D., Kioussis, D. and Beddington, R. S. (2000). The homeobox gene Hex is required in definitive endodermal tissues for normal forebrain, liver and thyroid formation. Development 127, 2433-2445.

Massague, J. and Wotton, D. Transcriptional control by the TGF-beta/Smad signalling system. EMBO J. 19, 1745-1754.

Matzuk, M. M., Kumar, T. R., and Bradley, A. (1995b). Different phenotypes for mice deficient in either activins or activin receptor II. Nature 374, 356 –360.

Meier, S. (1981). Development of the chick embryo mesoblast: morphogenesis of the prechordal plate and cranial segments. Dev. Biol. 83, 49-61.

Meno, C., Shimono, A., Saijoh, Y., Yashiro, K., Mochida, K., Ohishi, S., Noji, S., Kondoh, H. and Hamada, H. (1998). Lefty-1 is required for left-right determination as a regulator of lefty-2 and nodal. Cell 94, 287–297.

Minguillon, C. and Logan, M. (2003). The comparative genomics of T-box genes. Briefings in functional genomics and proteomics 2, 224-233.

Mitrani, E. and Shimoni, Y. (1990). Induction by soluble factors of organized axial structures in chick epiblasts. Science 247, 1092-1094.

Mitrani, E., Ziv, T., Thomsen, G., Shimoni, Y., Melton, D. A., and Bril, A. (1990). Activin can induce the formation of axial structures and is expressed in the hypoblast of the chick. Cell 63, 495-501.

Munsterberg, A. E. and Lassar, A. B. (1995). Combinatorial signals from the neural tube, floor plate and notochord induce myogenic bHLH gene expression in the somite. Development 121, 651-660.

Munsterberg, A. E., Kitajewski, J., Bumcrot, D. A., McMahon, A. P. and Lassar, A. B. (1995). Combinatorial signaling by sonic hedgehog and wnt family members induces myogenic bHLH gene expression in the somite. Genes and Development 9, 2911-2922.

Naiche, L. A., Harrelson, Z., Kelly, R. G. and Papaioannou, V. E. (2005). T-box genes in vertebrate development. Annual Reviews in Genetics 39, 219-239.

Nakamura, H., Katahira, T., Sato, T., Watanabe, Y. and Funahashi, J. (2004). Gain- and loss-of-function in chick embryos by electroporation. Mechanisms of Development 121, 1137-1143.

Niederreither, K., McCaffery, P., Drager, U. C., Chambon, P. and Dollé, P. (1997). Restricted expression and retinoic acid-induced downregulation of the retinaldehyde dehydrogenase type 2 (RALDH-2) gene during mouse development. Mechanisms of Development 62, 67-78.

Nieuwkoop, P. (1954). Neural activation and transformation in explants of competent ectoderm under the influence of fragments of anterior notochord in urodeles. J. Embryol. Exp. Morphol. 2, 175–193.

Nieuwkoop, P. D. (1969a). The formation of the mesoderm in urodelean amphibians. I. The induction by the endoderm. Wilhelm Roux' Arch. Entw Mech. Org. 162, 341-373.

Nieuwkoop, P. D. (1969b). The formation of mesoderm in urodelean amphibians. II. The origin of the dorso-ventral polarity of the mesoderm. Wilhelm Roux's Arch. Entwicklungsmech. Org. 163, 298–315.

Nieuwkoop, P. D. and Ubbels, G. A. (1972). The formation of mesoderm in urodelean amphibians. IV. Quantitative evidence for the purely 'ectodermal' origin of the entire mesoderm and phyrangeal endoderm. Wilhelm Roux's Arch. Entwicklungsmech. Org. 169, 185-199.

Nomura, M. and Li, E. (1998). Smad2 role in mesoderm formation, left-right patterning and craniofacial development. Nature 393, 786-790.

Oh, S. P., and Li, E. (1997). The signaling pathway mediated by type IIB activin receptor controls axial patterning and lateral asymmetry in the mouse. Genes and Development 11, 1812–1826.

Ohyama, K., Ellis, P., Kimura, S. and Placzek, M. (2005). Directed differentiation of neural cells to hypothalamic dopaminergic neurons. Development 132, 5185-5197.

Ohyama, K., Das, R. and Placzek, M. (2008). Temporal progression of hypothalamic patterning by a dual action of BMP. Development 135, 3325-3331.

Olson, E. N. and Srivastava, D. (1996). Molecular pathways controlling heart development. Science 272, 671-676.

Osada, S. I. and Wright, C. V. E. (1999). Xenopus nodal-related signaling is essential for mesendodermal patterning during early embryogenesis. Development 126, 3229-3240.

Osmond, M. K., Butler, A. J., Voon, F. C. T. and Bellairs, R. (1991). The effects of retinoic acid on heart formation in the early chick embryo. Development 113, 1405-1417.

Papaioannou, V. E. and Silver, L. M. (1998). The T-box gene family. BioEssays 20, 9-19.

Papapetrou, C., Edwards, Y. H. and Sowden, J. C. (1997). The T transcription factor functions as a dimer and exhibits a common human polymorphism Gly-177-Asp in the conserved DNA-binding domain. FEBS Lett. 409, 201-206.

Patten, I. and Placzek, M. (2000). The role of Sonic hedgehog in neural tube patterning. Cell. Mol. Life Sci. 57, 1695-1708.

Patten, I., Kulsea, P., Shen, M., Fraser, S. and Placzek, M. (2003). Distinct modes of floor plate induction in the chick embryo. Development 130, 4809-4821.

Pera, E. M. and Kessel, M. (1997). Patterning of the chick forebrain anlage by the prechordal plate. Development 124, 4153-4162.

Perea-Gomez, A., Vella, F. D. J., Shawlot, W., Oulad-Abdelghani, M., Chazaud, C., Meno, C., Pfister, V., Chen, L., Robertson, E., Hamada, H., Behringer, R. R. and Ang, S. L. (2002). Nodal Antagonists in the Anterior Visceral Endoderm Prevent the Formation of Multiple Primitive Streaks. Developmental Cell 3, 745-756.

Piccolo, S., Agius, E., Leyns, L. Bhattacharyya, S., Grunz, H., Bouwmeester, T. and De Robertis, E. M. (1999). The head induce Cerberus is a multifunctional antagonist of Nodal, BMP and Wnt signals. Nature 397, 707-710.

Piccolo, S., Sasai, Y., Lu, B. and De Robertis, E. M. (1996). Dorsoventral patterning in Xenopus: inhibition of ventral signals by direct binding of chordin to BMP-4. Cell 86, 589-598.

Placzek, M. (1995). The role of the notochord and floor plate in inductive interactions. Current Opinion in Genetics and Development 5, 499-506.

Placzek, M., Dodd, J. and Jessell, T. M. (2000). The case for floor plate induction by the notochord. Current Opinion in Neurobiology 10, 15-20.

Placzek, M., Jessell, T. M. and Dodd, J. (1993). Induction of floor plate differentiation by contact-dependent, homeogenetic signals. Development 117, 205-218.

Placzek, M., Tessier-Lavigne, M., Yamada, T., Jessel, T. M. and Dodd, J. (1990). Mesodermal control of neural cell identity: floor plate induction by the notochord. Science 250, 985-988.

Pogoda, H. M., Solnica-Krezel, L., Driever, W. and Meyer, D. (2000). The zebrafish forkhead transcription factor FoxH1/Fast1 is a modulator of Nodal signaling required for organizer formation. Current Biology 10, 1041–1049.

Psychoyos, D. and Stern, C. D. (1996). Fates and migratory routes of primitive streak cells in the chick embryo. Development 122, 1523-1534.

Rebagliati, M. R., Toyama, R., Fricke, C., Haffter, P. and Dawid, I. B. (1998). Zebrafish nodal-related genes are implicated in axial patterning and establishing left-right asymmetry. Developmental Biology 199, 261–272.

Reijntjes, S., Gale, E. and Maden, M. (2004). Generating gradients of retinoic acid in the chick embryo: Cyp26C1 expression and a comparative analysis of the Cyp26 enzymes. Developmental Dynamics 230, 509-517.

Reissmann, E., Jornvall, H., Blokzijl, A., Andersson, O., Chang, C., Minchiotti, G., Graziella Persico, M., Ibanez, C. F. and Brivanlou, A. H. (2001). The orphan receptor ALK7 and the Activin receptor ALK4 mediate signaling by Nodal proteins during vertebrate development. Genes and Development 15, 2010–2022.

Reversade, B., Kuroda, H., Lee, H., Mays, A. and De Robertis, E. M. (2005). Depletion of Bmp2, Bmp4, Bmp7 and Spemann organizer signals induces massive brain formation in Xenopus embryos. Development 132, 3381–3392.

Rivera-Pérez, J. A., Mallo, M., Gendron-Maguire, M., Gridley, T. and Behringer, R. R. (1995). Goosecoid is not an essential component of the mouse gastrula organizer but is required for craniofacial and rib development. Development 121, 3005-3012.

Roelink, H., Augsburger, A., Heemskerk, J., Korzh, V., Norlin, S., Ruiz i Altaba, A., Tanabe, Y., Placzek, M., Edlund, T., Jessell, T. M. and Dodd, J. (1994). Floor plate and motor neuron induction by vhh-1, a vertebrate homolog of hedgehog expressed by the notochord. Cell 76, 761-775.

Roelink, H., Porter, J. A., Chiang, C., Tanabe, Y., Chang, D. T., Beachy, P. A. and Jessell, T. M. (1995). Floor plate and motor neuron induction by different concentrations of the amino-terminal cleavage product of sonic hedgehog autoproteolysis. Cell 81, 445-455.

Rossant, J., Zirngibl, R., Cado, D., Shago, M. and Gigue`re, V. (1991). Expression of a retinoic acid response element-hsplacZ transgene defines specific domains of transcriptional activity during mouse embryogenesis. Genes and Development 5, 1333–1344.

Rowitch, D. H., S-Jacques, B., Lee, S. M., Flax, J. D. Snyder, E. Y. and McMahon, A. P. (1999). Sonic hedgehog regulates proliferation and inhibits differentiation of CNS precursor cells. Journal of Neuroscience 19, 8954-8965.

Ryan, K., Garrett, N., Mitchell, A. and Gurdon, J. B. (1996). Eomesodermin, a key early gene in Xenopus mesoderm differentiation. Cell 87, 989-1000.

Sampath, K., Rubinstein, A. L., Cheng, A. M. S., Liang, J. O., Fekany, K., Solnica-Krezel, L., Korzh, V., Halpern, M. E. and Wright, C. V. E. (1998). Induction of the zebrafish ventral brain and floorplate requires cyclops/nodal signalling. Nature 395, 185-189.

Sasai, Y., Lu, B., Steinbeisser, H. and De Robertis E. M. (1995). Regulation of neural induction by Chd and Bmp-4 antagonistic patterning signals in Xenopus. Nature 376, 333-336.

Sasai, Y., Lu, B., Steinbeisser, H., Geissert, D., Gont, L. K. and De Robertis, E. M. (1994). Xenopus chordin: a novel dorsalizing factor activated by organizer-specific homeobox genes. Cell 79, 779-790.

Sargent, T. D., Jamrich, M. and Dawid, I. B. (1986). Cell interactions and the control of gene activity during early development of Xenopus laevis. Developmental Biology 114, 238-246.

Saude, L., Woolley, K., Martin, P., Driever, W. and Stemple, D. L. (2000). Axis inducing activities and cell fates of the zebrafish organizer. Development 127, 3407-3417.

Schier, A. F., Neuhauss, S. C., Helde, K. A., Talbot, W. S. and Driever, W. (1997). The one-eyed pinhead gene functions in mesoderm and endoderm formation in zebrafish and interacts with no tail. Development 124, 327-342.

Schier, A. F. (2003). Nodal signaling in vertebrate development. Annu. Rev. Cell. Dev. Biol. 19, 589–621.

Schlueter, J., Männer, J. and Brand, T. (2006). BMP is an important regulator of proepicardial identity in the chick embryo. Developmental Biology 295, 546-558.

Schoenwolf, G. C., Garcia-Martinez, V. and Dias, M. S. (1992). Mesoderm movement and fate during avian gastrulation and neurulation. Developmental Dynamics 193, 235-248.

Schulte-Merker, S., Smith J. C. and Dale, L. (1994). Effects of truncated activin and FGF receptors and of follistatin on the inducing activities of BVg1 and activin: Does activin play a role in mesoderm induction. EMBO J. 13, 3533–3541.

Seilez, I., Thisse, B. and Thisse, C. (2005). FoxA3 and goosecoid promote anterior neural fate through inhibition of Wnt8a activity before the onset of gastrulation. Developmental Biology 290, 152-163.

Seleiro, E. A. P., Connolly, D. J. and Cooke, J. (1996). Early developmental expression and experimental axis determination by the chicken Vg1 gene. Current Biology 6, 1476-1486.

Shah, S. B., Skromne, I., Humme, C. R., Kessler, D. S., Lee, K. J., Stern, C. D. and Dodd, J. (1997). Misexpression of chick Vg1 in the marginal zone induces primitive streak formation. Development 124, 5127-5138.

Shiau, C. E., Lwigale, P. Y., Das, R. M., Wilson, S. A. and Bronner-Fraser, M. (2008). Robo2-Slit1 dependent cell-cell interactions mediate assembly of the trigeminal ganglion. Nature Neuroscience 11, 269-276.

Shawlot, W., Wakamiya, M., Kwan, K. M., Kania, A., Jessell, T. M. and Behringer, R. R. (1999). Lim1 is required in both primitive streak-derived tissues and visceral endoderm for head formation in the mouse. Development 126, 4925-4932.

Shawlot, W. and Behringer, R. R. (1995). Requirement for Lim1 in head-organizer function. Nature 374, 425-430.

Shih, J. and Fraser, S. E. (1995). Distribution of tissue progenitors within the shield region of the zebrafish gastrula. Development 121, 2755-2765.

Shih, J. and Fraser, S. E. (1996). Characterizing the zebrafish organizer: microsurgical analysis at the early-shield stage. Development 122, 1313-1322.

Sirard, C., de la Pompa, J. L., Elia, A., Itie, A., Mirtsos, C., Cheung, A., Hahn, S., Wakeham, A., Schwartz, L., Kern, S. E., Rossant, J. and Mak, T. W. (1998). The tumor suppressor gene Smad4/Dpc4 is required for gastrulation and later for anterior development of the mouse embryo. Genes and Development 12, 107–119.

Sirotkin, H. I., Gates, M. A., Kelly, P. D., Schier A. F. and Talbot, W. S. (2000). Fast1 is required for the development of dorsal axial structures in zebrafish. Current Biology 10, 1051–1054.

Skromne, I. and Stern, C. D. (2002). A hierarchy of gene expression accompanying induction of the primitive streak by Vg1 in the chick embryo. Mechanisms of Development 114, 115–118.

Smith, J. C., Price, B. M., Green, J. B., Weigel, D. and Herrmann, B. G. (1991). Expression of a Xenopus homolog of Brachyury (T) is an immediate-early response to mesoderm induction. Cell 67, 79–87.

Smith, W. C. and Harland, R. M. (1992). Expression cloning of noggin, a new dorsalizing factor localized to the Spemann organizer in Xenopus embryos. Cell 70, 829-840.

Song, J., Oh, S. P., Schrewe, H., Nomura, M., Lei, H., Okano, M., Gridley, T. and Li, E. (1999). The type II activin receptors are essential for egg cylinder growth, gastrulation, and rostral head development in mice. Developmental Biology 213, 157–169.

Song, J., Yue, Q. and Munsterberg, A. (2011). Time-lapse imaging of chick cardiac precursor cells. Methods Mol. Biol. 769: 359-72.

Spemann, H. and Mangold H. (1924). Über induktion von embryonalanlagen durch implantation artfremder organisatoren. Wilhelm Roux Arch. Entw. Mech. Org. 100: 599-638.

Spemann, H. (1938). Embryonic Development and Induction. New Haven, Yale University Press.

Stemple, D. L., Solnica-Krezel, L., Zwartkruis, F., Neuhauss, S. C., Schier, A. F., Malicki, J., Stainier, D. Y., Abdelilah, S., Rangini, Z., Mountcastle-Shah, E. and Driever, W. (1996). Mutations affecting development of the notochord in zebrafish. Development 123, 117-128.

Steinbeisser, H., Fainsod, A., Niehrs, C., Sasai, Y. and De Robertis, E. M. (1995). The role of gsc and BMP-4 in dorsal-ventral patterning of the marginal zone in Xenopus: a loss-of-function study using antisense RNA. EMBO Journal 14, 5230-5243.

Stennard, F., Carnac, G. and Gurdon, J. B. (1996). The Xenopus T-box gene, Antipodean, encodes a vegetally localised maternal mRNA and can trigger mesoderm formation. Development 122, 4179-4188.

Stern, C. D. (2001). Initial patterning of the central nervous system: How many organizers?. Nature Reviews Neuroscience 2, 92-98.

Stern, C. D., Yu, R. T., Kakizuka, A., Kintner, C. R., Mathews, L. S., Vale, W. W., Evans, R. M. and Umesono, K. (1995). Activin and its receptors during gastrulation and the later phases of mesoderm development in the chick embryo. Developmental Biology 172, 192-205.

Sudarwati, S. and Nieuwkoop, P. D. (1971). Mesoderm formation in the Anuran Xenopus laevis (Daudin). Wilhelm Roux' Archive 166: 189–204.

Sumoy, L., Keasey, J. B., Dittman, T. D., and Kimelman, D. (1997). A role for notochord in axial vascular development revealed by analysis of phenotype and the expression of VEGR-2 in zebrafish flh and ntl mutant embryos. Mechanisms of Development 63 (1) 15-27.

Sun, A., Jin, P., Tian, T., Gu, Y., Chen, Y. –G. and Meng, A. (2006). Activation and roles of ALK4/ALK7-mediated maternal TGFβ signals in zebrafish embryo. Biochem. Biophys. Res. Commun. 345, 694-703.

Sun, X., Saitsu, H., Shiota, K. and Ishibashi, M. (2008). Expression dynamics of the LIM-homeobox genes, Lhx1 and Lhx9, in the diencephalon during chick development. Int. J. Dev. Biol. 52, 33-41.

Suzuki, A., Thies, R. S., Yamaji, N., Song, J. J., Wozney, J. M., Murakami, K. and Ueno, N. (1994). A truncated bone morphogenetic protein receptor affects dorsal–ventral patterning in the early Xenopus embryo. Proc. Natl. Acad. Sci. 91, 10255–10259.

Suzuki, T., Takeuchi, J., Koshiba-Takeuchi, K. and Ogura, T. Tbx Genes Specify Posterior Digit Identity through Shh and BMP Signaling. Developmental Cell 6, 43–53.

Swartz, M., Eberhart, J., Mastick, G. S. and Krull, C. E. (2001). Sparking new frontiers: using in vivo electroporation for genetic manipulations. Developmental Biology 233, 13–21.

Szeto, D. P. and Kimelman, D. (2004). Combinatorial gene regulation by Bmp and Wnt in zebrafish posterior mesoderm formation. Development 131, 3751–3760.

Tao, Q., Yokota, C., Puck, H., Kofron, M., Birsoy, B., Yan, D., Asashima, M., Wylie, C. C., Lin, X. and Heasman, J. (2005). Maternal wnt11 activates the canonical wnt signaling pathway required for axis formation in Xenopus embryos. Cell 120, 857-871.

Tada, M., Casey, E. S., Fairclough, L. and Smith, J. C. (1998). Bix1, a direct target of Xenopus T-box genes, causes formation of ventral mesoderm and endoderm. Development 125 (20) 3997-4006.

Takahashi, S. Yokota, C., Takano, K., Tanegashima, K., Onuma, Y., Goto, J. and Asashima, M. (2000). Two novel nodal-related genes initiate early inductive events in Xenopus Nieuwkoop center. Development 127, 5319-5329.

Takaya, H. (1961). Significance of the notochord for the differentiation and growth of the embryonic trunk in amphibia. Embryologia 6, 123-134.

Talbot, W. S., Trevarrow, B., Halpern, M. E., Melby, A. E., Farr, G., Postlethwait, J. H., Jowett, T., Kimmel, C. B. and Kimelman, D. (1995). A homeobox gene essential for zebrafish notochord development. Nature 378, 150-157.

Tanabe, Y. and Jessell, T. M. (1996). Diversity and pattern in the developing spinal cord. Science 274, 1115-1123.

Tanaka, M. and Tickle, C. (2004). Boundary formation in chick somite and wing development is mediated by Tbx18. Developmental Biology 268, 470–480.

Teillet, M., Watanabe, Y., Jeffs, P., Duprez, D., Lapointe, F. and Le Douarin, N. M. (1998). Sonic hedgehog is required for survival of both myogenic and chondrogenic somitic lineages. Development 125, 2019-2030.

Thisse, C., Thisse, B., Halpern, M. E. and Postlethwait, J. H. (1994). Goosecoid expression in neurectoderm and mesendoderm is disrupted in zebrafish cyclops gastrulas. Developmental Biology 164, 420–429.

Toyama, R., O'Connell, M. L., Wright, C. V., Kuehn, M. R. and Dawid, I. B. (1995). Nodal induces ectopic goosecoid and lim1 expression and axis duplication in zebrafish. Development 121, 383-391.

Trousse, F., Giess, M.C., Soula, C., Ghandour, S., Duprat, A.M. and Cochard, P. (1995). Notochord and floor plate stimulate oligodendrocyte differentiation in cultures of the chick dorsal neural tube. J. Neurosci. Res. 41, 552–560.

Trowe, O., Maier, H., Schweizer, M., Kispert, A. (2008). Deafness in mice lacking the T-box transcription factor Tbx18 in otic fibrocytes. Development 135, 1725-1734.

Twal, W., Roze, L. and Zile, M. H. (1995). Anti-retinoic acid monoclonal antibody localizes all-trans-retinoic acid in target cells and blocks normal development in early quail embryo. Developmental Biology 168, 225-234.

Uchiyama, H., Kobayashi, T., Yamashita, A., Ohno, S. and Yabe, S. (2001). Cloning and characterization of the T-box gene *Tbx6* in Xenopus laevis. Development, Growth and Differentiation 43, 657-669.

Varlet, I., Collignon, J. and Robertson, E. J. (1997). Nodal expression in the primitive endoderm is required for the specification of the anterior axis during mouse gastrulation. Development 124, 1033–1044.

van Straaten, H. W. M., Hekking, J. W. M., Beursgens, J. P. W. M., Terwindtrouwenhorst, E. and Drukker, J. (1989). Effect og the notochord on proliferation and differentiation in the neural tube of the chick embryo. Development 107, 793-803.

van Straaten, H. W. M. and Hekking, J. W. M. (1991). Development of floor plate, neurons and axonal outgrowth pattern in the early spinal cord of the notochord-deficient chick embryo. Anat. Embryol. 184, 55-63.

Vesque, C., Ellis, S., Lee, A., Szabo, M., Thomas, P., Beddington, R. and Placzek, M. (2000). Development of chick axial mesoderm: Specification of prechordal mesoderm by anterior endodermderived TGFbeta family signalling. Development 127, 2795-2809.

Vincent, S. D., Dunn, N. R., Hayashi, S., Norris, D. P. and Robertson, E. J. (2003). Cell fate decisions within the mouse organizer are governed by graded Nodal signals. Genes and Development 17, 1646 -1662.

Waddington, C. H. (1932). Experiments on the development of chick and duck embryos cultivated in vitro. Philos. Trans. R. Soc. Lond. (Biol.) 221, 179-230.

Waldrip, W. R., Bikoff, E. K., Hoodless, P. A., Wrana, J. L. and Robertson, E. J. (1998). Smad2 signaling in extraembryonic tissues determines anterior-posterior polarity of the early mouse embryo. Cell 92 (6) 797–808.

Wang, S., Krinks, M., Lin, K., Luyten, F. P. and Moos, M. (1997). Frzb, a secreted protein expressed in the Spemann organizer, binds and inhibits Wnt-8. Cell 88, 757–766.

Wardle, F. C. and Papaioannou, V. E. (2008). Teasing out T-box targets in early mesoderm. Current Opinion in Genetic Development 18, 418-425.

Watabe, T., Kim, S., Candia, A., Rothbacher, U., Hashimoto, C., Inoue, K. and Cho, K. W. (1995). Molecular mechanisms of Spemann's organizer formation: conserved growth factor synergy between Xenopus and mouse. Genes and Development 9, 3038-3050.

Watabe-Rudolph, M., Schlautmann, N., Papaioannou, V. E. and Gossler, A. (2002). The mouse rib-vertebrae mutation is a hypomorphic Tbx6 allele. Mech. Dev. 119, 251–256.

Watanabe, M. and Whitman, M. (1999). Fast-1 is a key maternal effector of mesoderm inducers in the early Xenopus embryo. Development 126, 5621-5634.

Weinstein, M. Yang, X., Li, C., Xu, X., Gotay, J. and Deng, C. X. (1998). Failure of egg cylinder elongation and mesoderm induction in mouse embryos lacking the tumor suppressor smad2. PNAS 95, 9378-9383.

Whitman, M. (2001). Nodal signaling in early vertebrate embryos: themes and variations. Developmental Cell 1, 605–617

Wilson, S. I. and Edlund, T. (2001). Neural induction: toward a unifying mechanism. Nature Neuroscience 4, 1161-1168.

Wolpert, L., Beddington, R., Brockes, J., Jessell, T., Lawrence, P. and Meyerowitz, E. Principles of development (2002)

Wylie, C., Kofron, M., Payne, C., Anderson, R., Hosobuchi, M., Joseph, E. and Heasman, J. (1996). Maternal beta-catenin establishes a 'dorsal signal' in early Xenopus embryos. Development 122, 2987-2996.

Yamada, G., Mansouri, A., Torres, M., Stuart, E. T., Blum, M., Schultz, M., De Robertis, E. M. and Gruss, P. (1995). Targeted mutation of the murine Goosecoid gene results in craniofacial defects and neonatal death. Development 121, 2917-2922.

Yamada, T., Placzek, M., Tanaka, H., Dodd, J. and Jessell, T.M. (1991). Control of cell pattern in the developing nervous system: Polarizing activity of the floor plate and notochord. Cell 64, 635-647.

Yamada, T., Pfaff, S. L., Edlund, T. and Jessell T. M. (1993). Control of cell pattern in the neural tube motor neuron induction by diffusible factors from notochord and floor plate. Cell 73, 673–686.

Yamada, M., Revelli, J. –P., Eichele, G., Barron, M. and Schwartz, R. J. (2000). Expression of chick Tbx-2, Tbx-3, and Tbx-5 genes during early heart development: evidence for BMP2 induction of Tbx2. Developmental Biology 228, 95–105.

Yamamoto, M., Meno, C., Sakai, Y., Shiratori, H., Mochida, K., Ikawa, Y., Saijoh, Y. and Hamada, H. (2001). The transcription factor FoxH1 (FAST) mediates Nodal signaling during anterior-posterior patterning and node formation in the mouse. Genes and Development 15, 1242-1256.

Yanagisawa, K. O., Fujimoto, K. O., Fujimoto, H. and Urushthara, H. (1981). Effects of the Brachyury (T) mutation on morphogenetic movement in the mouse embryo. Developmental Biology 87, 242-248.

Yasugi, S. and Nakamura, H. (2000). Gene transfer into chicken embryos as an effective system of analysis in developmental biology. Dev. Growth. Differ. 42,195–197.

Yasuhiko, Y., Haraguchi, S., Kitajima, S., Takahashi, Y., Kanno, J. and Saga, Y. (2006). Tbx6-mediated Notch signaling controls somite-specific Mesp2 expression. PNAS 103, 3651-3656.

Zamir, E. A., Czirók, A., Cui, C., Little, C. D., Rongish, B. J. (2006). Mesodermal cell displacements during avian gastrulation are due to both individual cell autonomous and convective tissue movements. PNAS 103, 19806-19811.

Zhang, J., King, M. L., Houston, D., Payne, C., Wylie, C., and Heasman, J. (1998). The role of maternal VegT in establishing the primary germ layers in Xenopus embryos. Cell 94 (4) 515–524.

Zhou, X., Sasaki, H., Lowe, L., Hogan, B. L. and Kuehn, M. R. (1993). Nodal is a novel TGF-beta-like gene expressed in the mouse node during gastrulation. Nature 361, 543–547.

Zhu, L. Belo, J. A., De Robertis, E. M. and Stern, C. D. (1999). Goosecoid regulates the neural inducing strength of the mouse node. Developmental Biology 216, 276-281.

Zile, M. H. Vitamin A requirement for early cardiovascular morphogenesis specification in the vertebrate embryo: insights from the avian embryo. Exp. Biol. Med. 229, 598-606.

Zimmerman, L. B., De Jesus-Escobar, J. M. and Harland, R. M. (1996). The Spemann organizer signal noggin binds and inactivates bone morphogenetic protein 4. Cell 86, 599-606.

Ziv, T., Shimoni, Y. and Mitrani, E. (1992). Activin can generate ectopic axial structures in chick blastoderm explants. Development 115, 689-694.